INFORMATION TO USERS

This manuscript has been reproduced from the microfilm master. UMI films the text directly from the original or copy submitted. Thus, some thesis and dissertation copies are in typewriter face, while others may be from any type of computer printer.

The quality of this reproduction is dependent upon the quality of the copy submitted. Broken or indistinct print, colored or poor quality illustrations and photographs, print bleedthrough, substandard margins, and improper alignment can adversely affect reproduction.

In the unlikely event that the author did not send UMI a complete manuscript and there are missing pages, these will be noted. Also, if unauthorized copyright material had to be removed, a note will indicate the deletion.

Oversize materials (e.g., maps, drawings, charts) are reproduced by sectioning the original, beginning at the upper left-hand corner and continuing from left to right in equal sections with small overlaps.

ProQuest Information and Learning
300 North Zeeb Road, Ann Arbor, MI 48106-1346 USA
800-521-0600

ENTROPY AND SOLVENT STRUCTURE EFFECTS IN ELECTROCHEMICAL ADSORPTION AT MERCURY

by

L. G. M. Gordon

A thesis submitted in partial fulfillment
of the requirements for the degree of
Doctor of Philosophy
in the
Department of Chemistry
University of Ottawa

August 1969

B. E. Conway
Professor of Chemistry
Research Supervisor

L. G. M. Gordon
Ph. D. Candidate

PREFACE

The adsorption of uncharged substances at a mercury electrode at controlled potentials was first investigated by Gouy and studied more quantitatively by Frumkin who assumed the validity of the Langmuir-type relation for the configurational term in the isotherm but took into account particle-particle interactions. Further studies of the adsorption of neutral organic molecules have been stimulated by the effects these adsorbates have on electrochemical reactions such as corrosion, electrodeposition of metals and kinetic exchange currents. Of basic interest is the situation at an electrode, particularly Hg, where the electrical condition of the interface can be independently controlled. This is not generally possible at gas-solid interfaces nor in the case of adsorption at insulator/solution interfaces.

More recently, the assignment of isotherms to represent the adsorption behaviour of neutral molecules has become an important aspect of the study of the mercury electrode interface and is important in the study of the kinetics of organic electrode reactions. This problem has been most fully investigated by Parsons who in the course of his researches showed that the standard free energy of adsorption had a quadratic dependence on the electrode charge density, a relation which agreed with predictions which can be derived from the early simple models of Frumkin and Butler.

The structure of the interphase region of the ideally polarised mercury electrode has been investigated using methods involving capacitance and surface tension measurements but both these techniques are rather insensitive (when compared with spectral

studies of gas-solid interfaces) since they measure composite quantities associated with the presence of both solute and solvent. It is for this reason that various molecular models proposed for the interphase have not been completely satisfactory.

Many of the interpretations of the adsorption characteristics rely heavily on data obtained at one temperature. Thus the enthalpy and entropy components of the free energy of adsorption cannot be found, so that much decisive information on the structure of the interphase remains unknown.

The studies constituting the present work were selected in order to increase the understanding of the orientation, interaction and structural effects involving both solute and solvent in the ad-layer so that more refined molecular models might be developed. During these investigations, it became possible to study with a co-worker the surface reaction order of the kinetics of reduction of acetophenone in the case where surface concentrations of the reactant could directly be determined by the electrocapillary technique.

Although the literature contains a wealth of material pertaining to the general phenomena of adsorption and comprehensive treatises of Adam and of Davies and Rideal have been written, it was thought useful to introduce the work reported in this thesis with a general review of the characteristics of interfaces with the aim of comparing and supporting those ideas that arise in electrocapillary studies.

The work has been reported in the following papers.

1. New Techniques for Electrocapillary measurements using the Lippmann Electrometer, B. E. Conway and L. G. M. Gordon, J. Electroanal. Chem., 15, 7 (1967).

2. Further Developments in the Techniques for Electrocapillary Measurements, L. G. M. Gordon, J. Halpern and B. E. Conway, J. Electroanal. Chem., 21, p. 3 (1969).

3. Reaction Order and Adsorption in the Kinetics of Organic Electrode Reactions, B. E. Conway, E. J. Rudd and L. G. M. Gordon, Disc. Faraday Soc., 45, 87 (1968).

4. Entropy and Structural Effects in the Electrochemical Adsorption of Pyridine at Mercury, B. E. Conway and L. G. M. Gordon, J. Phys. Chem., In press, November (1969).

5. Some Common Problems with the Double-Layer and Ionic Solutions, B. E. Conway and L. G. M. Gordon, J. Phys. Chem., In press, November (1969).

ACKNOWLEDGMENT

I wish to extend my sincere thanks to Professor B. E. Conway for his willingness to discuss the many problems that have arisen in this work. His enthusiasm and originality have helped the author in the course of the research and his time and advice have always been freely given.

The author is also indebted to the Ontario Government and to the Sprague Electric Company, North Adams, Mass., U. S. A., for the awards of fellowships for the years 1967-69. Financial support for part of this research was also provided by the National Research Council of Canada.

Discussion with my colleagues of the electrochemistry group have been of great assistance. Technical help received from Mr. Serrat of the University of Ottawa Computing Centre staff and the workshop staff of the Chemistry Department is acknowledged with gratitude.

TABLE OF CONTENTS

Page

CHAPTER IV

CHAPTER V

LIST OF FIGURES

LIST OF TABLES

ABSTRACT

Interphase structure studies in the electrochemical adsorption of neutral organic substances at the mercury electrode have been carried out by electrocapillary measurements. New techniques have been developed which increase the accuracy and greatly facilitate the required measurements.

Use has been made of a Langmuir type of adsorption equation to evaluate the standard free energy of adsorption of pyridine from an aqueous 0.03M $NaClO_4$ solution over a range of temperatures. This study enabled the entropies and heatsof the electrochemical adsorption to be investigated as functions of electrode charge density and coverage.

The adsorption behaviour of acetophenone and its pinacol, 2, 3-diphenyl-butane-2, 3-diol, were examined in order to provide information required in the interpretation of the kinetic reaction orders for the electrochemical reduction of acetophenone at mercury. The pinacol, the main product of the reduction in acid solution, was found to be more adsorbable than the acetophenone, but the kinetic investigations indicated that the presence of pinacol did not affect the rate of reaction. The order of the surface reaction was found to be dependent on the coverage.

An important solvent effect was observed in the comparison of the surface pressure-surface coverage relations obtained for several systems (acetophenone, pinacol and naphthalene in methanolic and aqueous methanolic solutions) in which the same supporting electrolyte was used. The adsorption characteristics of the same solute from various solvents were found to be different, but were similar for different solutes adsorbed from the same

solvent. This behaviour, in conjunction with other effects reported, led to a critical assessment of the value of considering solute-solute interactions in the description of the observed "non-ideal" Langmuir-type behaviour.

The orientation of dipolar neutral adsorbates as a function of charge and surface concentration (and its correlation with the molecular area of the adsorbed species) has been investigated and previous interpretations have been modified.

A comparison between the results for the adsorption of pyridine from aqueous $NaClO_4$ and KCl solutions has been made in terms of the analyses based on the Langmuir and Volmer isotherms.

A new method for evaluating the true free energy, entropy and heat of adsorption of neutral molecules at a mercury electrode in the region of low surface concentration where adsorption is considered "ideal", was investigated. In this study, use was made of the Volmer equation of state.

The adsorption of D- and L-mandelic acid in the presence of L-lactic acid was investigated in order to evaluate possible stereospecific effects in adsorption. However, the differences which were observed in the corresponding surface pressures can be interpreted in terms of intra- and intermolecular esterification processes in the ad-layer, a situation which renders identification of true stereospecific effects somewhat ambiguous.

A review of a number of critical aspects of adsorption phenomena is presented in which the emphasis is placed on structural effects in the adsorbed phase.

CHAPTER I

INTRODUCTION

1.1 ELECTRICAL AND 'CHEMICAL' FACTORS IN ADSORPTION

The forces giving rise to adsorption are no different, in principle, from those in any other interaction phenomenon involving atoms or molecules. The interaction forces operating between the various species in an interphase are basically electromagnetic in origin, involving the electrons and nuclei of the system. Thus it is to be expected that correlations can be found between the various theories of adsorption which have been developed for the different types of interfaces. Since the present original work involves the interpretation of structural effects in adsorption at the mercury-solution interface, a review of structural effects found at other types of interfaces will first be useful. At electrode interfaces, the possibility of separately controlling the electrical and chemical variables in adsorption is an important aspect of electrochemical adsorption studies.

1.1.1 The Solid-Gas Interface

The solid-gas interface differs from the electrode-solution interface in many ways, but primarily the distinction lies in the presence of a solvent in the latter case, which (a) gives rise to a greater variety of interactions in the surface, but (b) allows control of the electrical field which arises at most surfaces.

Attractive forces pertinent to physical adsorption may be divided into several categories. In the presence of an interfacial

electric field, an adsorbate with a permanent dipole moment tends to have its dipole aligned with the field, and the existence of such parallel dipoles in the adsorbed phase introduces a mutual repulsion that may or may not be greater than the normal dispersion forces of attraction between the adsorbate molecules. If the adsorbed molecule possesses no permanent dipole or multipole moment, and a permanent electric field is absent at the surface, then adsorption arises from "non-polar" dispersion forces only. Between these two extreme cases there remains the type of adsorption in which the electric field of an adsorbent surface induces a dipole in a non-polar molecule and thus an interaction in addition to that produced by the dispersion forces arises.

When the electrical forces of attraction between the adsorbate and adsorbent become relatively large, then it is possible, depending on the electronic properties of the latter, for some degree of electron transfer to take place, and the interaction is then termed chemisorption. The molecules or radicals are then oriented to give the maximum overlap of the orbitals involved. This type of adsorption differs in the following ways from physical adsorption. In general it is accompanied by a larger heat of adsorption and a higher energy of activation, has a certain specificity with respect to the surface involved, is usually limited to formation of a monolayer and appreciably modifies the intrinsic electrical fields existing at the surface in the absence of the adsorbate.

An analysis of the electrical conditions at a solid-gas interface becomes complex when the following factors are taken into account: (a) perturbations of the field by the adsorbate, and of the adsorbate by the field; (b) lateral interactions between the adsorbate molecules and (c) intrinsic heterogeneity of the surface.

In principle, a quantum mechanical treatment would be desirable but due to the complexity of the system it is necessary to resort to various, often relatively crude, approximations. In fact, reference must usually be made directly to the determination of adsorption isotherms, which require for their analysis the choice of a feasible and appropriate model, together with a number of supporting assumptions.

However, before discussing the treatment of isotherms (§ 1.5), it should be pointed out that the effect of variation in the electronic nature of the surface phase can be studied as a function of the surface coverage. The asymmetrical distribution of electrons at a clean interface between a metallic conductor and vacuum gives rise to a double-layer of charge across which exists a potential drop called the intrinsic surface potential, χ. If this double-layer is changed by adsorption upon the interface, then there will be a change in χ which can be measured and which leads to changes in the magnetic and electric properties of the interfacial region (to be distinguished as the "interphase") such as conductivity, magnetic susceptibility and dielectric constant. In addition, evidence can be obtained about the redistribution of electrons within the adsorbate molecules by i. r., n. m. r., and e. s. r. spectroscopy.

The change, $\Delta\chi$, in surface potential, produced by the adsorbate film, is often called the "surface potential" of the adsorbed film and it is interesting to note that even the adsorption of non-polar xenon atoms gives rise to considerable surface potentials[1]. (For review see ref. 2).

1.1.2 Liquid-Vapour Interface

The surface free energy of a pure liquid is related to the energy required to transport a molecule from the bulk phase in which it experiences no net force, to the surface phase in which the unbalanced forces are directed towards the interior of the liquid.

Another aspect of the properties of the liquid-vapour interface, which has been qualitatively established, is the high degree of orientation of unsymmetrical molecules that must occur there. This idea was introduced by Hardy[57] and upheld by Langmuir[56] and Harkins[5] who based their conclusions on independent evidence or models. Further experimental evidence[3] is available to show that molecular orientation at liquid surfaces produces effects which extend to a considerable depth and these result in a consequent modification of the properties of the liquid in its surface zone.

In the case of these liquids, the molecules of which are asymmetric, this surface zone usually results from the preferential orientation of surface molecules with their most polar region(s) directed into the liquid[4, 5]. In the case of water with its four asymmetrical polar "vertices" it is found that the most energetically favourable orientation of the surface molecules will be that in which both positive vertices (the H atoms) are directed towards the interior of the liquid[6]. Because of hydrogen-bonding requirements, any preferential orientation of surface molecules will allow extension of the ice-like structure for some distance below the surface[7] and, as a result, the surface layer molecules will be, on the average, only second nearest neighbours and thus their energy of lateral interaction in the immediate surface zone can be relatively small. In addition, it should be noted that any breakdown of the surface layer structure (e.g. this possibility

could arise with adsorption) will also result in some structure-breaking in the water layers directly below the surface.

Any alignment of the dipoles of the solvent in the surface, like such effects at a gas-solid interface, sets up a surface potential, χ, across the surface phase. A dissolved substance which adsorbs at the surface and displaces previously oriented solvent molecules may change the dipole surface potential by an amount $\Delta\chi$. For adsorbed neutral molecules which replace adsorbed solvent

$$\Delta\chi = \frac{4\pi\bar{\mu}n}{\varepsilon} \qquad (1)$$

where n is the surface concentration of neutral molecules, μ is a complex function which depends on the molecular surface areas of solute and solvent as well as the usual factors of molecular orientation and dipole moments, and ε is the (usually unknown) effective dielectric constant of the surface layer. $\Delta\chi$ is a measure of the charge redistribution within the surface phase and this process can be due to at least one of three possibilities: a) unequal adsorption of ions of opposite charge; b) adsorption and orientation of dipolar molecules; and c) deformation of polarizable molecules in the force field of the interface.

The study of surfaces and interphases is very complicated and to some extent unsatisfactory when the distribution of charge is unknown or uncontrolled, as it is at the gas-solid interface. In the next section, it will be shown how some of these difficulties are substantially overcome when electrode interfaces are the subject of study.

1.2 ELECTRICAL 'CONTROL' OF ADSORPTION AT ELECTRODE INTERFACES

Although the potential drop across an electrode-solution interphase cannot be measured absolutely, its relative magnitude compared with that at the interphase of a reference electrode (the electrode and solution of which are kept at a constant equilibrium composition) can be determined.

By applying an e.m.f. across the working electrode (the one under study) and a third electrode (counter electrode), it is possible to control the potential of the former. Changes in the applied e.m.f. result in a change of potential at the working electrode, the magnitude of which is measured by a potentiometer in the reference electrode circuit. This system allows the redistribution of charge to be analysed. In cases where charge transfer across the interface is negligible, a complete, quantitative and thermodynamically unambiguous treatment of the adsorption of ions and molecules and their effect on the electrode surface charge can be made at fixed potentials. Conversely, at constant electrode charge, the adsorption of ions and molecules will affect the potential profile in the interphase. For neutral dipolar molecule adsorption, the redistribution of local charge will be greatest when the dipoles are perpendicular to the surface. In addition, the variation of the potential (E) with the surface concentration of adsorbate (Γ), at zero electrode surface charge (e.c.m.), gives an indication of the orientation of the dipoles. This can be seen from the equation

$$\Delta E_{q=0} = \frac{4\pi\mu}{\epsilon}\Gamma \qquad (2)$$

which is analogous to equation (1). Any non-linearity of the ΔE vs Γ relation could indicate that μ/ϵ is varying with Γ and that reorientation of the adsorbate and structural changes in the interphase

are taking place. However, equation (2) is too simple to allow an unambiguous interpretation to be made, i. e. equation (2) does not consider the solvent interactions and reorientations (see § 4. 3).

At high field strengths in the interphase, under conditions where orientation saturation occurs, the adsorbate molecules can be further polarized to an extent which is dependent on their polarizability.

1. 3 COMPETITIVE ADSORPTION AT SOLID-SOLUTION INTERFACES

Since investigations of the adsorption of non-electrolytes at solid surfaces have led to the recognition of the role of the solvent in the ad-layer, it is important to consider such results when attempting to interpret structural aspects of electrode-solution interphases. Normally it is not possible to study the adsorption of neutral molecules at electrodes by the techniques used at large surface area solid* -solution interfaces because of the difficulty in producing and maintaining equipotential surfaces. However, spectroscopic investigations of this type[8] have been successful although the useful potential range is in some cases rather limited.

The study of adsorption of non-electrolytes from solution at solids remained somewhat restricted until it was realised that solute and solvent are in many cases indistinguishable, and that the solvent is involved in the adsorption process. This indistinguishability is certainly true for systems where the two components are completely miscible but the term solute and solvent may retain some usefulness in systems where there is limited solubility. Further, it has recently been indicated that there may be a distinction between adsorption of 'solid' and 'liquid' solutes[9] (see below in the discussion on temperature effects).

---

*The term solid in this section has its usual meaning and will not necessarily include electrodes unless they are specifically mentioned.

Two concepts of adsorption have been applied to mixtures. 'Preferential' or 'selective' adsorption corresponds to the term surface excess (§1.4.1) which is a measure of the extent to which the bulk liquid is impoverished with respect to one component because the surface layer is correspondingly enriched. The second is 'absolute' adsorption which refers to the actual quantity of that component present in the adsorbed phase. It is a true surface concentration.

Since measurements are normally based on the decrease in bulk concentration of one component, preferential adsorption is the relevant representation. Although consideration of absolute adsorption would appear to lead to a better understanding of the adsorption process, arguments have been put forward to suggest that preferential adsorption is less unambiguous[10].

From experimental evidence, it is quite clear that at a liquid-solid interface the interaction of each component of the solution with the solid surface is important and to these factors may have to be added the lateral interactions between the two adsorbate components. It is evident that differences of adsorptive forces can be responsible for preferential adsorption. In general, the observed phenomena can be understood qualitatively in terms of varying degrees of polarity exhibited by the surface and the adsorbate.

In the absence of specific polar groups, the π-electrons of aromatic systems cause aromatic compounds to be adsorbed preferentially at polar solids with respect to corresponding aliphatic compounds of similar molecular weight studied at comparable solution concentrations[11]. This behaviour is in contrast with that at the liquid-vapour interface[12] where it has been shown that cyclohexane is preferentially adsorbed from the benzene-cyclohexane system. This indicates the importance of specificity of solid

adsorbate interactions. For the mercury electrode-methanol solution interface, this type of behaviour was also noted by Gerovich and Rybalchenko[13] who showed that the adsorption of non-polar organic compounds at large positive surface charges increased with the degree of unsaturation, particularly with delocalised systems.

Interactions in the bulk liquid are also an important factor in determining the adsorption behaviour. It has been found that on the homogeneous surface of "graphon", benzene is preferentially adsorbed from both methanol and n-butanol. This is obviously due in part to the nature of the interaction at the solid surface. The marked difference in degree of preferential adsorption between the two systems, however, suggests that another factor is important[16]. The n-butanol solvates the benzene more strongly and therefore reduced preferential adsorption is found. This is also thought to be the case at electrodes where cations are hydrated to a greater extent than anions and so the latter exhibit a greater adsorbability.

Adsorption by charcoal from a pyridine-water system[9(p. 55),17] shows that when one component is strongly adsorbed (in this case pyridine), and the second is weakly adsorbed, enhanced adsorption of the second component may result from its interaction by hydrogen-bonding with the component which is more strongly held by the surface. Behaviour of this type also arises at the mercury electrode-solution interface[15] where an aqueous 1M KCl solution shows negative adsorption of Cl^- at negative surface charges but positive adsorption in the presence of adsorbed pyridine, i.e. the adsorbed pyridine enhances the Cl^- ion surface concentration.

If a molecule is highly unsymmetrical, the orientation which it adopts may considerably alter the number of molecules which can occupy unit area of surface. For example, the molecule of stearic acid when adsorbed with its hydrocarbon chain along the

surface occupies approximately five times the area which is required when the chain is oriented perpendicular to the surface. It adopts the latter configuration only when the surface is polar. Since, in some cases, it is difficult to determine exactly how much of a given component is present in the adsorbed phase, its orientation in that phase cannot be determined directly. In contrast to these circumstances, orientations of dipolar molecules at the mercury-solution interface can be indicated semiquantitatively by observing the effect of the adsorbate on the electrode potential of the mercury at constant surface charge (usually taken as zero at the e.c.m.), as discussed in § 1.2. This is the basis of the Esin and Markov effect examined in more detail in section 4.3 with respect to results obtained in the present work.

For adsorption from completely miscible liquids, selectivity generally decreases with rise in temperature[9, (p. 60)]. With decreasing temperature, multilayer adsorption is likely to occur as the critical solution temperature is approached[9, (pp. 77-80)]. However, in some systems, it has been shown that multilayer adsorption of one component occurs (incipient phase separation) if it is adsorbed below its melting point. The adsorption at electrodes of solutes in the vicinity of their melting points has not been investigated as a function of temperature; however, a study of multilayer formation on the mercury electrode has been made by Frumkin et al.[73].

1.4 THE IDEAL POLARIZED ELECTRODE

Thermodynamic analysis of electrode-electrolyte interfaces is considerably simplified in the absence of electrode reactions[61]. When charge-transfer reactions at an electrode are negligible the electrode is said to be ideally polarised, and applied potentials only serve to redistribute the charge within the interphase and charge the metal surface. The most important example of an ideally polarisable interface is the mercury electrode in aqueous solution which acts as an ideally polarised electrode because of the high overvoltage for hydrogen evolution, i.e. charge transfer across the double-layer proceeds at negligible rates except at the highest cathodic potentials. The range of potentials that can be covered with other metals is somewhat narrower than that for mercury but can be extended when non-aqueous solutions are used.

1.4.1 The Gibbs Adsorption Equation

The most accurate and complete procedures for studying electrochemical adsorption at electrode interfaces are (a) the electrocapillary method (§ 3.1) which is based on the measurement of the dependence of surface tension of a liquid metal such as mercury on potential[28] and adsorbate concentration; and (b) the capacity method where the electrode double-layer capacity is directly measured by means of an a.c. impedance method or by transients.

The starting point for the derivation of the electrocapillary equation is the Gibbs adsorption equation for the interface,

$$-d\gamma = \sigma dT + \sum_i \Gamma_i d\bar{\mu}_i + \sum_n \Gamma_n d\mu_n + q_M dE \qquad (3)$$

In this equation, γ is the interfacial tension, σ the superficial density of excess entropy, μ's and $\bar{\mu}$'s are the chemical potentials of the neutral components and the electrochemical potentials of the charged components of the bulk solution, respectively; q_M is the surface charge density on the electrode metal and the Γ terms are the surface excesses of the indicated components. The Γ terms have the significance of relative surface excesses of the respective components and represent the differences between the amounts of substances per unit area of interface up to some dividing plane (determined by the condition Γ(solvent) = 0) parallel to the surface when adsorption has occurred and the amount that would be present if the solution composition were homogeneous up to the metal surface. For pure mercury, all $\Gamma d\mu$ terms associated with the metal phase will be zero and therefore need not be incorporated in equation (3).

From the Gibbs adsorption equation, relations can be obtained which give the extensive variable in terms of variation of the corresponding intensive quantities under conditions where all other variables, except the one concerned, are maintained constant. Thus:

$$-\left(\frac{\partial \gamma}{\partial T}\right)_{\mu_i, \mu_n, E} = \sigma \qquad (4)$$

$$-\left(\frac{\partial \gamma}{\partial \mu_i}\right)_{\mu_n, E, T} = \Gamma_i \qquad (5)$$

$$-\left(\frac{\partial \gamma}{\partial \mu_n}\right)_{\mu_i, E, T} = \Gamma_n \qquad (6)$$

$$-\left(\frac{\partial \gamma}{\partial E}\right)_{T, \mu_i, \mu_n} = q_M \qquad (7)$$

The plot of γ vs E is known as the electrocapillary curve and at its maximum (e.c.m.) q_M is zero and the corresponding potential is E_z the potential of zero charge (p.z.c.).

The surface pressure ϕ_E at constant E is defined by the equation

$$\phi_E = \gamma_b - \gamma \tag{8}$$

where the subscript "b" refers to the solution in the absence of adsorbate. Thus ϕ_E can replace $-\gamma$ in the partial differential equations above since γ_b is constant and independent of μ. An alternative procedure[20] is to define a parameter,

$$\xi = \gamma + q_M E \tag{9}$$

so that, at constant charge, the surface pressure becomes

$$\phi_q = \xi_b - \xi$$

$$= (\gamma_b - \gamma) + q_M(E_b - E) \tag{10}$$

Using this definition of surface pressure results in a set of equations similar to (4), (5) and (6).

Much discussion has been recorded on the choice of the electrical variable in electrochemical adsorption studies. Ideally, experimental conditions in the investigations of isotherms should be selected for which the 'electrical part' of the free energy of adsorption is kept constant.

Damaskin[21] recommended the use of the potential as was initially stated by Frumkin[22]. However, Grahame[23] pointed out that ϕ_1 (see § 1.4.2 (i)) contained a component arising from the particle-particle interactions in the ad-layer. This meant that constancy of ϕ_1 did not ensure constancy of particle-electrode

interactions. In addition, there is the added uncertainty that the potential across the diffuse-layer also may not remain constant.

As a result of these difficulties, Parsons[20] suggested that under conditions of constant charge, electrode-particle interactions are maintained almost constant. Under constant total metal-solution p. d., however, the components of potential drops in the overall interphasial potential differences, may vary with composition of the double-layer and the contribution from the excess charge on the metal may not be constant. Under the condition of constant q_M, the latter difficulty is absent. Parsons added later[26] that these interactions might still vary somewhat, even at constant charge, as a result of a variation of the dielectric constant in the inner layer with the amount of adsorbed substance. However, in the plots of ϕ_E vs E and ϕ_q vs q_M for the adsorption of n-butanol from the supporting electrolyte solutions of KF and KCl, Parsons showed that the curves had essentially the same shape (independent of the nature of the anions) when q_M was chosen as the variable and the maxima occurred at a constant value of q_M ($-2\ \mu$ coulomb cm^{-2}). On the other hand, the ϕ_E vs E curves had a shape dependent on the concentration of specifically adsorbed Cl^- ion. Recently, further studies[25] have shown that the dependence of the free energy of adsorption (obtained from isotherms) on the electrical variable is approximately quadratic, but the dependence is more accurately quadratic if charge rather than potential is used as the variable.

Finally the Gibbs adsorption equation does not lead to a definite adsorption isotherm from which the thermodynamic quantities ΔG°, ΔS°, and ΔH° for the adsorption process can be obtained. It is necessary to resort to other equilibrium thermodynamic equations (isotherms) which involve assumptions concerning the equation of state of adsorbed material or assumptions concerning the details of molecular interactions in the interphase (see § 1.5).

A critical analysis of the Gibbs description of adsorption has been presented recently by Flood[19] and, with regard to recent work, the application of the Gibbs adsorption equation to electrode studies has been most fully expounded by Mohilner[27].

1.4.2 Structure of the Surface Phase

The Gibbs thermodynamic analysis of the surface phase yields the relative surface excesses, but cannot, without some model, give information about the structure in terms e.g. of ion distribution and orientation of molecules.

1.4.2 (i) The Distribution of Ions in the Surface Phase

The early model of Helmholtz[28], applied to colloids, pictured the double-layer of charges (on the surface and in the solution) as a "fixed layer" and hence equivalent electrically to a parallel plate capacitor. Gouy[29] and Chapman[30] pointed out that the Helmholtz model neglected the disordering effect of the thermal energy which causes the ions to be distributed in a way analogous to that in the Deby-Hückel ionic atmosphere around a single ion. The third development of the model was due to Stern[31] who took into account (a) the possibility that the ions may have finite sizes and approach the electrode only to within a certain critical distance and (b) that chemisorption effects could be significant. Grahame[32] showed that the distance of closest approach was different for anions and cations and this extension led to the following qualitative picture of the electrical double layer at a metal/electrolyte interface:

a) The metallic phase at potential ϕ_M, in general, bears a net electrical charge q_M which has been shown (§ 1.4.1) to have a well-defined thermodynamic significance and can be measured absolutely.

b) An inner layer exists adjacent to the metal surface which can contain 'specifically' adsorbed ions, the electrical centres of which lie on a locus called the inner Helmholtz plane (I. H. P.) at potential ϕ_1. This layer also contains oriented solvent dipoles and any adsorbed neutral solute molecules from the bulk solution. The total charge residing in this plane is written as q_-^1 where the superscript and subscript indicate association with the I. H. P. and negative anion charge, respectively. When the solvation energy of the ions is large they will tend not to be specifically adsorbed and their centres will be at their distance of closest approach in a layer known as the outer Helmholtz plane (O. H. P.) at which the potential is ϕ_2 (ψ_1 in the earlier Russian literature).

c) The diffuse layer or ionic atmosphere conjugate to the charged interface is bounded by the O. H. P. and extends into the bulk of the solution; it contains non-specifically adsorbed ions which are held by coulombic forces.

The positive and negative charges in the diffuse layer (from ϕ_2 to ϕ_S) are given by

$$q_{\pm}^{2-s} = \pm \left(\frac{RT\varepsilon C}{2\pi}\right)^{1/2} \left(\exp\left[\frac{-z_{\pm}F\phi_2}{2RT}\right] - 1\right) \qquad (11)$$

where C is the bulk concentration. In general, the following equation will hold

$$-q_M = q_S = q_+^{2-s} + (q_-^{2-s} + q_-^1) \qquad (12)$$

$$= z_+ \Gamma_+ F + z_- \Gamma_- F$$

where q_S is the total charge in the double layer, $-q_M$ that on the metal and Γ_+, and Γ_- are the experimentally determinable components of adsorbed ionic charge, expressed as surface excesses.

The development of this model was due to the progressive understanding of the interfacial tension and capacitance data for the electrode-electrolyte interphase. The capacitance (C) of the double layer arises from the fact that charges of equal and opposite sign reside on opposite sides of the interface across which transfer of charge is negligible. The variation of the charge with potential gives a differential capacitance. q_M and C are related mathematically by

$$q_M = \int_{E_{e.c.m.}}^{E} C\,dE \qquad (13)$$

and also, in relation to the surface tension, by

$$\gamma = \gamma_{e.c.m.} - \iint_{E_{e.c.m.}}^{E} C\,dE^2 \qquad (14)$$

Grahame's model and its mathematical treatment[32] has received wide acceptance and can be found more fully discussed in the original papers and in standard reviews and texts[33, 34].

1.4.2 (ii) Further Modifications to the Theory of the Structure of the Double Layer

The preceding theory neglects the role played by the solvent in the adsorption process and was developed specifically to account for the ionic distribution in the interphase. It is of considerable importance, however, to investigate also the adsorption of neutral molecules in order to obtain from the adsorption phenomena evidence of orientation, distortion and solvation effects; these, in the main, will arise in the surface monolayer (dipole-charge interactions having much shorter range than charge-charge interactions).

(a) Frumkin's Theory[22]

Frumkin's quantitative theory of adsorption of neutral molecules from solution was the earliest treatment. It related the change of free energy of the double-layer to changes of capacity at constant potential upon substitution of the adsorbate for the solvent and ions. The principal equation can be written

$$\Delta\bar{G}^{o} = \Delta G^{o} + \frac{1}{2}(C - C')\,\phi_M^2 + \left(\frac{\mu}{\ell} - \frac{\mu'}{\ell'}\right)\phi_M \qquad (15)$$

where the superscript "prime" indicates the condition of saturation of the electrode surface by the adsorbate and the absence of the superscript denotes the absence of the adsorbate. C is the double-layer capacity of an element of unit area; ℓ is the theoretical distance between the plates of the 'capacitor', and μ is the dipole moment of the solvent or solute adsorbate perpendicular to the interface. ϕ_M is equated to the rational potential $(E - E_z)$.

The second term on the right-hand-side of equation (15) accounts for the variation of energy of the interphase due to the decrease in its dielectric constant and the increase in effective "plate separation" when the adsorbate is introduced. The third term is associated with the change in effective total dipole moment of the species in the interphase due to the adsorption process and consequent replacement of solvent dipoles.

According to equation (15), there is a maximum in the adsorption when

$$\phi_M = \phi_{M,max} = -\frac{\mu/\ell - \mu'/\ell'}{C - C'} \qquad (16)$$

and the corresponding $\Delta\bar{G}^{o}$ is

$$\Delta\bar{G}^{o}_{max} = \Delta G^{o} - \frac{(\mu/\ell - \mu'/\ell')^2}{2(C - C')} \qquad (17)$$

Equation (15) can now be rewritten

$$\Delta\bar{G}^{o} = \Delta\bar{G}^{o}_{max} + \frac{1}{2}(C - C')(\phi_M - \phi_{M,max})^2 \qquad (18)$$

Thus ΔG^{o} is obtained as a function of directly measurable quantities. As shown by Parsons[35], equation (15) can be transposed so that charge is the electrical variable:

$$\Delta\bar{G}^{o} = \Delta\bar{G}^{o}_{max} + \frac{1}{2}\left(\frac{1}{C'} - \frac{1}{C}\right)(q_M - q_{M,max})^2 \qquad (19)$$

where

$$q_{M,max} = -\frac{4\pi(\mu/\epsilon - \mu'/\epsilon')}{1/C' - 1/C} \qquad (20)$$

and

$$\Delta\bar{G}^{o}_{max} = \Delta G^{o} - \frac{[4\pi(\mu/\epsilon - \mu'/\epsilon')]^2}{2(1/C' - 1/C)} \qquad (21)$$

This model then has been based on the macroscopic concept of dielectric energies and thus lacks a molecular character.

(b) Butler's Theory[37]

Whereas in Frumkin's theory use is made of macroscopic concepts as a basis for the calculation of the potential dependence of the free energy of adsorption, in Butler's theory this quantity is expressed in terms of molecular properties; in this respect, it is similar to his theory of salting-out of non-electrolytes by the field of ions in solution. Butler calculated the electrical part of $\Delta\bar{G}^{o}$ from the work done when an element of volume V of solvent S is replaced by the same volume of adsorbate A. Thus

$$\Delta\bar{G}^{o} = \Delta G^{o} + [\tfrac{1}{2}(\alpha_A - \alpha_S)X^2 + (P_A - P_S)X]V \qquad (22)$$

where α is the polarisability, P the permanent polarisation per unit volume and X the field strength. Equation (22) can be treated in the same way as equation (15). However, the field strength is not directly measurable and it is therefore necessary to express X in terms of $(\phi_M - \phi_{M,max})$ or $(q_M - q_{M,max})$ but this transformation involves further assumptions. Bockris et al.[38] raised the following two objections to this theory.

(i) bulk dielectric constants of solvent and adsorbate were used to calculate their polarisabilities at the interface whereas Conway[39] has shown that dielectric saturation effects occur in the double layer causing a decrease in the dielectric constant.

(ii) the assumption that the orientation of dipoles does not change with the potential is questionable. This latter objection, although widely held, does not appear to be founded on decisive experimental evidence. It is however, theoretically justified[40].

The Inner Layer Capacitance

From the description of potentials given in § 1.4.2 (i), it is seen that the total (Galvani or absolute) potential drop from metal to bulk solution is given by

$$\phi_M - \phi_S = (\phi_M - \phi_2) + \phi_2 = \phi_M \qquad (23)$$

when $\phi_S = 0$ is taken as a reference state.

Then

$$\frac{\partial \phi_M}{\partial q_M} = \frac{\partial (\phi_M - \phi_2)}{\partial q_M} + \frac{\partial \phi_2}{\partial q_M} \qquad (24)$$

or

$$1/C = 1/C_{M-2} + 1/C_{2-S} \qquad (25)$$

where the subscripts M, 2 and S have the usual association with the metal phase, the O. H. P. and the bulk solution, respectively, i.e. C is the total differential double-layer capacity which is a series combination of the inner and diffuse layer capacities as shown in equation (25). The last term is computed from the Gouy-Chapman theory by differentiating equation (11) with respect to ϕ_2, while C is measured experimentally. This then allows C_{M-2} to be evaluated. In the absence of specific adsorption, C_{M-2} (or $\partial q_M / \partial(\phi_M - \phi_2)$) was found to vary quite markedly with q_M and temperature, and a molecular model which would satisfactorily explain this behaviour would necessarily involve the physical and chemical nature of the adsorbed layer of solvent. C_{M-2} showed the following behaviour: (a) an increase with positive charge; (b) an increase for large negative charges; (c) a hump which in aqueous solutions occurs at about +2 μcoulomb. $cm.^{-2}$ and which disappears at higher temperatures; (d) absence of the hump in methanolic solutions and (e) displacement of the hump to very negative charges for formamide and N-methyl formamide solvents. Bockris et al.[40] have listed a number of other critical facts which arise when specific adsorption is involved.

(c) Theory of McDonald and Barlow[41]

This theory was developed to explain the experimental measurements of Grahame for NaF in water at $0^{\circ}C$ to $85^{\circ}C$ and KF in methanol at $25^{\circ}C$ and is a modified version of an earlier treatment[42]. Since the univalent electrolytes were assumed to be unadsorbed, the inner layer was considered charge-free and thus

$$- q_M = q_+^{2-s} + q_-^{2-s} \qquad (26)$$

McDonald and Barlow considered the inner layer to be an hexagonally close-packed monomolecular layer. All dipole orientations were assumed possible and the dielectric 'constant' was regarded as dependent on the orientation distribution of the dipoles; this contribution to the dielectric constant thus tends towards zero at sufficiently high fields (X). This assumption of non-aligned dipoles in the surface layer at the e.c.m. (also taken to be the case in (d) and (c)) is in complete contrast with the observations at liquid surfaces and gas-solid interfaces (§§ 1.1.1, 1.1.2) where there is some intrinsic orientation. This choice was made to account for the decrease in C_{M-2} at certain cathodic potentials where dielectric saturation was said to occur.

The theoretical formulation of C_{M-2} from a molecular model was made in the following way. X, the field strength, is related to the potential drop across the inner layer by the relationship

$$\phi_M - \phi_2 = X.d \qquad (27)$$

where d is the thickness of the layer and equals d_o when X = 0. A normalized thickness t is then defined by

$$t = d/d_o \qquad (28)$$

and thus the inner layer capacitance is

$$C_{M-2} = dq_M/d(\phi_M - \phi_2) = (dq_M/dX)(dX/d(\phi_M-\phi_2)) \qquad (29)$$

It should be pointed out that $d(\phi_M-\phi_2) \neq dX$ (see equation (27)) since d is also a variable and so dq_M/dX involves the differential dielectric constant. It then becomes possible to obtain

$$C_{M-2} = (\frac{1}{d_o})(dq_M/dX) + [1 + \frac{d(\ln t)}{d(\ln X)}]^{-1} \qquad (30)$$

and it was noted that dq_M/dX and t both depend on X when the layer exhibits dielectric saturation and compression.

The theory explains some aspects of the behaviour of C_{M-2} referred to above by considering the effects of electrostriction (which is the change in volume occurring in a dielectric fluid subjected to an electric field), and compression of the uncharged layer which arises from the pressure exerted by the attraction of the two oppositely charged regions on either side of the inner layer.

(d) The Theory of Mott and Watts-Tobin[43, 44]

In an approach similar to that of McDonald and Barlow, Watts-Tobin and Mott[43, 44] attempted to interpret theoretically the measured capacitance of the mercury-electrolyte double layer. The model differed from the others discussed in this section (§1.4.2) in that they suggested: (a) that mercury atoms could be pulled out of the surface by the electric field to form ad-atoms; (b) that the adsorbed water was oriented so that there were always three of its "bond-forming" directions pointing towards the metal, and (c) that adsorption of hydroxyl ions gave rise to an increasing capacity at markedly positive surface charge densities. Later Austin and Parsons[45] disproved suggestion (c) by showing from capacity measurements that C_{M-2} was not affected by the pH of the solution.

Nancollas et al.[108] extended the theory of Watts-Tobin to account for non-equivalent orientations of the solvent molecules and found that the predictions made from the modified theory were in close agreement with the experimental results.

(e) The Theory of Bockris, Devanathan and Muller[40] (B. D. M.)

These authors investigated theoretically the effects of charge on the inner layer capacitance in the presence and absence of adsorbed ionic and neutral aliphatic molecules. The investigation was therefore more comprehensive than those of (c) and (d), more sophisticated than that in (b) and more descriptive as a molecular model than that in (a).

As this thesis is concerned mainly with neutral organic molecule adsorption, this aspect of the B. D. M. model will be summarised here. The essential empirical facts of neutral aliphatic molecule adsorption that Bockris et al. considered necessary to explain were:

(i) that the relation between coverage Θ and electrode charge q_M are parabolic and symmetrical on the charge scale;

(ii) that the Θ - q_M relation is dependent on the nature of the organic molecules (this was implicit in Frumkin's model);

(iii) that coverage passes through a maximum in the range of q_M -2 to -3 μ coulomb. cm.$^{-2}$.

The model was not intended to be applicable to aromatic molecules since no account was to be taken of π-bond formation.

Since the orientation of the aliphatic molecules at the interface would affect the energy of interaction, a molecular description of this phenomenon was necessary in the development of this model. It was suggested that the hydrocarbon group pointed towards the metal, a conclusion which was supported by the following evidence.

a) There is a close relationship between the free energies of solution and of adsorption of several classes of organic molecules, i. e. the adsorption is strongly influenced by interactions between the polar group and the solvent.

b) The orientation taken up by the molecule was that which leads to the most favourable free energy of adsorption (calculations were made from molecular models).

c) The shift of the p. z. c. upon the addition of aliphatic substances to solution is in the positive direction for all species studied although these included molecules with dipole moments greater than that of

water. Were the organic polar groups in contact with the mercury, the shift of the p. z. c. would have depended on the group.

In the model, the solvent molecules are regarded as being distributed between two states of orientation in which the dipoles are aligned either with or against the field, i. e. in opposite directions. The populations of the dipoles in 'up' and 'down' states, $N_\uparrow$ and $N_\downarrow$ are dependent on the field and the mutual lateral interactions between the oriented dipoles (attractive when two dipoles are aligned in opposite directions, repulsive when they are aligned in the same direction).

As in the Langmuir isotherm (kinetic derivation), the equilibrium between water adsorbed on the electrode in an 'up' (or 'down') position, and that in solution is given by

$$k_w C_w (1 - \Theta_\uparrow - \Theta_\downarrow) = k_\uparrow \Theta_\uparrow \tag{31}$$

$$k_w C_w (1 - \Theta_\uparrow - \Theta_\downarrow) = k_\downarrow \Theta_\downarrow \tag{32}$$

where k's are rate constants for adsorption and C_w is the concentration of water in the bulk solution. From equations (31) and (32)

$$\Theta_\uparrow / \Theta_\downarrow = e^{2x} \tag{33}$$

where kTx is the sum of the energies of the dipole arising from orientation in the field and from the mutual interaction. Then

$$\frac{\Theta_\uparrow - \Theta_\downarrow}{\Theta_\downarrow + \Theta_\uparrow} = \tanh x$$

$$= \frac{N_\uparrow - N_\downarrow}{N_\uparrow + N_\downarrow} = \frac{N_\uparrow - N_\downarrow}{N_T} \tag{34}$$

where N_T is the total number of solvent molecules. The energy of the 'up' water is

$$kTx = \mu X + E.c \frac{N_{\downarrow}}{N} - E.c. \frac{N_{\uparrow}}{N.} \qquad (35)$$

$$= -(\text{energy for the 'down' water})$$

where c is the effective coordination number, E is the lateral interaction energy between a pair of adjacent dipoles and X (the field strength) is given by

$$X = -4\pi q_M/\varepsilon \qquad (36)$$

Hence, from equations (34) and (35),

$$\frac{N_{\uparrow} - N_{\downarrow}}{N_T} = \tanh\left[-\frac{E.c}{kT} \frac{(N_{\uparrow} - N_{\downarrow})}{N_T} + \frac{\mu X}{kT}\right] \qquad (37)$$

$$= R \text{ , a factor characterising the distribution.}$$

Now the average water molecule has an electrical component of energy on the surface of

$$\Delta G_{\phi} = \frac{N_{\uparrow}}{N_T} \left(\mu X + \frac{N_{\downarrow}}{N_T} E.c - \frac{N_{\uparrow}}{N_T} E.c\right)$$

$$- \frac{N_{\downarrow}}{N_T} \left(\mu X + \frac{N_{\downarrow}}{N_T} E.c - \frac{N_{\uparrow}}{N_T} E.c\right)$$

$$= \frac{N_{\uparrow} - N_{\downarrow}}{N_T} \left[\mu X - \frac{(N_{\uparrow} - N_{\downarrow})}{N_T} E.c\right]$$

$$= R[\mu X - R\, E.c] \qquad (38)$$

Now assuming that this is the only lateral interaction term in the surface phase, the isotherm for the adsorption process becomes

$$\frac{\Theta_{org}}{1 - \Theta_{org}} = \frac{C_{org}}{C_w} \exp\left[\frac{-\Delta G^o_{ads}}{RT}\right] . \exp\left[nR\left(\frac{\mu X}{kT} - R \frac{E.c}{kT}\right)\right] \qquad (39)$$

where ΔG^o_{ads} refers to the difference between electrode-water and electrode-solute interactions and n is the number of water molecules displaced by a solute molecule at the surface.

Qualitative agreement with experiment for the relation between surface coverage and surface charge is obtained even though solute-solute and solute-solvent interactions in the inner layer are not considered. Frumkin[46(p.168)] has criticised this model on the grounds that: (a) the distortion polarisability of the water molecule is omitted in the free energy calculations where only orientation polarisation is considered; (b) the increase in the electrical energy of the double-layer due to the substitution of water for organic substance at constant charge is not allowed for and (c) since the organic molecules will have their polar groups outside the inner layer, no effect on the potential distribution should be found. Criticism (c) in the present author's opinion, is not completely valid since non-polar groups in the inner layer would change its dielectric constant and displace polar solvent molecules (see equation (1)). An experiment concerning this point is reported in a later section of this thesis (§4.6). It has also been shown that the p. z. c. in the case of amyl alcohol adsorption was dependent on the coverage[47].

The theory also assumes the Langmuir isotherm to be applicable for the adsorption from solution, an assumption which has not been completely justified. Delahay[34(p. 73)] has made a critical and thorough assessment of theories (c), (d) and (e).

(f) Theory of Hills and Payne[58]

Hills and Payne measured the temperature and pressure coefficients of the integral capacity (K) of the mercury-aqueous solution (0.1 N NaF) double layer, where the inner layer is charge free, and found a minimum in $(\partial K/\partial T)_q$ at ca. -2 μ coulomb. cm.$^{-2}$ and a maximum in $(\partial K/\partial P)_q$ at ca. -8 μ coulomb cm.$^{-2}$. In the interpretation of their results the diffuse layer contribution was neglected so that $dK = dK^i$ where the superscript i signifies that the quantity refers to the inner Helmholtz layer. Then

$$K^i = \varepsilon^i/4\pi x_2$$

where x_2 is the distance of the O. H. P. from the surface. The coefficients described therefore represent the temperature and pressure dependence of the ratio ε^i/x_2.

From the variations of the surface excess volume $(\partial\gamma/\partial P)_{q_M}$ and surface excess entropy $(-\partial\gamma/\partial T)_{q_M}$ as functions of the electrode charge density, Hills and Payne concluded that the number of water molecules in the ad-layer is variable. The authors, however, retained the idea put forward in the theories previously discussed in this section, that orientation and polarisation of the ad-water occurs, but argued that these considerations were not the only factors affecting the inner layer capacity.

In this, as in the B. D. M. model, a plane of water molecules is considered to lie between the metal and the solvated fluoride ions but as the concentration of water in this layer decreases, the solvated ions can move closer to the electrode taking up 'interstitial' positions in the ad-layer. With increasing positive polarisation, the surface water concentration increases because of the interaction of the solvent dipoles with the field and the specific interactions of

the oxygen atoms with the mercury. This model has been extended to the systems in which the anion is specifically adsorbed.

In conclusion, it is apparent that unlike the treatment for the diffuse layer, the description of the inner layer is by no means complete. The inner layer capacitance seems to have some dependence on the adsorbed ions but is also very dependent upon the solvent. This latter point is clearly illustrated by the work of Randles and White[48] who showed that there was a capacitance hump in aqueous nitrate solutions at all concentrations but not for the pure salts when molten.

1.5 ADSORPTION ISOTHERMS

The electrolyte-solution interphases are always at least two component systems, so that mixed or "competitive" adsorption must be considered if the most realistic treatment (cf. § 1.3) is to be made. However, much work has been done on the basis of models in which the solvent is considered as a continuum. It follows, on the basis of such a model, that the replacement of part of the adsorbed solvent by a more strongly adsorbed species leaves the remaining part of the adsorbed solvent in an unperturbed state. Such a picture of the solvent in the ad-layer is certainly an over-simplication, if not an inaccurate representation of the real situation.

An adsorption isotherm describes the variation, at constant temperature and electrode charge (or, less preferably, at constant potential) (see § 1.4.1) of the surface concentration with the bulk activity.

In most cases treated in this thesis, it was found that the difference in magnitude between the relative surface excess and the surface concentration, calculated on the basis of a 6 Å surface layer thickness, was negligible.

When there is equilibrium of a species between the adsorbed state and the bulk of the solution at an ideal polarised electrode, the corresponding electrochemical potentials are equal. Thus

$$(\bar{\mu}^{o} + RT \ln [f(\Gamma)]_{ads} = (\bar{\mu}^{o} + RT \ln C)_{bulk}$$

where $f(\Gamma)$ is a function of the surface concentration and $\bar{\mu}^{o}$ can formally be replaced by μ^{o} for neutral substances. This equation or isotherm can be rewritten as

$$f(\Gamma) = C. \exp[-\Delta\bar{G}^{o}/RT] \qquad (40)$$

where

$$\Delta\bar{G}^{o} = \bar{\mu}^{o}_{ads} - \bar{\mu}^{o}_{bulk}$$

is the standard free energy of adsorption.

Now Γ is related to the surface pressure ϕ through a two-dimensional equation of state ($\phi = F(\Gamma)$) the choice of which will be dependent on the adsorption conditions and the nature of the interactions, etc. From the equation of state the isotherm is derived, using the thermodynamic differential equation

$$d(\bar{G}_{ads}) = A\, d\phi \qquad (41)$$

where $A (=1/\Gamma)$ is the area available per adsorbate molecule in the interphase, i.e. the surface dilution.

For example, the Volmer equation of state (see eqn. (63)) is

$$\Gamma = \frac{\phi}{RT + b\phi} \qquad (42)$$

Then, using eqn. (41) and integrating,

$$\bar{G}_{ads} = \int \frac{RT + b\phi}{\phi}\, d\phi = b\phi + RT \ln \phi + K \qquad (43)$$

and K can be equated with $\bar{G}^{o}_{ads}$

Also

$$\bar{G}_{bulk} = \bar{G}^{o}_{bulk} + RT \ln C \qquad (44)$$

At equilibrium $\Delta\bar{G} = \bar{G}_{ads} - \bar{G}_{bulk} = 0$

$$\text{i.e. } \bar{G}^{o}_{bulk} - \bar{G}^{o}_{ads} = \Delta\bar{G}^{o}$$

$$= RT \ln C - b\emptyset - RT \ln \emptyset$$

$$\text{i.e. } C.\exp[-\Delta\bar{G}^{o}/RT] = \emptyset.\exp[b\emptyset/RT] \qquad (45)$$

Substitution from equation (63) can allow the relation (45) to be expressed in a form containing Γ's instead of $\emptyset$'s corresponding to the adsorption "isotherm". The most common adsorption isotherms encountered in the study of electrochemical adsorption have been listed by Parsons[49] (see also ref's. 27, 34). The simplest of these is based on Henry's Law in which the adsorbate is treated as a two-dimensional ideal gas in which the surface concentration is taken as proportional to bulk concentration - hence the term "Henry's Law". This isotherm can be modified in a number of ways to take into account non-ideality and so there arises the virial, Volmer and the Helfand, Frisch and Lebowitz types of isotherms[26]. In a similar

way, the Langmuir isotherm which, for adsorption from liquid phases, is based on substitutional adsorption of equal sized particles[36], can be modified to allow for (a) the difference in size of solute and solvent molecules (Flory-Huggins isotherm) and (b) particle-particle interactions or heterogeneity of the surface (Frumkin isotherm).

A suitable choice of isotherm for representation or treatment of a particular set of results can sometimes be made by considering the variation of the free energy of adsorption with surface coverage which results when the data are analysed initially in terms of an isotherm, e.g. the Langmuir, which neglects particle-particle interactions. For example, the analysis of experimental results for adsorption in terms of deviations from a Henry's Law or a Langmuir type isotherm can lead to variations of the apparent free energy of adsorption which change linearly with coverage if either the "virial" or the Frumkin type isotherm (in its original form[62, 22]) is really applicable. Similarly, the correctness of the form of the configuration term $\Theta/1 - \Theta$ can also be tested; e.g. it may require revision in terms of the relative area ratio for adsorbate and solvent referred to above (see also Chapter V).

1.6 SOME ASPECTS OF ADSORPTION IN RELATION TO ELECTRODE KINETICS

Under the influence of the well-established ideas of reaction orders in chemical kinetics, Vetter[53, 54], Conway and Salomon[55] and Conway, Rudd and Gordon[74] examined the question of reaction orders in the kinetics of electrode processes. The difficulty met with in the study of electrochemical reactions involving ionic species is that the local ion concentration and potential profile in the double-layer must be considered. For non-specifically adsorbed ions in dilute solutions, the appropriate double-layer concentration

effects are easily calculated as treated by Frumkin[73]. For reactions of neutral organic substances, ionic double layer effects can be avoided by working in excess electrolyte of constant concentration and only changing the concentration of the organic reactant. The reaction orders (R) then depend only on (a) the reaction mechanism, (b) the type of isotherm for the adsorption of the neutral reactant, and (c) the degree of reactant coverage Θ and the corresponding equilibrium bulk concentration C involved in any particular steady-state rate. Since both the rate and coverage depend on the electrode potential, R values must usually be considered with respect to potential. If the current density i is a linear function of Θ^n the reaction order is

$$R = \left(\frac{d \ln i}{d \ln C}\right)_v = \left(\frac{d \ln i}{d \ln \Theta}\right)_v \cdot \left(\frac{d \ln \Theta}{d \ln C}\right)_v \qquad (46)$$

The first term of the product is n, the true surface reaction order, while the second term must be derived from the reactant isotherm, $\Theta = f(C)$ or $\ln \Theta = f(\ln C)$ by differentiation. The surface reaction order, n, significant for the kinetics of the interfacial reaction and thus expressed in terms of Θ or Γ is obviously $(d \ln i/d \ln \Theta)_V$. The experimentally accessible quantity in direct kinetic measurement is $(d \ln i/d \ln C)_V$.

At solid electrode surfaces where the reaction is activation-controlled, the adsorbate coverage can influence the kinetics of the reaction in two ways[59].

(1) The rate will increase with the surface concentration of the electroactive species (as seen in equation (46)), for positive reaction orders.

(2) The increase in surface coverage increases the adsorbate-adsorbate interaction energy which, in conjunction with any heterogeneity effects, will affect the free energy of adsorption with a consequent effect on the rate constant.

CHAPTER II

AIMS OF THE WORK

In recent previous studies on the electrochemical adsorption of neutral molecules at the mercury electrode-aqueous solution interface the results have been interpreted in terms of orientation and interaction effects of the adsorbed solute. These effects were discussed in terms of Esin-Markov plots and in regard to the relationship between the free energy of adsorption and coverage. It was found convenient to evaluate the apparent standard free energy of adsorption ($\Delta\bar{G}^{o}$) in an isotherm of the type

$$\ln F(\Gamma) = -\frac{\Delta\bar{G}^{o}}{RT} + \ln C \qquad (47)$$

(where $F(\Gamma)$ is a function of Γ defined in § 1.5) and then to examine the form of the dependence of $\Delta\bar{G}^{o}$ on Γ and the surface charge. The analysis enables details of the orientation and interaction effects to be examined since the surface charge density, which is a basic factor in determining the adsorption phenomena under discussion, could be fixed at any magnitude in the range of potentials investigated (cf. § 1.1.1).

In the present work it was considered desirable to examine further some of the following aspects of the adsorption of neutral molecules at the mercury electrode-solution interface, with particular reference to enthalpy and entropy components of the free energy of adsorption.

a) Since the free energy of adsorption evaluated from the experimental observations is dependent on the choice of $F(\Gamma)$ employed in the analysis of the results, it was first necessary to consider the

suitability and limitations of the chosen function. ($F(\Gamma)$ is defined in § 1.5). For example, it is desirable to examine the significance of electrochemical adsorption results in terms of several isotherms, comparatively. Thus the Langmuir, Frumkin type and the Volmer isotherms and equations of state were applied in the present work.

b) The adsorption of neutral molecules at electrode surfaces is always accompanied by desorption of solvent molecules. Solvent displacement should therefore play an important role in the adsorption process, and thus it must be accounted for in the change of free energy of such a process. The ratio of the molecular area of the solute to that of the solvent must also be considered in the substitutional adsorption process. It was felt desirable to consider this question in some detail.

c) The role of the solvent implied in (b) above indicated that special attention should be focussed on the structure of the surface phase, e.g. by examining the entropy of adsorption of pyridine from aqueous $NaClO_4$ solutions as a function of surface charge density under isosteric conditions. Experimentally, this can be achieved by determining the free energies of electrochemical adsorption over a range of temperatures, electrode potentials and bulk concentrations. Such experiments also allow the evaluation of heats of adsorption which can be interpreted in terms of interaction effects and solvent structure in the interphase. Electrostatic calculations of the energy of polarisation of pyridine (dipole-field and electronic polarisation energy) at various fields, in comparison with that for 2 or 3 water molecules which it would replace, it was felt should be considered in the interpretations of the experimental results.

d) The type of solvent used in any investigation of adsorption at a mercury electrode-solution interface can influence the adsorption

equilibrium because of the interactions (attractive or repulsive) of the solvent with the solute in the ad-layer and in relation to its solvating properties in the bulk phase (see § 1.3). It therefore seemed important to make comparisons between the properties of an adsorbate, adsorbed from different solvents, taking into account either the different solvation energies of the solute in the bulk phases, or considering only those measurable quantities which apply to the surface phase such as charge density, surface pressure, potential and surface concentration.

A study was therefore made of the effect of varying the solvent on the adsorption of acetophenone. The solvents were: (i) pure methanol, (ii) 1:4 mole ratio water + methanol and (iii) 1:4 mole ratio water + methanol in which the concentration of acetophenone-pinacol was 0.1 M.

e) The three solvent systems employed in (d) above were chosen primarily to provide, for the first time, information necessary to establish the detailed relationship between the adsorption behaviour of acetophenone and the kinetics of its electrochemical reduction through evaluation of true surface orders of reaction. (The kinetic behaviour of the reaction concerned is the subject of another thesis from this Department and will therefore be referred to only briefly in the present thesis but the adsorption behaviour will be described in some detail.).

f) The evaluation of thermodynamic quantities for adsorption at the mercury electrode by means of electrocapillary measurements demands the execution of a large number of measurements both at closely spaced intervals of potential and with a variety of solution concentrations if satisfactory accuracy in the derived thermodynamic quantities is to be obtained. An important aim of the experimental part of the work was therefore to develop improved techniques for capillary electrometry which both increase the accuracy and facilitate the measurements (§ 3.1).

CHAPTER III

EXPERIMENTAL

3.1 IMPROVED ELECTROCAPILLARY TECHNIQUES

For studies of equilibrium electrochemical adsorption at mercury by surface tension measurements, the use of the Lippmann electrometer is preferable to the use of drop-weight techniques, particularly when slow adsorption processes, e.g., in the case of organic adsorbates, are involved. Recently the sessile drop method has also been used but it is unsuitable for experiments that require many points to be determined over a range of potentials and concentrations. The technique of capillary electrometer measurements hitherto developed, normally involves, however, rather tedious observations of (a) the position of a fine thread of mercury in a capillary as it is brought to a fiducial mark (e.g., cross-wires in a viewing microscope) near the end of the capillary, and (b) the height of mercury in a manometer when the mercury in the capillary has been brought to the fiducial mark. The latter measurement must usually be made with an accuracy of 0.003 cm. using a cathetometer. A new technique has been devised which materially simplifies both these measurements and eliminates some of the tedium attached to these two aspects of the determination of an electrocapillary curve which, for proper definition, requires some thirty points to be determined for any given temperature and concentration of adsorbate and electrolyte, if precise data on the thermodynamics of adsorption are to be deduced.

3.1.1 Resistance Indicator for Location of the Mercury Meniscus[121]

A new approach, based on the measurement of the resistance of the column of supporting electrolyte solution below the descending column of mercury in the capillary, has been developed successfully.

The lower meniscus of a column of mercury supported in the fine capillary is adjusted in the usual way[70, 66, 75] to a fiducial position (see below) by means of pressure from a gas line containing a reservoir bulb and communicating to the upper meniscus of the column of mercury (Figure 1) and to one side of a 1-in. diameter U-tube manometer. Fine adjustment is made according to the procedure of Parsons and Joshi[75] by manipulating a screw-operated copper bellows connected by glass-metal seals to the gas line. In the optical measurements which were carried out as a control procedure to test the reliability of the new method, the position of the mercury thread in the capillary was viewed by means of a binocular stereo-zoom microscope (5-50 x magnification). Such a microscope has a good depth of focus and the mercury thread can be easily seen.

The circuit shown in Figure 2 was set up and comprises the usual d. c. polarisation arrangement using helipot potential dividers (or a potentiostat) and a Radiometer pH-millivoltmeter for measurement of the potential of the mercury electrode with respect to that of a standard reference electrode in a third compartment of the cell. The circuit differs from those conventionally used in previous work by inclusion of a shielded 1:4 transformer (T_2) (of the type used for conductance bridges) through which a low level a. c. signal, of amplitude ΔV, can be injected from an oscillator (O) (Figure 2) into the d. c. polarising circuit between the counter-electrode and the capillary electrode (W) of mercury. The alternating current passing in the capillary electrode part of the circuit will be

Figure 1

Schematic diagram of apparatus. (E), electrode connections; (E'), electrical contacts; (W), water jacket; (Ma), manometer; (Bm), binocular microscope; (C), capillary (see inset); (L), lamp; (B), bellows; (R_2), bulb; (R_1), reservoir.

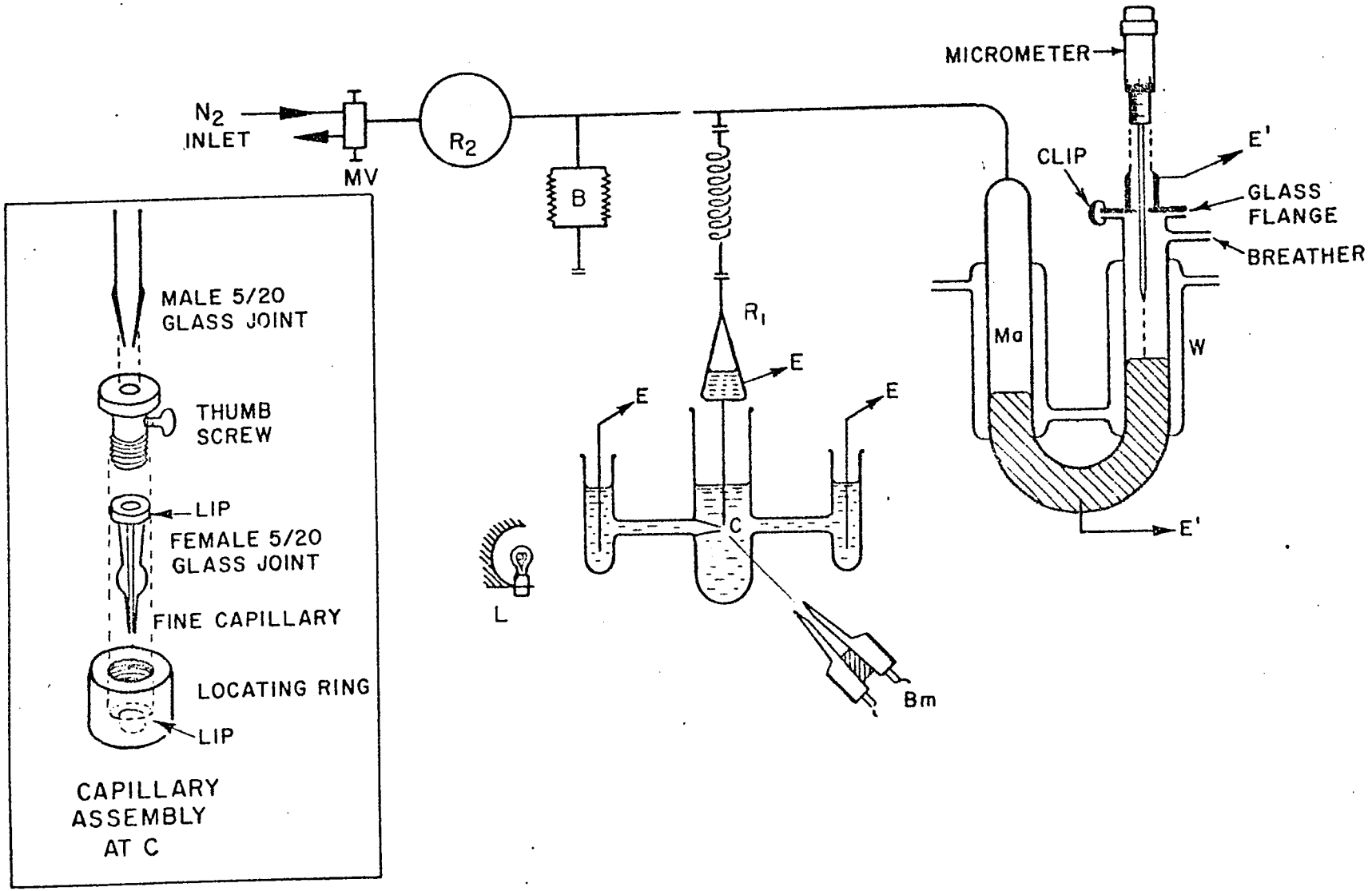
MICROMETER
N_2 INLET
MV
R_2
B
R_1
E
E
E
E'
CLIP
GLASS FLANGE
BREATHER
Ma
W
E'
C
L
Bm
MALE 5/20 GLASS JOINT
THUMB SCREW
LIP
FEMALE 5/20 GLASS JOINT
FINE CAPILLARY
LOCATING RING
LIP
CAPILLARY ASSEMBLY AT C

Figure 2

Electrical circuit for indication of the position of the mercury meniscus in the capillary. (W), Working electrode - Hg capillary; (R), reference electrode, 0.1N calomel; (C) counter electrode, 0.1N calomel or Pt; (X), tuned amplifier and Null detector, General Radio Co., Type 1232-A, Ser. No. 1281; (Y), Radiometer, Type PHM_4C No. 46833, Copenhagen; (O), wide band oscillator, Model 200CD, Tektronix; (T_1), transformer, Gen. Rad. Co., Type 578-B (step-down); (L_1), large inductance (35 H) or a.c. filter; (L_2), two variable inductances (I H) in series, Gen. Rad. Co., Type 107N, Ser. No. 9463; (R_1), helipot (20 Ω).

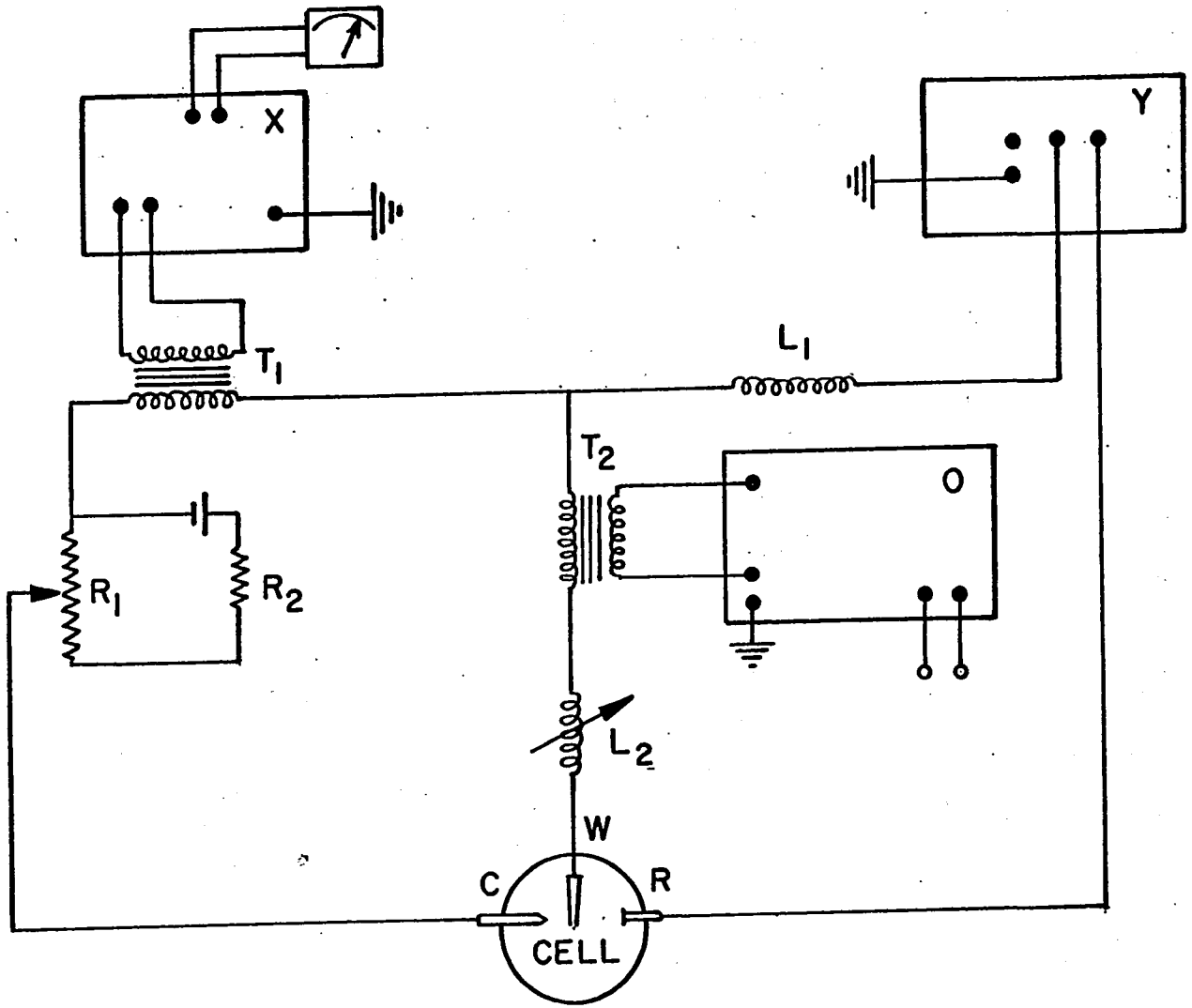
X
Y
T_1
L_1
T_2
O
R_1
R_2
L_2
W
C
R
CELL

determined mainly by the impedance, Z, offered to the current by the very thin column of electrolyte solution* (ohmic resistance, R) below the mercury meniscus in the capillary, in combination with the double-layer capacitance of the very small area of the meniscus in the capillary. These impedance contributions may be written Z_R (for the electrolyte column) and Z_c for the double-layer and are obviously in a series relation. Under "ideal polarisation"[76] conditions, any reaction resistance impedance contribution at the interface is infinite and being in parallel with the double-layer capacitance will not influence Z. For a given double-layer capacitance, the position of the mercury in the capillary will directly determine Z_R (=R), and hence the alternating current flowing in the circuit, since other resistances in the circuit are orders of magnitude smaller. Since the alternating current, i, and the resistance, R (proportional to the length of electrolyte column below the mercury meniscus), are hyperbolically related, viz.

$$iR = V_{a.c.} \qquad (48)$$

where $V_{a.c.}$ is the constant a.c. potential operating, the detection of the current flowing for a given $V_{a.c.}$ provides a very sensitive method for following the position of the mercury thread, since as the latter approaches the end of the capillary, the current i rapidly rises reciprocally in R. The results shown in Figure 3 demonstrate the reciprocal relation between i and R except very near the end of the capillary where R becomes so small that C presumably determines the impedance appreciably, and end-effects become significant.

---

* Direct measurement of the resistance of this column of electrolyte by means of an impedance or Wheatstone bridge is not possible owing to the low resistance solution paths which are provided in parallel through the reference and counter electrodes when the electrocapillary measurements are in progress.

Figure 3

Test of linearity of resistance response in relation to a. c. passing in detector circuit.

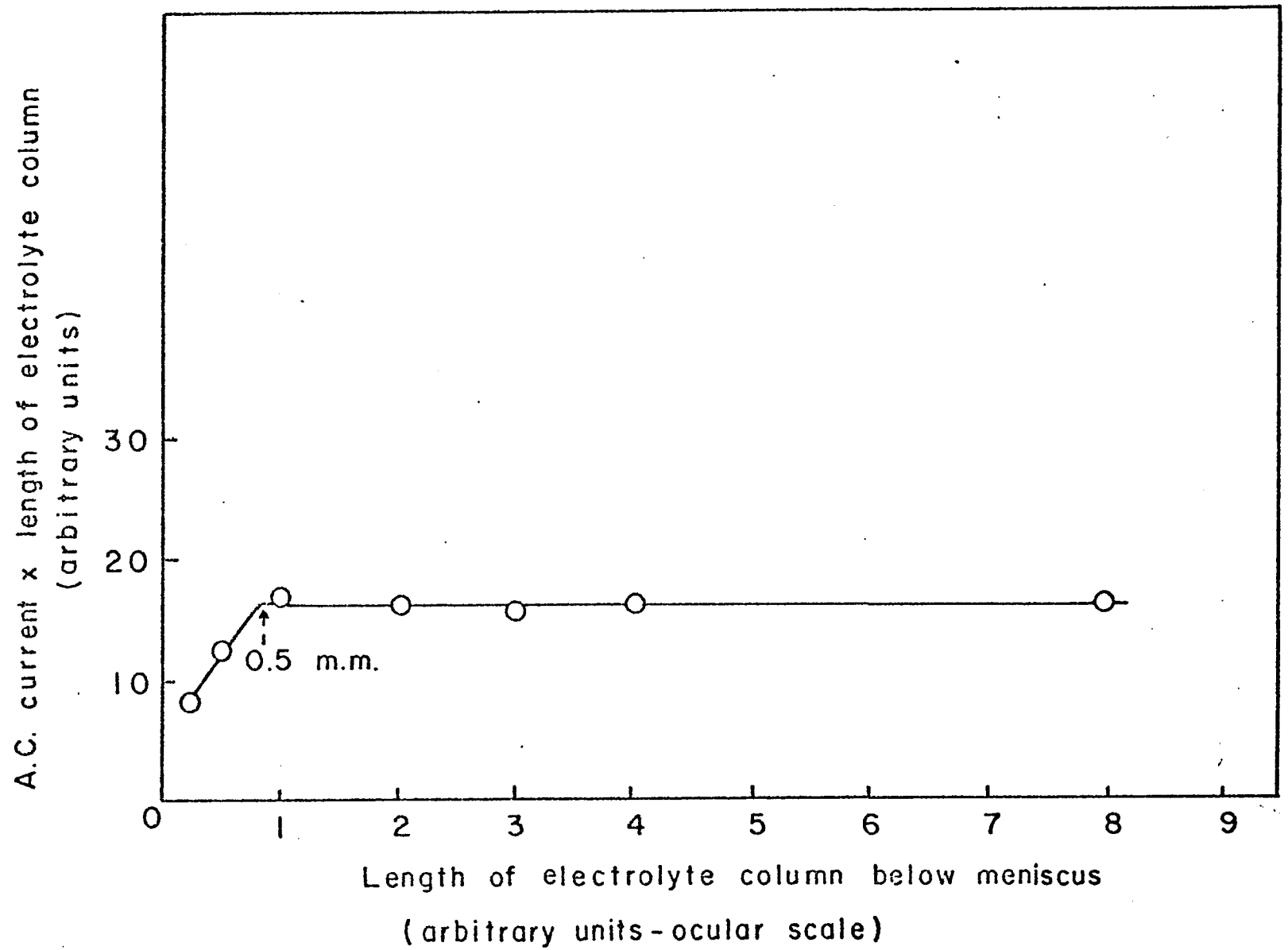
A.C. current x length of electrolyte column
(arbitrary units)
30
20
10
0
0.5 m.m.
1
2
3
4
5
6
7
8
9
Length of electrolyte column below meniscus
(arbitrary units - ocular scale)

The alternating current flowing in the polarisation circuit is passed through another step-down transformer, T_1, and the current in the secondary of this transformer is fed to a tuned General Radio Null Detector X operating on the same frequency as the input a.c. The rectified current displayed by means of a micro-ammeter is a function of the distance that the mercury thread has advanced down the capillary. For a given a.c. input voltage, the deflection can, with suitable adjustments (see below), be reproducibly and precisely related to the position of the mercury meniscus.

Since the resistance of each solution used in a series of runs varies from run to run, a single optical "calibration" must be made once for each electrocapillary curve by noting the meter deflection when the mercury meniscus, for the given solution, is brought to the same fiducial mark (as determined by optical viewing). The fiducial mark itself can be taken as one "optical scale division" in a ruled ocular above a ruling adjusted to be coincident with the bottom of the capillary.

Introduction of the small a.c. voltage in the working electrode circuit had no detectable effect on the level of the meniscus at a given d.c. polarisation potential.

(a) Capacitance effects

For a given d.c. voltage level at the mercury meniscus, microscopic changes of position of the mercury thread could be made to correspond to large (up to 30% full-scale) deflections at the detector meter. In test runs with 1 N aq. KCl, however, changes of d.c. polarisation potential produced a small but significant difference of the meter deflection for the same absolute position of the mercury in the capillary (determined by the conventional optical viewing method). Since the effect was dependent on the a.c. frequency, it was considered likely that the normal changes which the double-layer

capacity undergoes with potential were responsible for causing significant changes of impedance of the column of electrolyte in series combination with the interfacial double-layer capacitance, C, at the meniscus. The impedance offered by the transformers is also frequency-dependent. Since Z is determined by

$$Z = (R^2 + Z_c^2)^{1/2}, \tag{49}$$

and Z_c evidently causes in part the variation of Z with frequency and d.c. polarisation potential, an attempt was made to eliminate the latter effects by introduction of a variable inductance L_2 (0-1 H) in series with the capillary electrode so that the resulting impedance of the circuit would be

$$Z = (R^2 + (Z_c - Z_L)^2)^{1/2} \tag{50}$$

where L in Z_L is the total inductance of the a.c. circuit including any contributions from the transformers, and the current in the detector at any position of the mercury meniscus and any d.c. potential could be maximized (Z minimized) by adjustment of L_2. The variable inductance, L_2, then compensates for variations of Z_c, through changes of C with potential. In practice, L_2 is chosen sufficiently large that the variation of Z with d.c. potential (with the meniscus at a given position) is made negligible. This approach gave a very satisfactory solution to the problem that the meter needle deflection, as a function of position of the meniscus, was affected by the d.c. potential of the electrode. The second fixed inductance, L_1, screens the potentiometer, Y, from any residual a.c. signal from W through R (Figure 2).

(b) Frequency effects

The circuit designed had an impedance which varied with a. c. frequency, as mentioned above, presumably due to the presence of the inductance and transformers in series with the double-layer capacity of the mercury meniscus and the resistance of the electrolyte column. The frequency chosen (7-8 kHz) for the measurements was that for which the circuit was observed to have maximum admittance and the resulting sensitivity for the location of the meniscus was highest. All measurements were in fact made at 7 kHz after optimization of conditions had been achieved.

(c) Results obtained by the new procedure

Some typical results for surface tension measurements in 0.001 N and 0.002 N aq. KCl are shown in Figure 4, together with results for a solution of an organic electrolyte, N-methyl-pyridinium iodide. The central solid dots represent the measurements obtained by the conventional optical procedure while the circular points around the dots represent measurements on the same solution at the same potentials carried out by means of the new electrical method; they are indistinguishable. Since the differences are not sufficiently large to be represented on the usual scale of graphs for surface tension, or corresponding excess pressure as a function of electrode potential, a special plot of these differences, ΔP in pressure (determined by cathetometry) and $\Delta\gamma$ in surface tension, is shown in Figure 5 for various solutions and electrode potentials. The differences, ΔP, in Figure 5 correspond to mean $\Delta\gamma$ of only 0.03 dyn cm.$^{-1}$, which is well within the accuracy of conventional previous techniques.

3.1.2 Closed-circuit Television Technique[113]

A further modification which has been developed in the present work employs a small television camera which views the meniscus down one lens of a binocular zoom stereo-microscope and

Figure 4

Comparison of electrocapillary curves determined for aq. KCl soln. and N-methylpyridinium iodide by the electrical (O) and optical detection (•) procedures. (1) 0.001N aq. KCl; (2) 0.002N aq. KCl; (3) 0.01N aq. KCl + 0.1N N-methylpyridinium iodide.

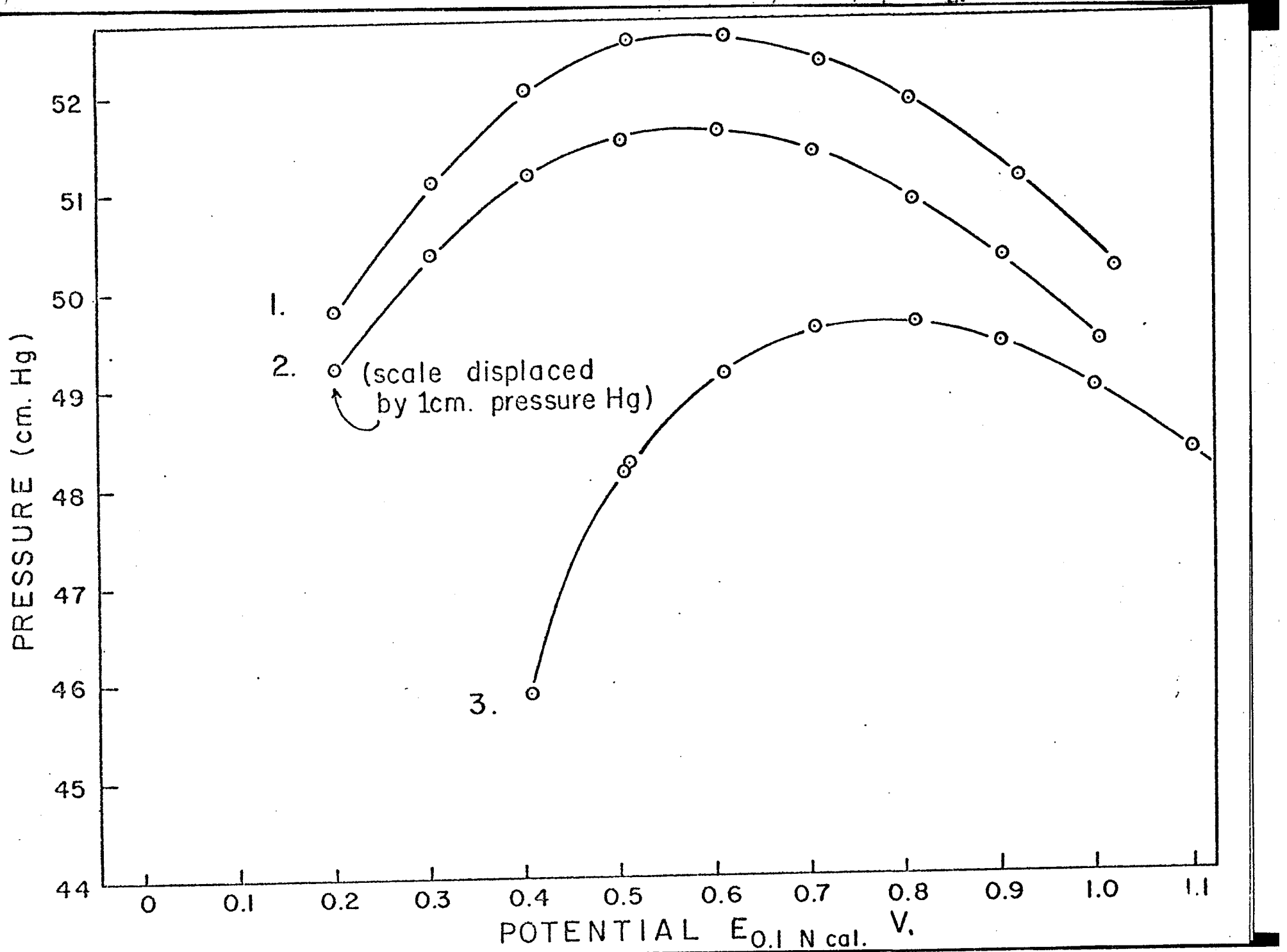
PRESSURE (cm. Hg)
52
51
50
49
48
47
46
45
44
1.
2.
(scale displaced
by 1cm. pressure Hg)
3.
0
0.1
0.2
0.3
0.4
0.5
0.6
0.7
0.8
0.9
1.0
1.1
POTENTIAL $E_{0.1\ N\ cal.}$ V.

Figure 5

Large-scale representation of differences, ΔP of the excess pressure, and $\Delta \gamma$ of surface tension, for various electrocapillary measurements determined by the optical and electrical methods as a function of electrode potential and for various solns. (P-values by cathetometry). (1) (Δ), 0.005N KCl; (2), (O), 0.01N KCl; (3) (X), 0.01N KCl + 0.1N N-methylpyridinium iodide; (4) (□), 0.1N KCl.

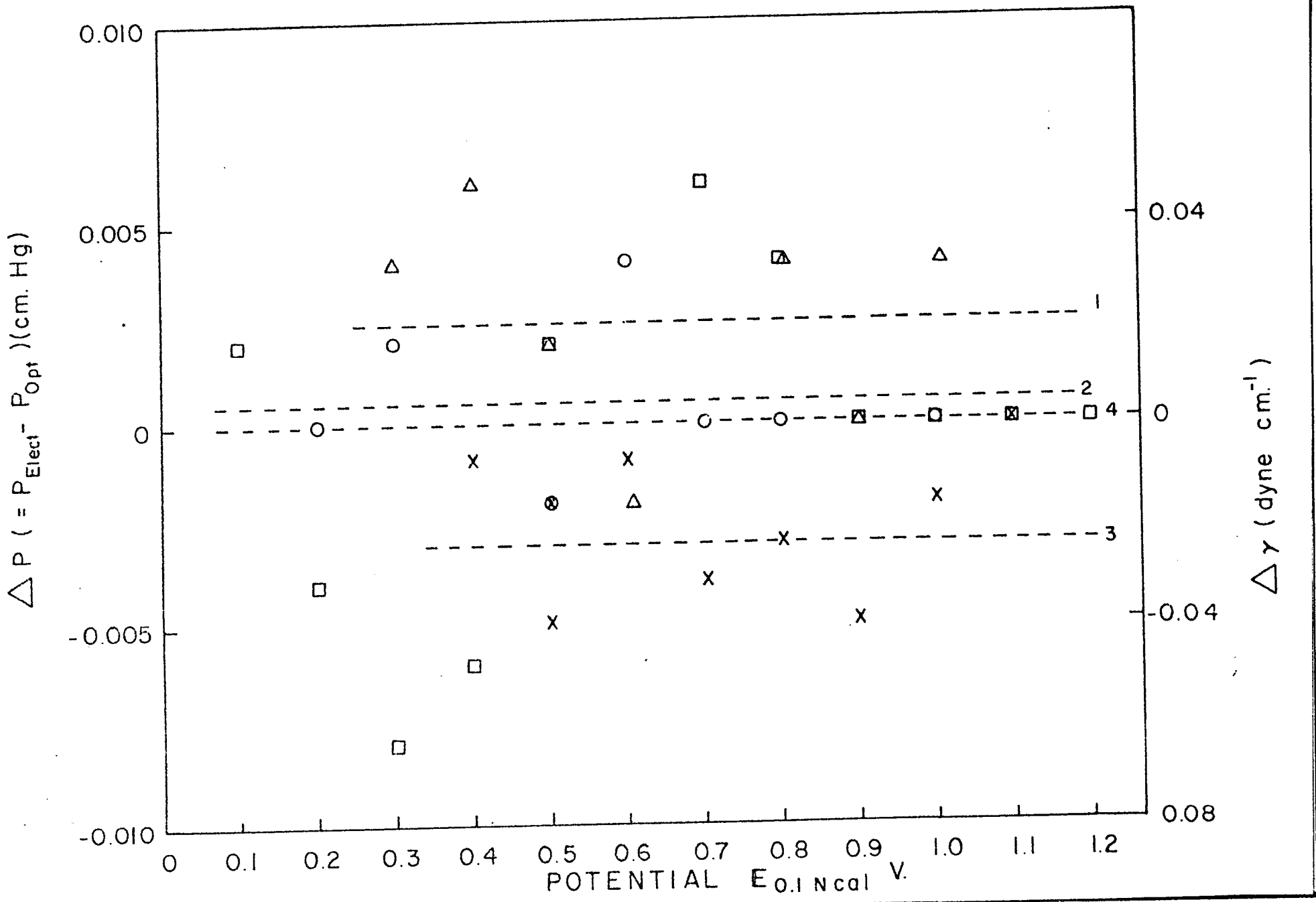
0.010
0.005
0
-0.005
-0.010
0
0.1
0.2
0.3
0.4
0.5
0.6
0.7
0.8
0.9
1.0
1.1
1.2
POTENTIAL $E_{0.1\,N\,cal}$ V.
ΔP (= P_{Elect} - P_{Opt})(cm. Hg)
$\Delta \gamma$ (dyne cm^{-1})
0.04
0
-0.04
0.08
1
2
3
4

communicates the scanned image to a 15" t.v. monitor screen. The second lens of the binocular microscope can be conveniently used to line up the optics of the system. The general layout of the apparatus is shown in Figure 6.

The capillary and mercury thread are illuminated from the side by means of a microscope lamp and adjustable mirrors, and optimally the thread can be made to appear as a clear dark line on a bright background. (See Figure 7, upper photograph). A fiducial mark or scale can be fixed on the outside of the monitor screen to provide a reference point for the lowest level to which the mercury is brought in each measurement (Figure 7, lower photograph). The magnification is such that the full width of a very thin capillary appears as a 25 cm. image on the screen and the mercury thread itself is seen as an image approximately 1 cm. wide. The thread can therefore be very precisely and conveniently positioned at the fiducial mark in each measurement with very little strain on the operator and the convenience of the procedure is incomparably superior to that of direct microscopic observations by eye.

A final convenient feature that can be added for semi-automatic operation (cf. [70]) is a micro-photoelectric cell affixed to the front of the screen at the position where the image of the thread is focussed. The local change of intensity of the light from the fluorescent screen is sufficient to give an on/off signal for termination of the excess pressure adjustment by means of metal bellows [75] and hence provides a basis for a self-regulating method.

3.1.3 Excess Pressure Measurements

The second important improvement introduced in the measurement technique was development of a direct reading micrometer-manometer. A U-tube manometer, with 1-in. diameter columns of mercury on each side, was provided with thermostat water jackets, W, on each side and a 2 1/2 in. glass flange (Figure 1)

Figure 6

Schematic drawing of T. V. microscope and illumination arrangement for electrocapillary measurements by the method of determining excess pressures.

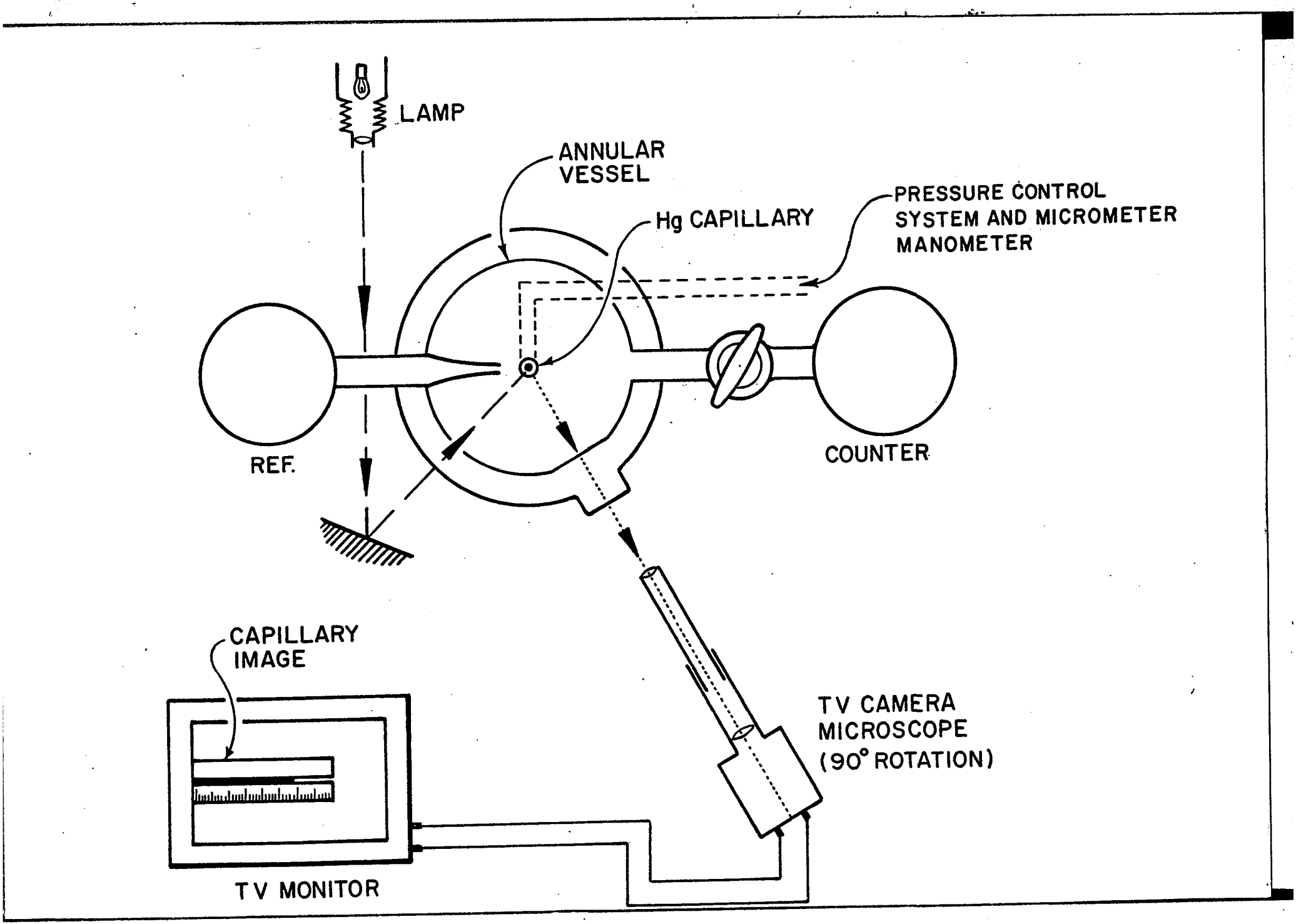
LAMP
ANNULAR VESSEL
Hg CAPILLARY
PRESSURE CONTROL SYSTEM AND MICROMETER MANOMETER
REF.
COUNTER
CAPILLARY IMAGE
TV CAMERA MICROSCOPE (90° ROTATION)
TV MONITOR

Figure 7

Photos of the magnified capillary and mercury thread on the T. V. monitor. Lower photo shows thread approaching fiducial position adjusted with respect to bottom of capillary image.

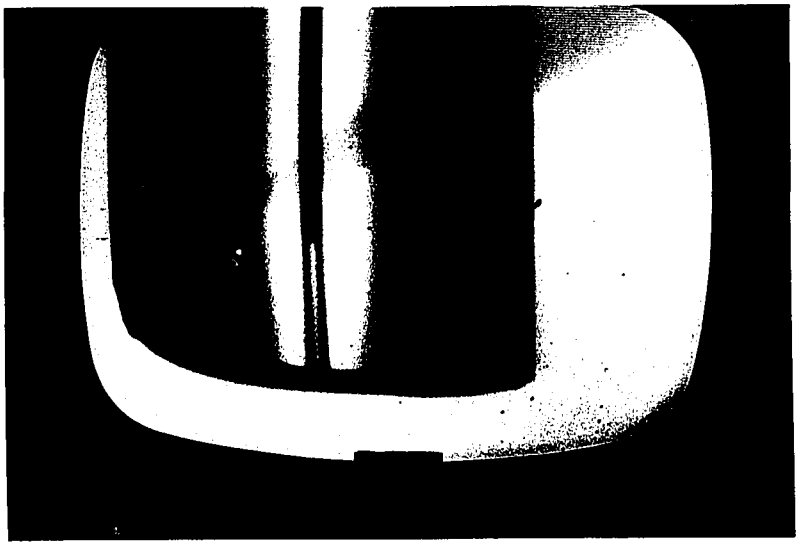

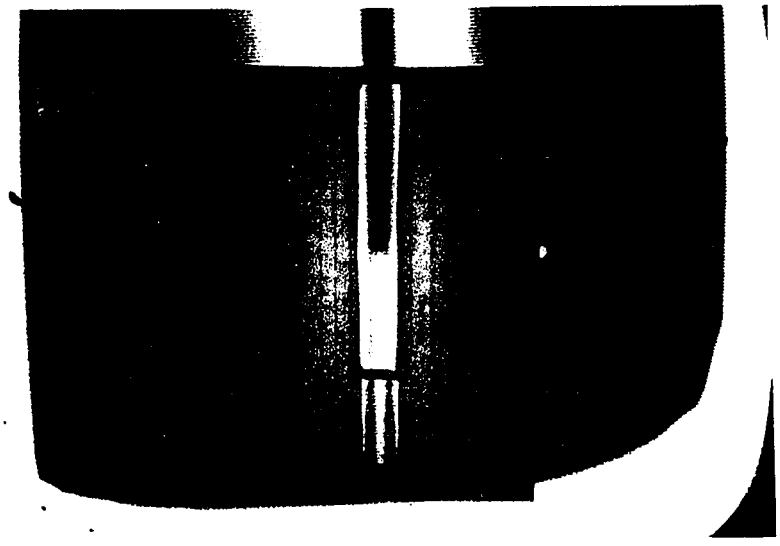

at one of the ends. The other side of the manometer was connected in the usual manner to the gas pressure and metal bellows assembly, and to the upper end of the capillary electrode by means of a flange seal joined to a glass-metal seal. The flange, G, was connected with metal clamps to a brass head in which was fixed a single-ended micrometer capable of measuring a displacement of 0.001 cm., with a 5-cm. traverse. This allowed total pressure changes of up to 10 cm. to be measured in the U-manometer from a previously fixed level. The shaft of the micrometer was securely connected to a 1/4-in. diameter stainless steel rod machined to a sharp 60°-bevel at the end. Adjustment of the micrometer allowed the point of the bevel to be brought into contact with the mercury meniscus in the manometer tube, a condition which could be exactly indicated by completion of an electrical circuit through the mercury, the micrometer and its shaft, and a 1.2-V battery operating through a 100-kΩ resistance. Contact was shown by the sudden deflection of a microammeter included in this circuit.

Since the micrometric pressure measurements are made with reference to only one side ot the manometer, it is important to have the manometer tubes of exactly the same diameter and of uniform bore. This was tested by making initial cathetometer measurements on both sides, together with the micrometer measurements, and showing that the mean of the heights on each side was equal (within 0.003 cm.) to the stationary level when no excess pressure was applied.

The combination of the direct reading manometer (the difference of levels of the upper and lower menisci of mercury in the capillary electrode must be separately measured but does not change significantly during the course of measurements on a single electrocapillary curve if a suitable mercury reservoir is used) and the mercury meniscus position detector, enables electrocapillary

measurements to be carried out with much greater facility than is possible with the usual techniques. Coupling of the micrometer with a 100-turn helipot or stepping motor would allow the possibility of direct recording of the excess pressure, through a divided reference voltage or digital recording arrangement.

The reproducibilities of the excess pressure measurements determined by cathetometry and by the micrometer method are compared in Figure 8. It is seen that use of the micrometer method improves reproducibility of ΔP substantially, and this is an important factor in the improvement of the overall reproducibility of the $\Delta \gamma$-measurements.

3.1.4 Capillary Design

In order to facilitate interchange of capillaries when necessary, a modification to the conventional arrangement was made. The capillary was constructed from a short piece of glass which could be attached to the main column and reservoir by means of a glass joint. The latter was held in position as shown in the inset in Figure 1 by means of a Teflon sleeve and collar provided with a screw thread to maintain a tight seal.

The upper end of the capillary assembly was provided with a 50-ml reservoir for mercury in the form of a small conical flask sealed to the column tube below, and to a flange above, through a glass-metal seal. The whole column tube and reservoir could be raised or lowered in the cell through a sliding glass sleeve constructed of ground "Tru-bore" tubing. An optimum level for optical viewing through a plane glass plate window in the cell could therefore be chosen by appropriate adjustments.

Figure 8

Reproducibility of excess pressure measurements by optical cathetometry and by direct micrometer measurements. Various symbols represent values of ΔP obtained for several settings of Hg level by three observers.

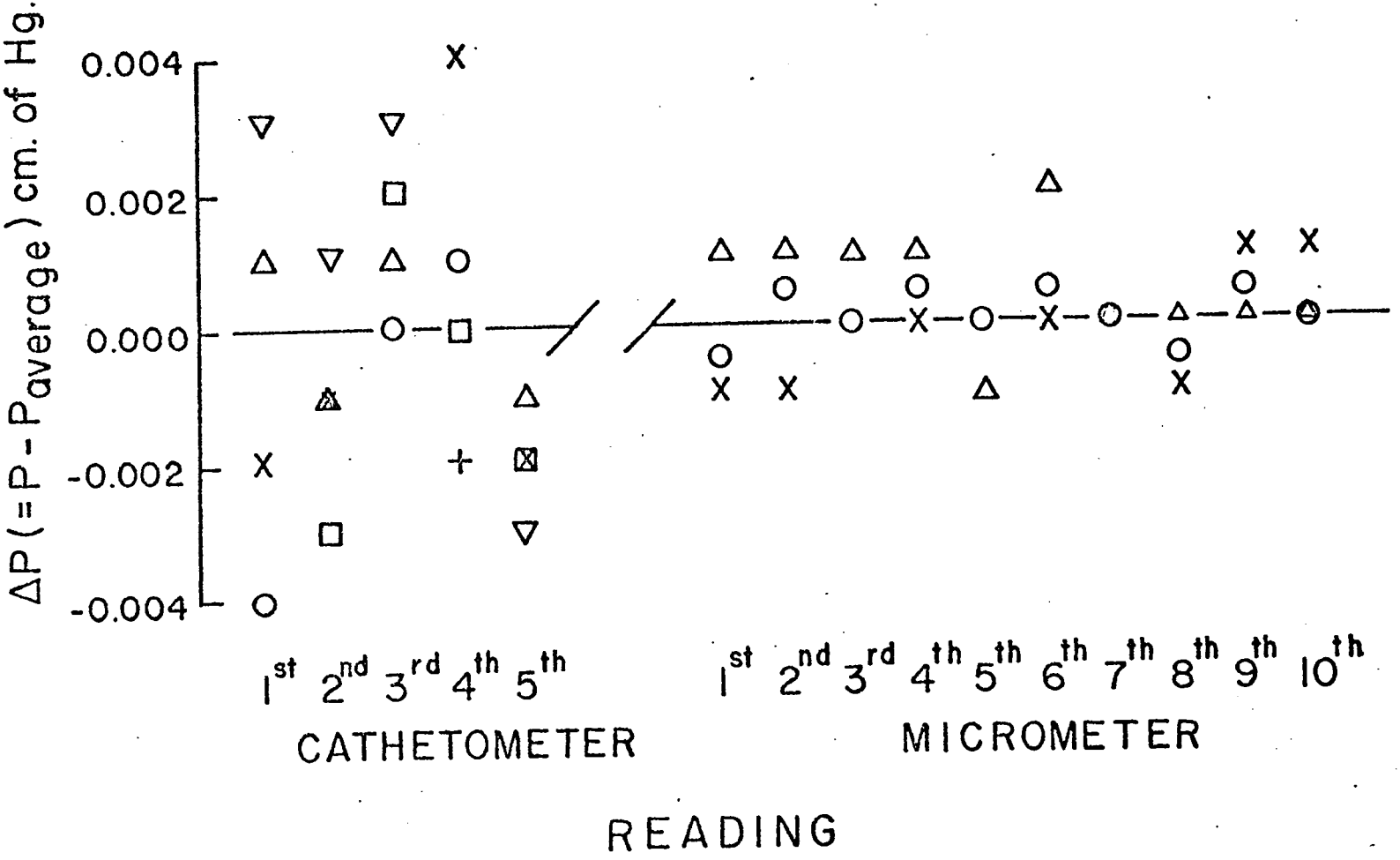
ΔP (= P - Paverage) cm. of Hg.
0.004
0.002
0.000
-0.002
-0.004
1st 2nd 3rd 4th 5th
CATHETOMETER
1st 2nd 3rd 4th 5th 6th 7th 8th 9th 10th
MICROMETER
READING

3.2 EXPERIMENTAL CONDITIONS

3.2.1 Purification of Chemicals

(a) Water was doubly distilled from aqueous alkaline permanganate in a still equipped with three spray traps; just prior to use, the water was distilled for a third time in a nitrogen atmosphere into an electrolyte solution preparation vessel.

(b) "Spectroanalysed" methanol (Fisher Scientific Company) was distilled before use in the acetophenone and naphthalene adsorption studies.

(c) Mercury was passed through a pinhole in a filter paper to eliminate any impurities gathered on its surface. When quite clean to the eye, the mercury was then sprayed from a fine capillary down a one-meter column filled with 5 per cent nitric acid in an apparatus of the type described by Vogel[18]. Further purification was made by anodic electrolysis in a mercurous nitrate-nitric acid solution to remove traces of alkali and alkaline earth metals. The mercury was then triply distilled in vacuo, the final distillation being made just before the mercury was required for use.

(d) "Purified" sodium perchlorate ($NaClO_4.H_2O$, Fisher Scientific Co.) was used without further purification as a supporting electrolyte in the adsorption study of pyridine. Its use was restricted to aqueous solutions at a concentration of 0.03 M (§ 4.4).

(e) AnalaR pyridine (British Drug Houses Ltd.) was distilled under nitrogen which provided an inert atmosphere so that aerial oxidation which otherwise tends to occur in the distillation of pyridine and related compounds (see § 4.4) is minimized.

(f) Naphthalene (technical grade), used in the substitutional adsorption studies in regard to the Esin-Markov effect, was twice recrystallised from n-butanol. (See § 4.6).

(g) "Analytical Reagent" grade potassium chloride (Mallinckrodt Chemical Co.) was used without further purification as a supporting electrolyte in one set of experiments on the adsorption of pyridine.

(h) "Reagent" grade sulphuric acid (Shawinigan) was used without further purification as the supporting electrolyte for solutions of acetophenone, pinacol and naphthalene.

(i) "Sigma" grade Mandelic and lactic acids (Sigma Chem. Co.) were used without further purification in the studies on steric effects in adsorption at mercury (§ 5.7).

(j) "Reagent" grade acetophenone (Fisher Chem. Co.) was distilled under reduced pressure in a nitrogen atmosphere. (See § 4.5).

(k) 2,3-diphenylbutane-2,3-diol (referred to as 'pinacol' in this thesis) was prepared from acetophenone by electrolysis and recrystallised from 95% ethanol (see § 4.5).

3.2.2 Reference Electrodes

(a) Calomel Electrodes

These were prepared by covering a mercury surface with a paste of calomel and mercury and shaking slightly to obtain an even coverage. A sodium or potassium chloride solution of known concentration was then added slowly. When sodium perchlorate was used as the supporting electrolyte in the working electrode compartment, the electrical contact with the calomel

electrode was made through a solution-wetted 10/30 joint to minimize diffusion of chloride ions out from the electrode. When not in use, the calomel electrode was stored in a chloride solution of the same concentration as that inside the electrode. Frequent checks of its potential against those of other reference electrodes were made.

(b) Hydrogen Electrode

Hydrogen electrodes employed in part of the work were constructed simultaneously in pairs from identical pieces of platinum gauze. These were platinised to different extents so that any impurities adsorbed from the solution would have a greater effect on the reference electrode of smaller real surface area so that a potential-difference between the two would be an indication of any impurity effects. If the potential difference became greater than 0.5 mV., the electrodes were discarded or cleaned and replatinised.

3.2.3 Thermostasis

The working and reference compartments of the capillary electrometer cell, the mercury column, of which the capillary is an integral part, and the manometer, were all double-walled so that thermostatted water could be circulated through the whole system. Fluctuations of temperature were less than $0.1^{\circ}C$. As the density ρ of mercury is dependent on the temperature, calculations of the pressure p from the head of mercury h ($p = h \rho g$), supported by the meniscus in the capillary, were made at each temperature employed in the experiments.

3.3 ESTIMATION OF ERRORS

Errors in the measurement of γ arise from the following sources. The first and most important of these arises from the difficulty in accurately adjusting the meniscus in the capillary at the fiducial mark (see §§ 3.1.1, 3.1.2). Secondly, unless the potential measurements are of sufficient accuracy, the values of γ could, in effect, be slightly in error especially at the extreme ends of the electrocapillary curve where $|d\gamma/dE|$ is large.

In fact, in these regions of high electrode charge, an accuracy of only 1 mV in potential could give rise to an error of up 1 dyn. cm.$^{-1}$ in γ, whereas in the vicinity of the e.c.m. such errors are negligible.

When the technique described in § 3.1.2 was used, the maximum experimental error was found to lie within $\pm$ 0.02 dyne. cm.$^{-1}$, a result which was obtained by repeating surface tension measurements several times at chosen fixed potentials controlled to $< \pm$ 0.5 mV. by means of a potentiostat.

Measurements of concentration of adsorbates were made either spectrophotometrically or volumetrically, or by both methods as in the case of acetophenone; the results were accurate to three significant figures or ca. 0.2%.

CHAPTER IV

RESULTS

4.1 COMPUTER ANALYSIS

The derived entities, surface charge density (q_M), relative surface excess (Γ) and surface pressure (ϕ) were computed using a programme similar to the one outlined by Lawrence et al.[60]. The surface charge density, q_M, was determined by taking the experimental values of surface tension γ at various electrode potentials E for a particular electrocapillary curve and computing the new variable $y = \gamma + kE$ where k is constant. The curve $y = f_1(E)$ now has a maximum at the value of E for which k is the slope of the original $\gamma = f_2(E)$ curve, i.e.

$$\frac{dy}{dE} = \frac{d\gamma}{dE} + k = 0 \qquad \text{(at the maximum)}$$

or

$$k = -\frac{d\gamma}{dE} = q_M$$

Thus, instead of choosing E and differentiating the electrocapillary curve at that point to obtain q_M, a value of q_M is selected for which E is then determined. In addition $y_{max} = \xi$ (defined by equation 11) and it is of importance to note that ξ does not depend upon an accurate differentiation of the electrocapillary curve.

The computer programme described above was also used to obtain the surface excesses. A function z was defined as $z = (\xi + KRT \ln C)_{q_M}$ where K is a constant, and the maximum of this curve indicated the value of C for the chosen value of K(= Γ). This

procedure was convenient since it allowed the results to be set out at fixed values of Γ (i.e. corresponding to isosteric conditions) without the normal interpolation procedures (with their inevitable errors) which are necessary when results are obtained at constant C. The quantities computed were ϕ_E, Γ_E, q_M, ξ, ϕ_q and Γ_q where subscripts E and q indicate that the derived quantities were obtained at constant potential or charge, respectively. The subscript q will in general be omitted.

Computed values of the surface charge density were in good agreement with those found graphically over the range of potential considered but points at the ends of the electrocapillary curve were subject to error. The differences between the p.z.c.'s found from the two methods were in most cases within 5 mV of each other except occasionally when relatively high solution concentrations gave rise to rather flattened electrocapillary curves and a difference of 20 mV sometimes arose. In the computation of the relative surface excesses, the curve-fitting [of the cubic equation $\xi = f(\ln C)$] was checked by obtaining the values of ξ at known concentrations from the above equation and comparing these with the original data. The comparison showed that in the majority of cases there was less than 0.5 dyne cm^{-1} difference and only about 1% of the points had differences greater than 0.7 dyne cm^{-1}. Since throughout the concentration range there was a random distribution of the magnitudes of the errors, the smallest values of the relative surface excess would carry the largest percentage errors. In all cases studied, this invariably occurred in the low concentration regions and values of the relative surface excess below 0.4×10^{-10} mole. $cm.^{-2}$ were found by comparison with the graphical method to be unreliable, otherwise good agreement between the two methods was obtained.

Lawrence et al.[60] found that in the curve fitting of the functions y and z, 3rd-order polynomials gave the most satisfactory results. These were therefore used in this work.

4.2 TEMPERATURE STUDIES

4.2.1 Characteristic Thermodynamic Functions

The characteristic thermodynamic functions of a homogeneous three-dimensional bulk phase are normally four in number but, as pointed out by Parsons[63], the application of thermodynamics to the surface phase at an electrode requires sixteen such functions. The isosteric heats of adsorption differ according to which one of the variables is kept constant in each pair of the following conjugate variables (γ, A) (A being the surface area), (q_M, E) and (P, V). ('Isosteric' is probably an unfortunate label for the condition of constant surface concentration, since there are always at least two components in the interphase in adsorption from solution and the nature of the solvent is of paramount importance. The essential feature requiring description is not surface coverage but surface composition and thus the surface phase may be more aptly described by the term 'isopleth'.) Of the above variables, it was found convenient to keep A, q_M, and P constant, the first being determined by the capillary radius at the fiducial mark, the second by methods indicated in the previous section and the third by allowing the interface to be at atmospheric pressure. Hills and Payne[58] considered that results at constant V (i.e. constant density) were more easily interpreted.

4.2.2 Temperature Dependence of Potential

Since the measured working electrode 'potential' E is the difference between the individual metal-solution potential differences V_M and $V_{M, ref}$, it is necessary when using the potential as the electrical variable to know how $V_{M, ref}$ varies with temperature so that the value of E obtained can be corrected for the temperature variation. However, the estimation of the temperature coefficient of the reference electrode potential is not straightforward, either practically or theoretically. Nevertheless, the absolute temperature coefficient of the reversible electrode potential can be non-thermodynamically estimated with much better accuracy than that for the absolute potential itself.

It is fortunate that the electrical variable, q_M, which has been shown to be preferable to potential (§ 1.4.1) in the analysis of electrochemical adsorption data can be measured absolutely and independently of the reference electrode potential even though this may change with temperature.

4.3 ESIN AND MARKOV EFFECT

It was shown by Esin and Markov[64] that the p.z.c. of a mercury electrode varies linearly with the logarithm of the bulk activity of the surface active ions. More recently this effect has been found by Devanathan and Peries[65] to apply to potentials at any constant charge q_M. An analogous phenomenon was also investigated for neutral molecule adsorption by Conway and Barradas[66] who studied aromatic heterocyclic compounds as adsorbates. In the case of specific ionic adsorption, the p.z.c. is well-defined since the curvature at the e.c.m. remains sharp as the bulk concentration changes, whereas the opposite effect occurs in the case of neutral molecule adsorption where a flattering of the electrocapillary curve

occurs with increasing concentration. Although, in this case, shifts in the p. z. c. with bulk concentration were found to be large, the scatter in the points does not allow an unequivocal confirmation of the linearity of the Esin-Markov effect. In fact Barradas et al.[67] showed later that $(\partial\Gamma / \partial q_M)_\mu$ in the cases studied was dependent on μ and because

$$(\partial\Gamma / \partial q_M)_\mu = (\partial E / \partial \mu)_{q_M}, \qquad (51)$$

the $E_{p.z.c.}$ *vs* log C (or μ) plot must be non-linear.

It is of interest to note that the assumption in Frumkin's model (§ 1. 4. 2(ii)a) for neutral molecule adsorption, viz.

$$q_M = q_{\Theta=0}(1 - \Theta) + q_{\Theta=1}\Theta \qquad (52)$$

relies on the L. H. S. of equation (51) being independent of bulk concentration; this, in fact, is not borne out experimentally in the cases previously cited in reference (67).

In the case of aromatic heterocyclic compounds, two regions were observed[66] in the $(E_b - E)_{p.z.c.}$ *vs* log C plots and these were interpreted in terms of two possible extreme orientations of the molecules; the flat and vertical orientations were associated with π-bonding and dipole-dipole image interactions with the surface, respectively.

Although the electrostatic formula of Helmholtz (cf. equation 2) which can be expressed in terms of the derivative.

$$(\partial E / \partial \Gamma)_{q_M} = 4\pi N\mu / \varepsilon \qquad (53)$$

(where N is Avogadro's number and Γ is expressed in moles cm^{-2}) is probably too simple to explain the details of the $(E_b - E)_{e.c.m.} = f(\Gamma)$ plots, it might well be a better indicator for discerning

orientation effects arising in the case of neutral molecules than is the Esin-Markov equation. However, since both treatments are similar and rather qualitative in most instances, only one form will normally be considered.

4.4 ADSORPTION OF PYRIDINE

4.4.1 Potential as a Function of Temperature and Bulk Concentration at Constant Charge

In Figure 9 there are two regions in the $\Delta E_{p.z.c.}$ vs Γ plots; although it is not justified to regard the various plots as linear, it would appear that reorientation occurs at $\Theta < 0.5$ where Γ_M has the value of 4.15×10^{-10} mole. cm^{-2} [68] for pyridine molecules lying in the "flat" position. As the temperature increases, the value of Θ for the transition region is lowered. At higher coverages there is an increase in the values of $\Delta E_{p.z.c.}$ with temperatures.

Esin-Markov plots are illustrated in Figure 10 for surface charge densities -2, 0, 4, and 8 $\mu C. cm.^{-2}$ and curves are drawn for the cases of lowest and highest temperatures. Ill-defined isosbestic points which are found on all sets of graphs appear at higher bulk concentrations for the more highly charged (especially positively charged) electrode surfaces. At zero and negative surface charges, the regions of very low and very high concentration show temperature effects on the shift of potential (at which the given charge is attained) which are the reverse of those found at positive surface charges. The rather 'flat' region at low concentrations extends into the higher concentration region as the charge becomes more negative (or less positive).

Figure 9

Variation of the potential of zero charge with surface concentration of pyridine at various temperatures

	Temperature °C	
	7.5	x
	20.0	●
0.03M $NaClO_4$	40.0	▽
	60.0	▲
	80.0	+
1N KCl	25.0	....O....

Figure 9a

Plots of $\Delta E_{p.z.c.}$ vs surface concentration (Γ) which are representative of those observed (——) and of those expected (----) if complete reorientation of the adsorbate molecules occur at Γ_a.

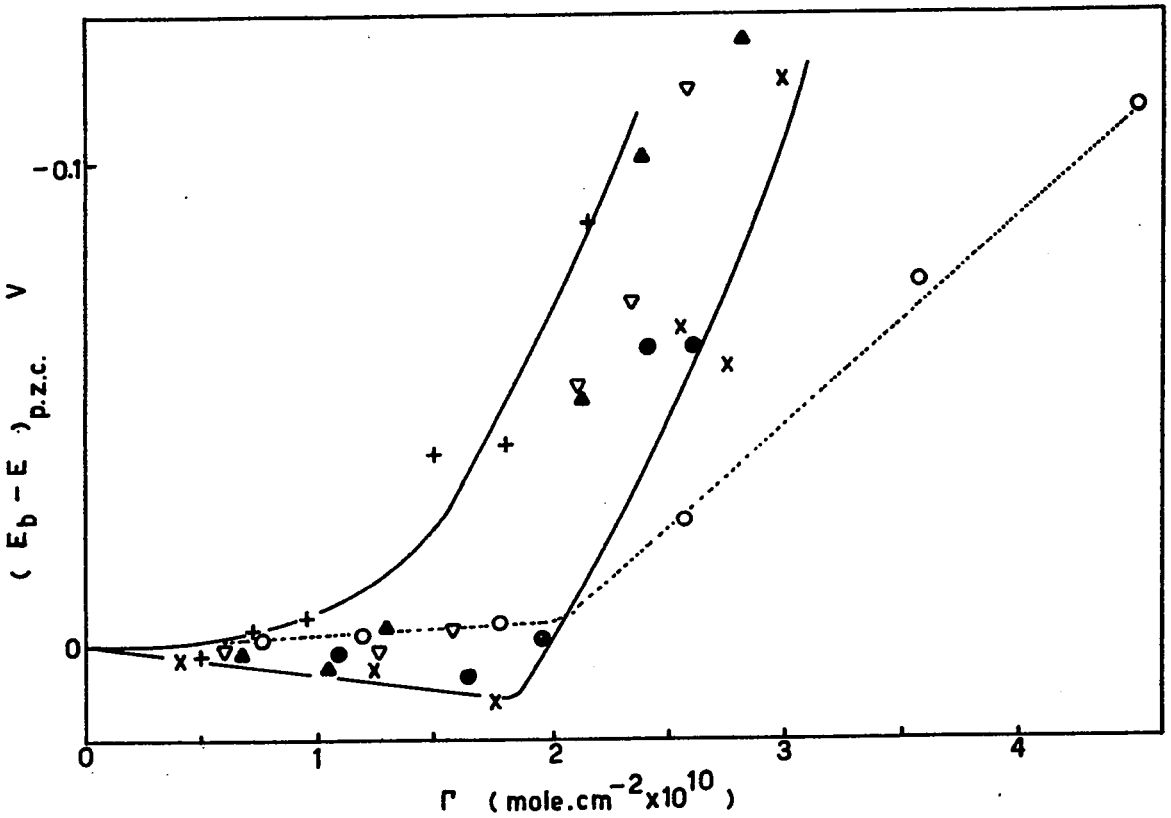
-0.1
0
0
1
2
3
4
(E_b - E)_p.z.c. V
Γ (mole.cm^-2 x10^10)

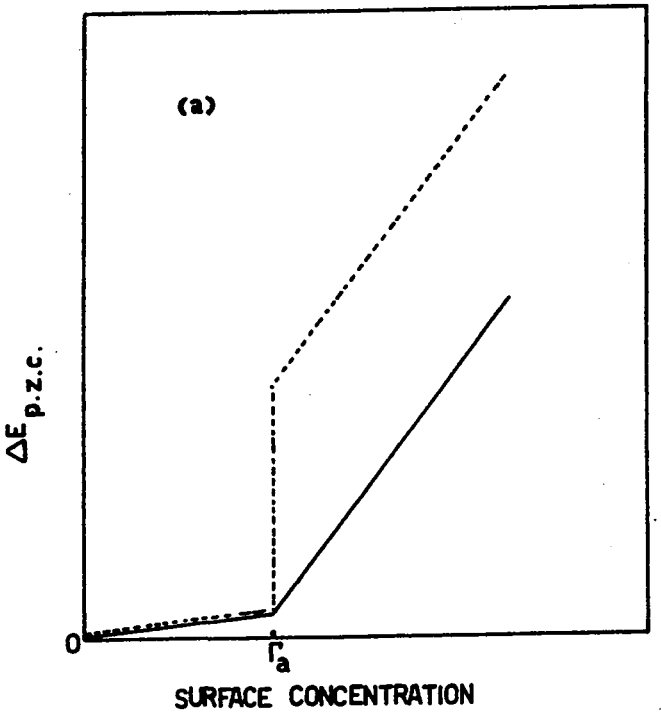
(a)
ΔE_p.z.c.
0
Γ_a
SURFACE CONCENTRATION

Figure 10

Variation of potential with bulk concentration of pyridine in 0.03M $NaClO_4$ solution at various temperatures and electrode charge densities (q_M).

Temperature ^oC	
7.5	x
20.0	●
40.0	Δ
60.0	▼
80.0	+

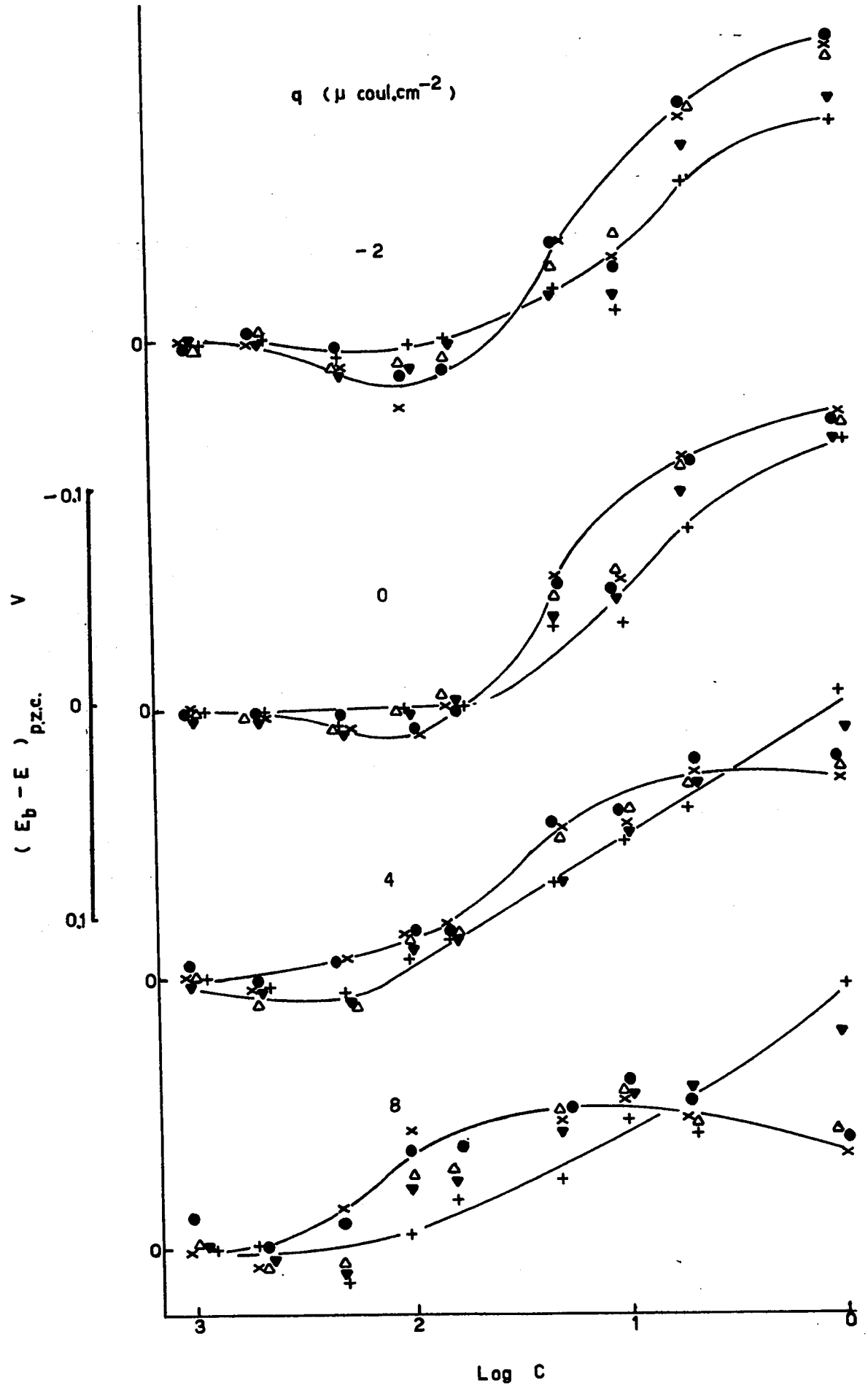
q (μ coul.cm^{-2})
-2
0
4
8
0
0
0
0
-0.1
0
0.1
V
$(E_b - E)_{p.z.c.}$
3
2
1
0
Log C

4.4.2 Temperature Effect on Surface Concentration

The isotherms shown in Figure 11 indicate that for a given bulk concentration, surface coverage of pyridine increases with increasing positive charge and decreasing temperature. In Figure 12, the relation between charge and temperature for given values of Γ_q and equilibrium concentration C is shown for three pairs of surface and bulk concentrations. The behaviour observed is somewhat analogous to that relationship, first pointed out by Bernal and Fowler[69], between the polarising power of an ion (associated with its charge density) and the temperature, in regard to their effects on the structure of water; i.e. the average energy required to break or make solvent structure could be achieved by either the introduction of charged ions or by the changing of the temperature. For the behaviour shown in Figure 12, the corresponding energy is associated with the adsorption process. In effect, the plots of Figure 12 show that in order to maintain a given value of Γ_q for a given bulk adsorbate concentration, the temperature must be increased if q_M is made more negative. This implies that the free energy of adsorption is increased (numerically) as the electrode becomes more cathodically charged, i.e. the ratio $-\Delta G^o/RT$ in the electrochemical isotherm must remain constant for various q_M and T to maintain a constant distribution of solute.

4.4.3 The Co-anion Effect

In Figure 9 it is seen that $(E_b - E)_{p.z.c.}$ is always positive for the system in which pyridine is adsorbed in the presence of 1M KCl. This is not the case in the low concentration region when 0.03M $NaClO_4$ is used as the supporting electrolyte. Secondly, much higher surface concentrations of pyridine are necessary to change the p.z.c. of KCl solutions to the same extent as that for

Figure 11

Variation of surface concentration (Γ) with bulk concentration (C) of pyridine at various temperatures and various values of q_M.
(a) +8 ; (b) +4 ; (c) 0 and (d) -4 μ coul. cm.$^{-2}$

Temperature	^{o}C
7.5	x
20.0	●
40.0	Δ
60.0	▼
80.0	+

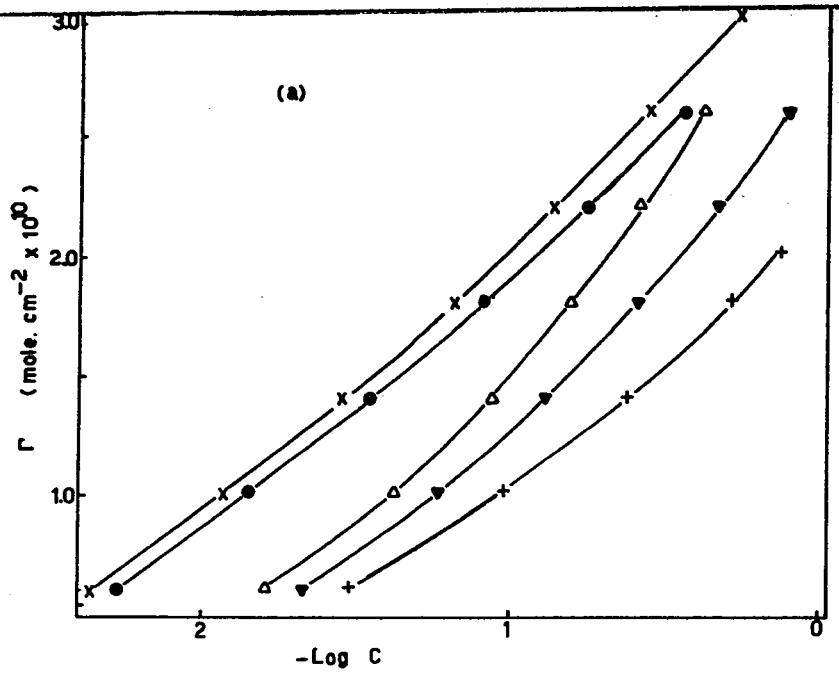
(a)
Γ (mole. cm^{-2} x 10^{10})
3.0
2.0
1.0
2
1
0
-Log C

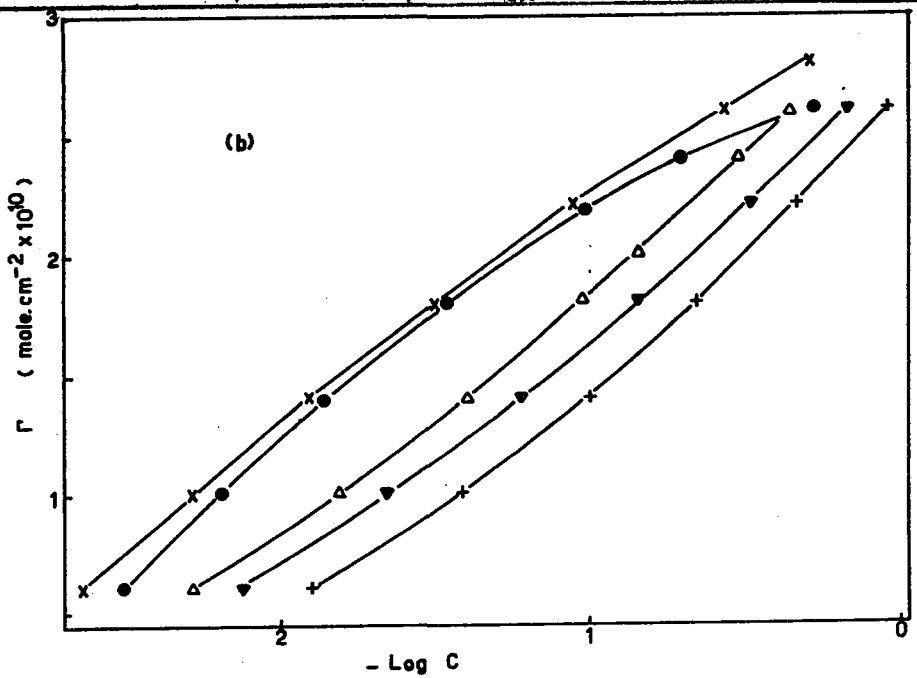
(b)
Γ (mole.cm^{-2} x 10^{10})
3
2
1
2
1
0
- Log C

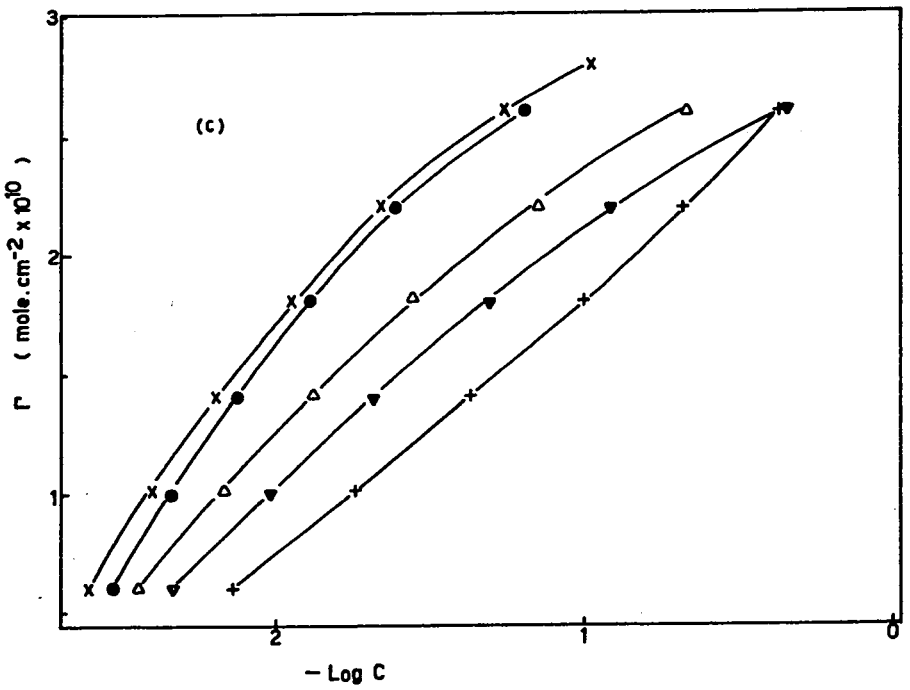
(c)
Γ (mole.cm^{-2} x 10^{10})
3
2
1
2
1
0
- Log C

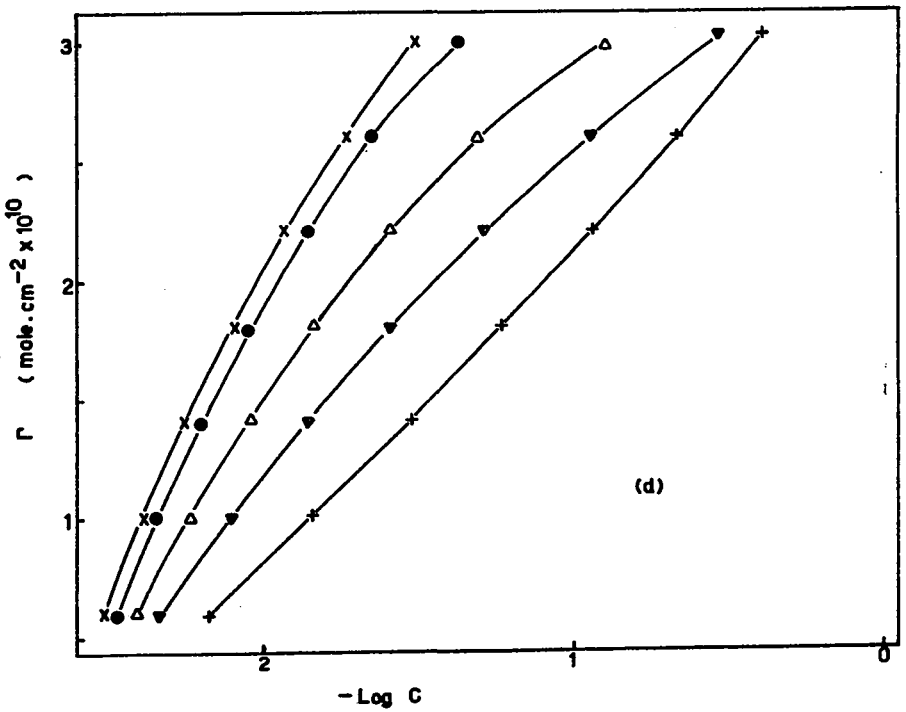
(d)
Γ (mole.cm^{-2} x 10^{10})
3
2
1
2
1
0
- Log C

Figure 12

Compensation effect between temperature and electrode charge density for constant distribution of pyridine in bulk and surface phases.

1M KCl	0.03M $NaClO_4$	(C) bulk concn. mole. l^{-1}	(Γ) mole. cm. $^{-2}$ 10^{10}
●	o	0.01	0.8
■	□	0.04	1.6
▲	△	0.1	2.4

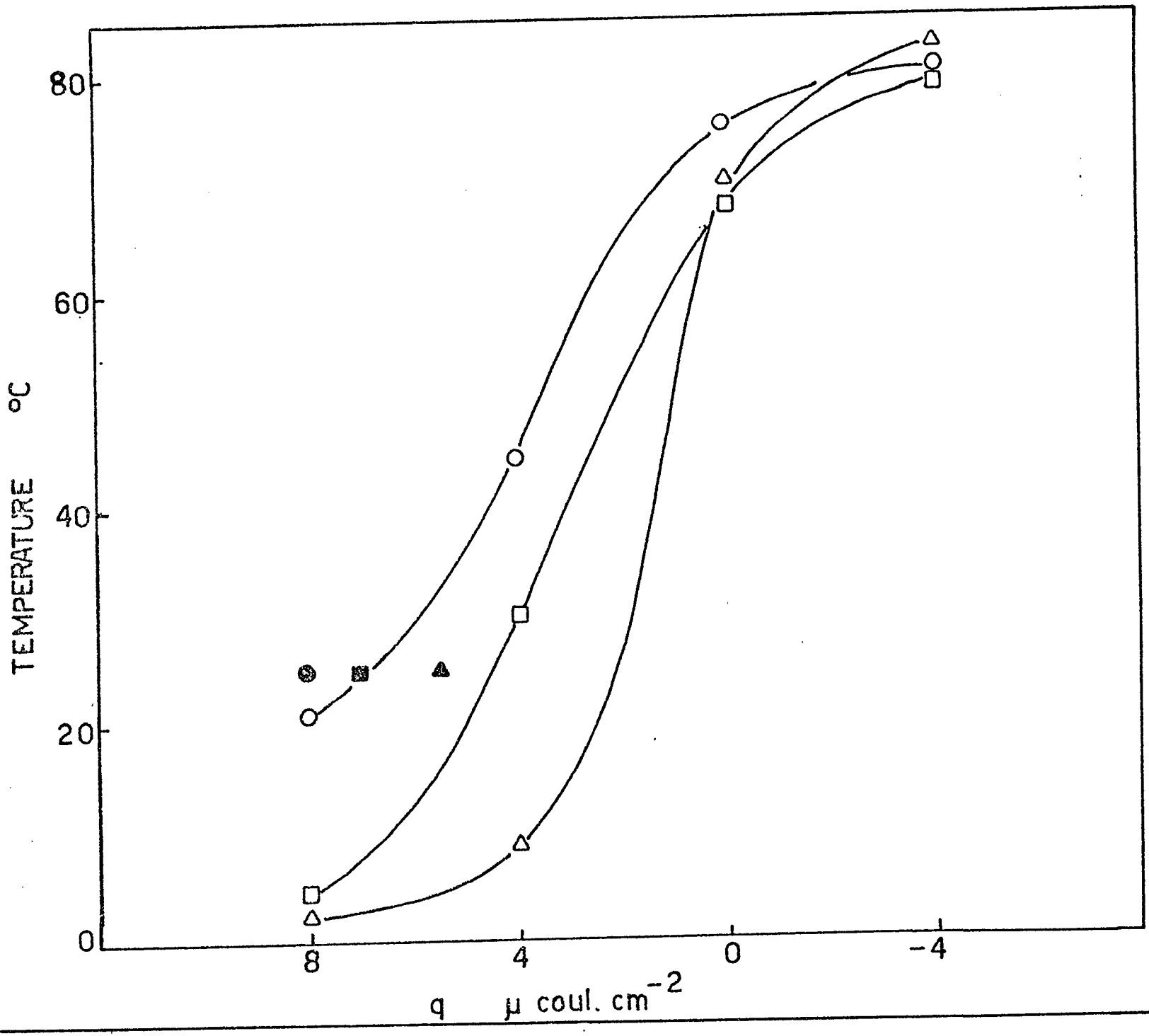
80
60
40
20
0
TEMPERATURE °C
8
4
0
-4
q μ coul. cm^{-2}

$NaClO_4$ solutions. This fact is of particular interest when it is considered in the light of the previously established synergetic effect in the simultaneous adsorption of pyridine and chloride ions[15].

The $\emptyset$ - Γ plots of Figures 13a and 13b indicate that at low surface coverages by pyridine, the surface pressures are greater in the presence of Cl^- ions (1M bulk concentration) than in the presence of ClO_4^- ions (0.03M bulk concentration). Not only are the latter ions present at a lower bulk concentration but they are also known to be much less adsorbable at the mercury electrode-aqueous solution interface than the former. These differences between the surface pressures of pyridine in the Cl^- and ClO_4^- solutions are greatest when the electrode charge is least positive (or most negative). However, with increased adsorbate coverage, the specificity of the effect of the co-anion decreases.

In Figure 12 the three corresponding points associated with the chloride solutions do not fall on the corresponding 'perchlorate curves' and thus the change of the electrolyte in the system is equivalent to a change in temperature accompanied by a change in electrode charge density.

4.5 ADSORPTION OF ACETOPHENONE AND ITS PINACOL

This study was carried out in order to provide the information required in the investigation of the kinetics of acetophenone reduction (in particular the reaction order of the reaction) at the mercury electrode, the study of which is reported in outline in §§ 1.6 and 5.6. The main product of the reduction in acid solution is the pinacol 2,3-diphenyl-butane-2,3-diol, which if adsorbed extensively would hinder the reaction. Therefore the characteristics of the adsorption of the pinacol were also investigated in this work.

Figure 13

Variation of surface pressure ϕ with surface concentration of pyridine at various electrode charge densities.

(a) Pyridine adsorbed from 0.03M $NaClO_4$ solution

q μ coul. $cm.^{-2}$	
8	△
4	+
0	□
-4	x

(b) Pyridine adsorbed from 1M KCl solution

q μ coul. $cm.^{-2}$	
12	o
8	△
4	+
0	▼
-4	o
-8	□

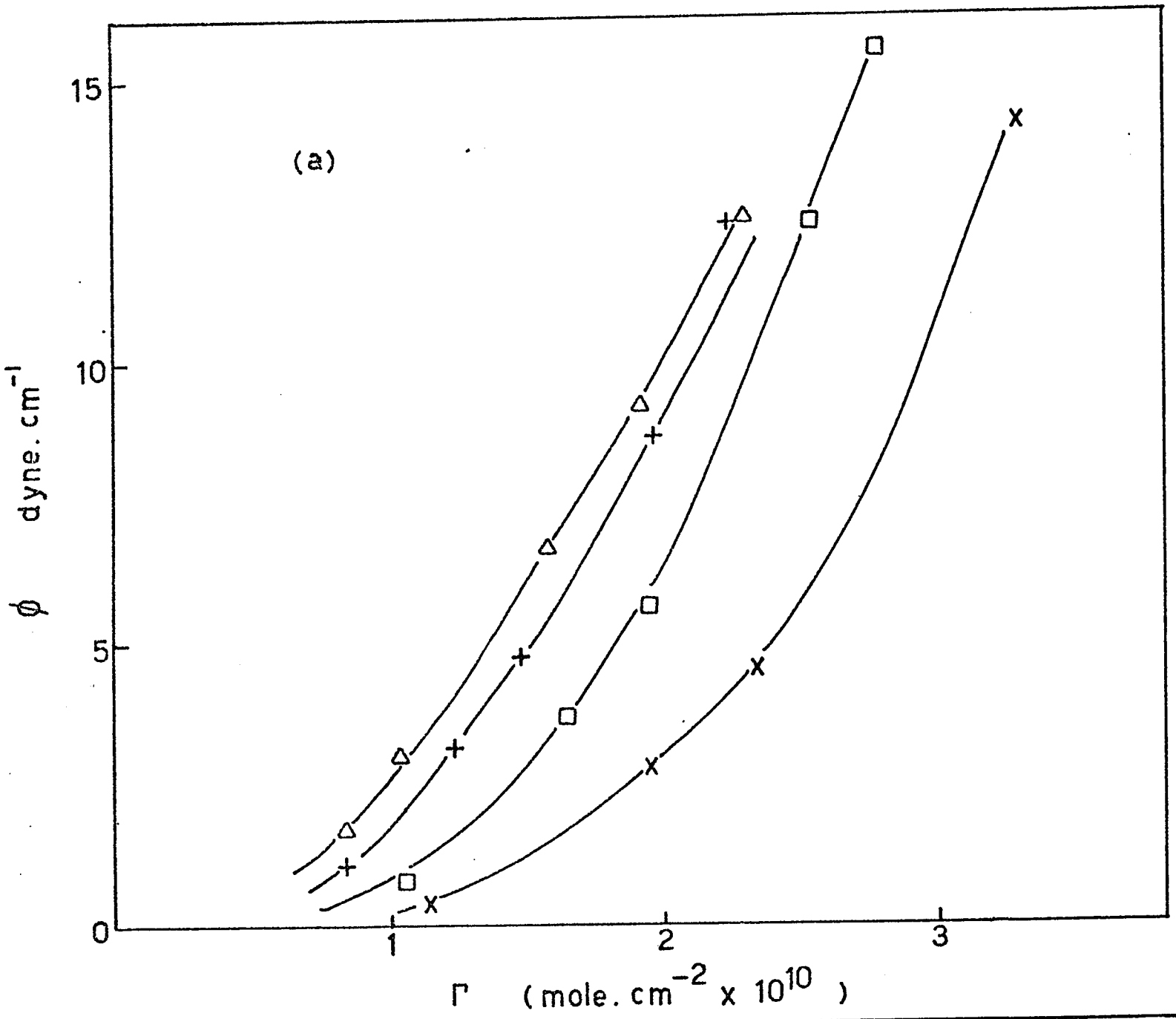
(a)
15
10
5
0
1
2
3
ϕ dyne. cm^{-1}
Γ (mole. cm^{-2} x 10^{10})

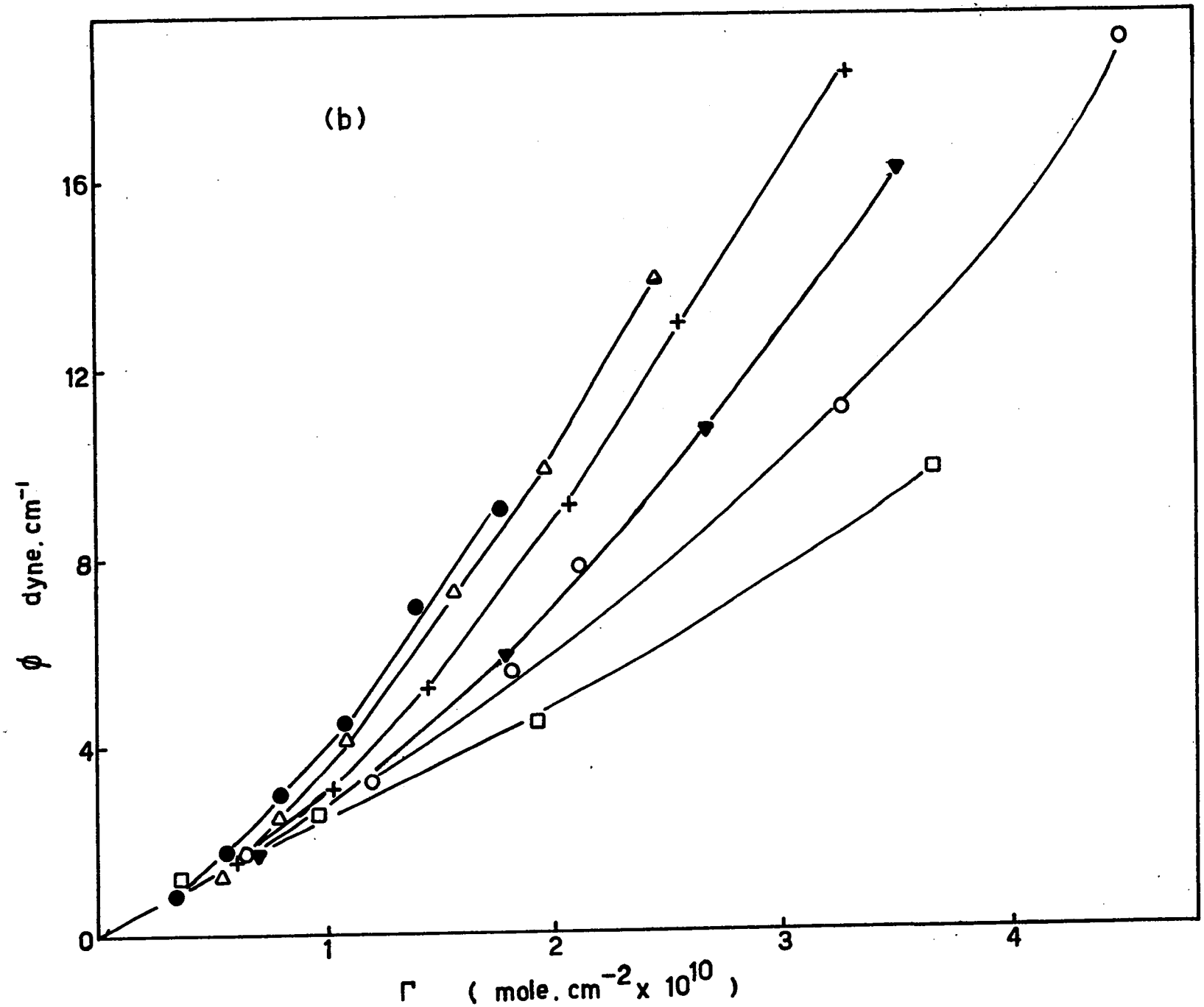
(b)
16
12
8
4
0
1
2
3
4
φ dyne. cm⁻¹
Γ (mole. cm⁻² x 10¹⁰)

Figure 14

Variation of potential of zero charge with bulk concentration for acetophenone and its pinacol.

Solvent (1M H_2SO_4)

methanol	acetophenone	●
1:4 mole ratio water + methanol	acetophenone	O
1:4 mole ratio water + methanol + 0.1M pinacol	acetophenone	Δ
1:4 mole ratio water + methanol	pinacol	+

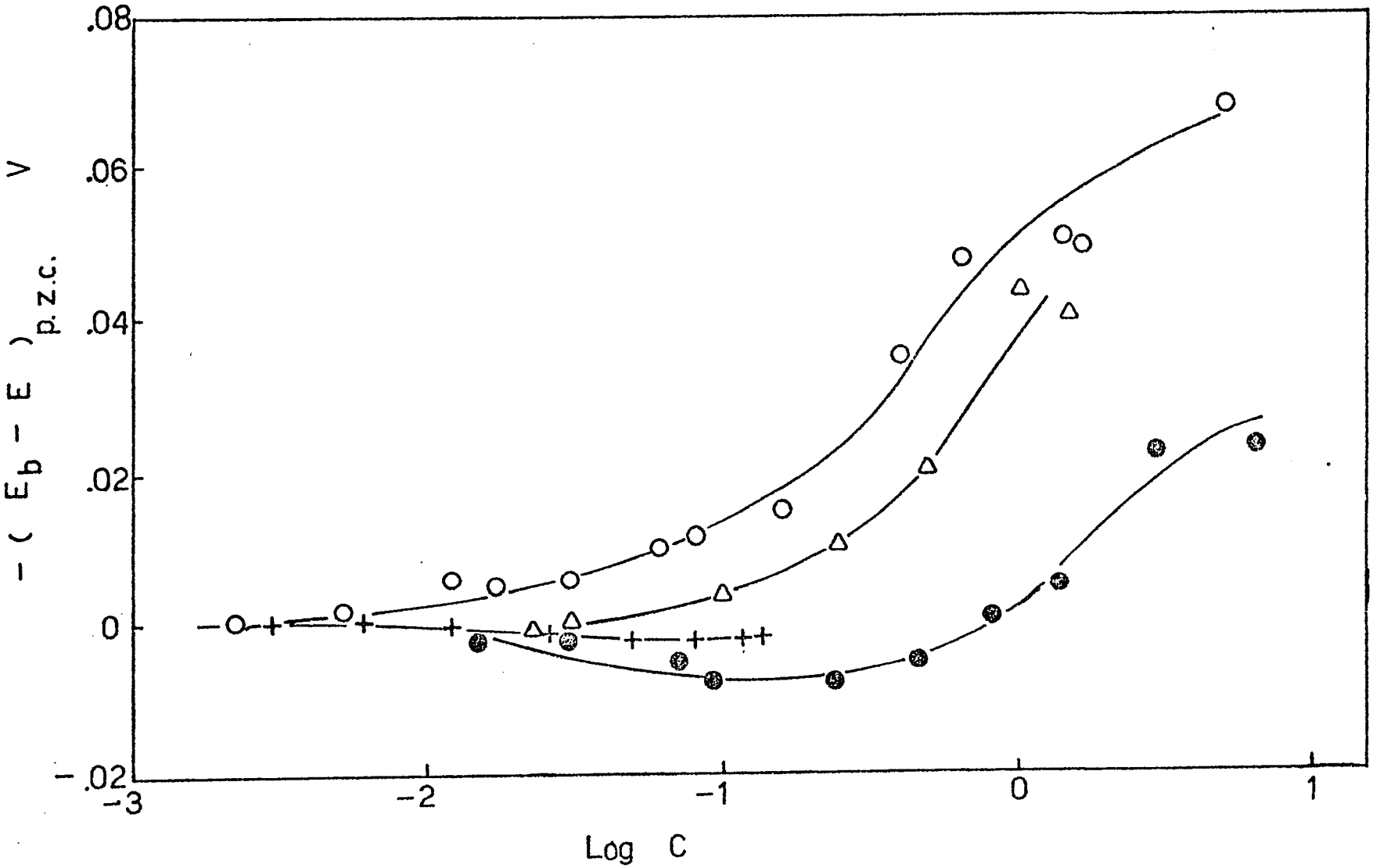
.08
.06
.04
.02
0
-.02
-3
-2
-1
0
1
Log C
- (E_b - E)_p.z.c. V

Electrocapillary measurements were made on the following three types of solution in the same solvent mixture (1:4 mole ratio water + methanol, 1M H_2SO_4) as that used in the kinetic runs: (a) acetophenone alone; (b) acetophenone in the presence of 0.1M pinacol (mentioned above) and (c) the pinacol alone. Thus information concerning the adsorption of the reactant, of the product separately and the reactant in the presence of a fixed concentration of the product could be obtained. The concentration of the pinacol used was sufficiently low that the chemical potentials of acetophenone in the presence and absence of pinacol were sensibly the same. Another experimental run in which acetophenone was adsorbed from 1M H_2SO_4 in pure methanol was also conducted.

4.5.1 Surface Concentrations

Since the surface excesses of acetophenone were relatively small over the concentration range considered, especially at appreciably negative values of q_M, the corresponding true surface concentrations differed significantly from them particularly at the highest equilibrium solution concentrations. From Figures 15a, b, c, it is seen that at high concentrations, there is a tendency for the adsorption of acetophenone from the various solvent systems to decrease in the order: "methanol-water-pinacol" > "methanol-water" > "methanol". However, at low concentrations, the three-component solvent mixtures (i.e. methanol-water + pinacol) gave rise to the lowest surface concentrations of acetophenone.

The Γ - log C description of the adsorption of pinacol (Figure 15d) (as in the Esin-Markov plot) differed greatly from those for acetophenone adsorption. The highest surface concentrations of the pinacol are reached at approximately one decade of bulk concentration lower than that for acetophenone under the same conditions of charge and solvent composition, so that the standard

Figure 15

Variation of surface concentrations of acetophenone and its pinacol with their bulk concentrations at various electrode charge densities

Solvent (1M H_2SO_4)	Solute
(a) methanol	acetophenone
(b) 1:4 mole ratio water + methanol	acetophenone
(c) 1:4 mole ratio water + methanol + 0.1M pinacol	acetophenone
(d) 1:4 mole ratio water + methanol	pinacol

q_M μ coul. cm.$^{-2}$	
16	x
12	•
8	Δ
4	+
0	∇

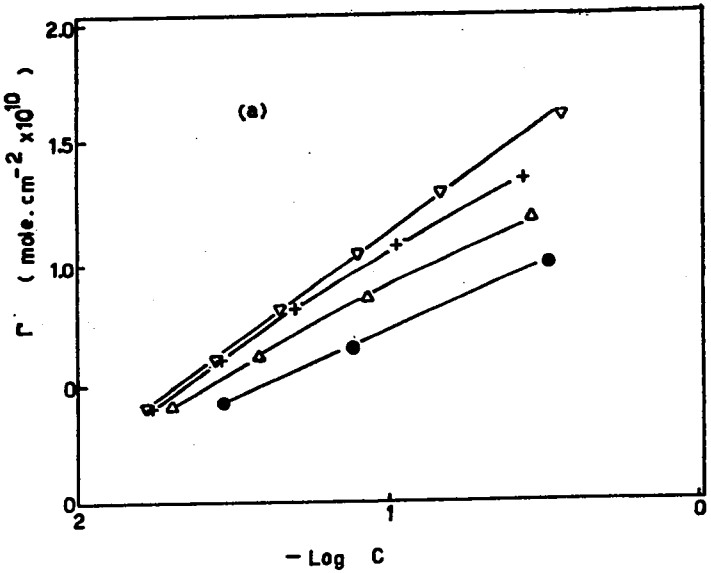
(a)
Γ (mole.cm⁻² x10¹⁰)
2.0
1.5
1.0
0
2
1
0
- Log C

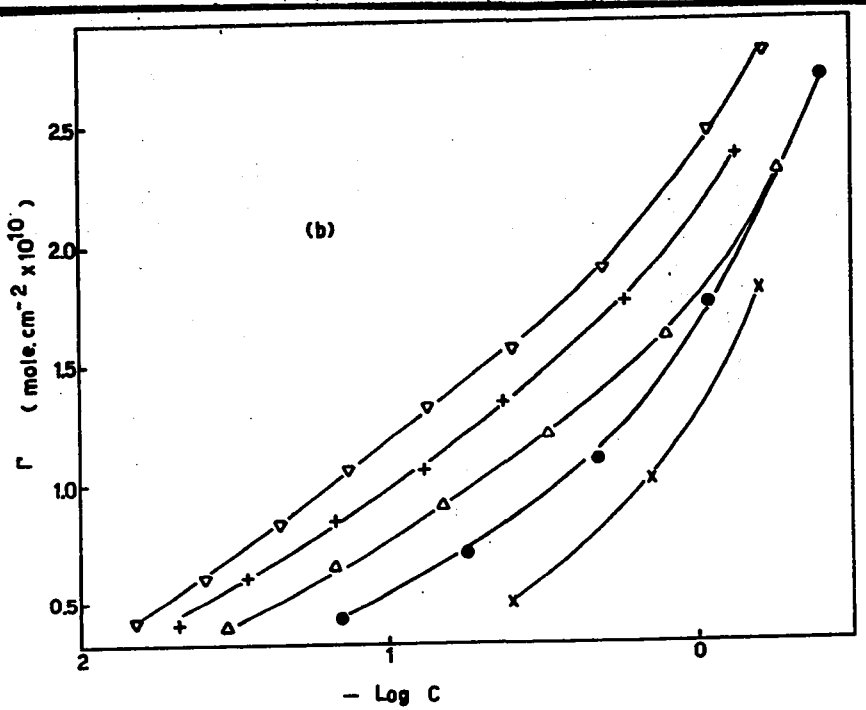
(b)
Γ (mole.cm⁻² x10¹⁰)
2.5
2.0
1.5
1.0
0.5
2
1
0
- Log C

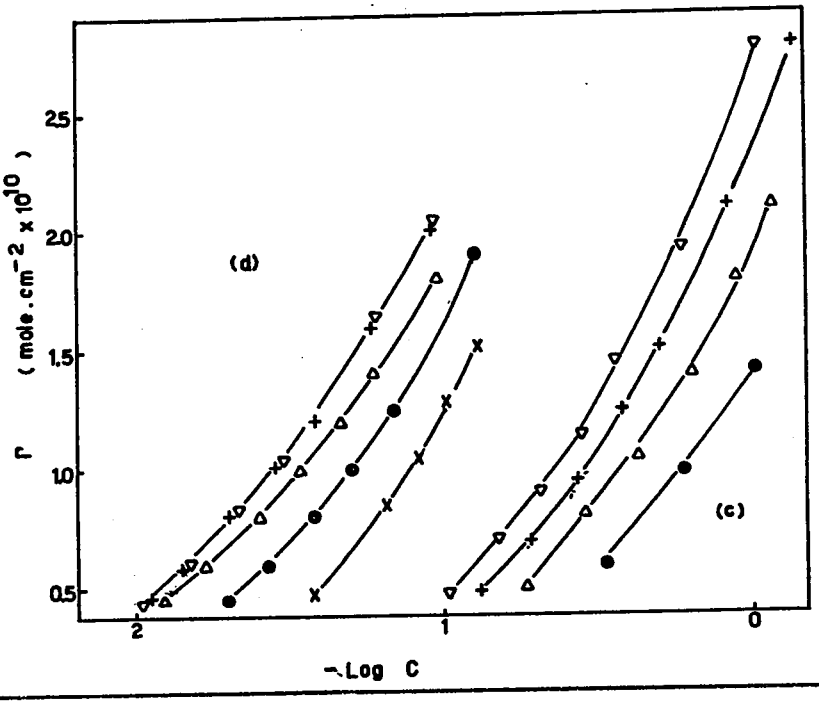
(d)
(c)
Γ (mole.cm⁻² x10¹⁰)
2.5
2.0
1.5
1.0
0.5
2
1
0
-Log C

free energy of adsorption of the pinacol is greater than that of acetophenone.

It should be noted that in studies of neutral molecule adsorption, the concentration and activities of the solute are considered to be equivalent but this may not be true at concentrations, say, above 2M where the solute can modify the properties of the solvent significantly. The data obtained for C > 2M in the electrocapillary investigations of acetophenone should therefore be treated with a little caution in this respect. However, the non-ideality effects are much less significant than for electrolytes at comparable concentrations.

As in the co-anion effect exhibited in the relation between ϕ and Γ for pyridine adsorption, there is a marked influence of solvent on the ϕ - Γ relationships for acetophenone adsorption (Figures 16a, b, c). This appears to be a good indication that the solvent plays an important role in determining the nature and magnitude of interactions occurring in the ad-layer (interphase) irrespective of the type of solvation that takes place in the bulk phase, since ϕ and Γ are quantities which are representative of the behaviour of molecules in the surface phase. It is apparent from this set of graphs that for all electrode charge densities considered, the surface pressure decreases at corresponding surface concentrations as water is introduced (20%) into the methanol and further decreases as pinacol is added to the 20% water-methanol solvent mixture. This behaviour may be quite general since the second component added is water which is less adsorbable than methanol in the concentration range studied[70] while the third component, pinacol, is the most readily adsorbed as found in the present work (cf. Figure 15d with Figures 15a, b, c).

The plots of Figure 16a differ characteristically from those of Figures 16b, c, in that definite changes in the slopes of

Figure 16

Variation of surface pressure ($\emptyset$) with surface concentration of acetophenone and its pinacol at various electrode charge densities.

Solvent (1M H_2SO_4)	Solute
(a) methanol	acetophenone
(b) 1:4 mole ratio water + methanol	acetophenone
(c) 1:4 mole ratio water + methanol + 0.1M pinacol	acetophenone
(d) 1:4 mole ratio water + methanol	pinacol

q_M μ coul. cm.$^{-2}$	
16	x
12	o
8	Δ
4	+
0	∇

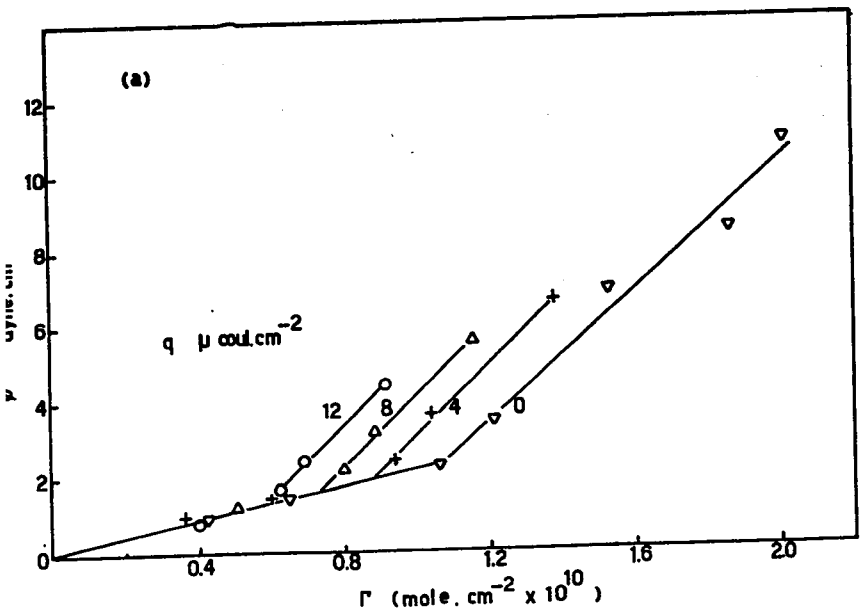
(a)
q μ coul.cm⁻²
12
8
4
0
Γ (mole. cm⁻² x 10¹⁰)

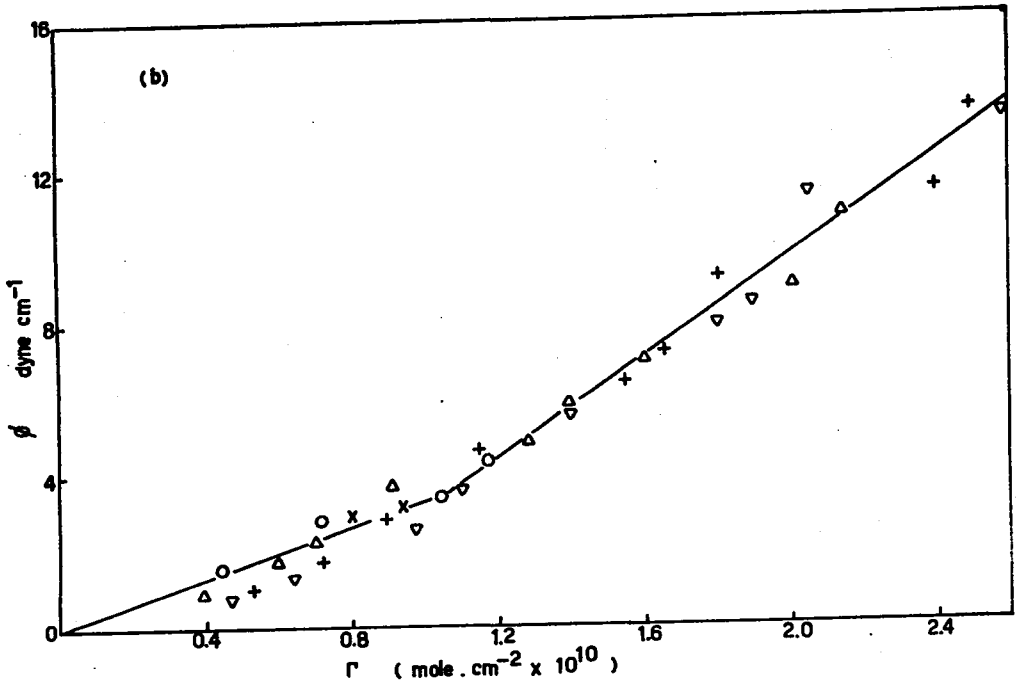
(b)
ϕ dyne cm⁻¹
Γ (mole. cm⁻² x 10¹⁰)

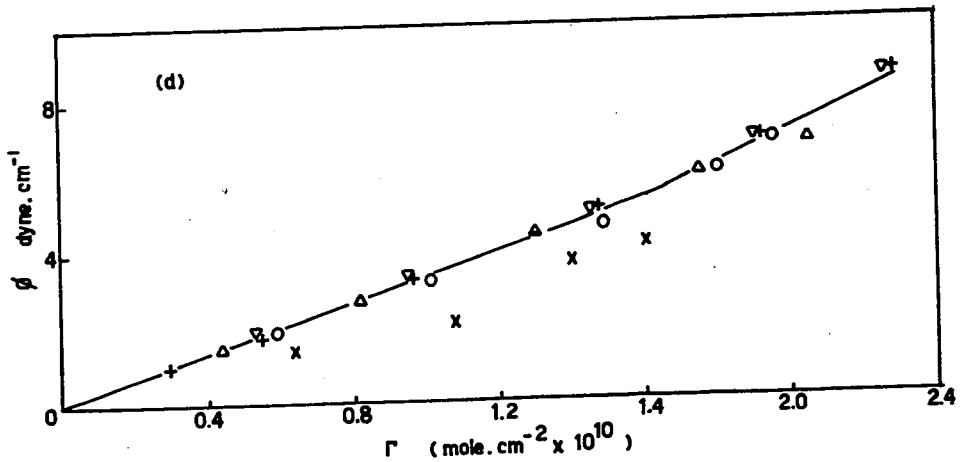
(d)
ϕ dyne. cm⁻¹
Γ (mole. cm⁻² x 10¹⁰)

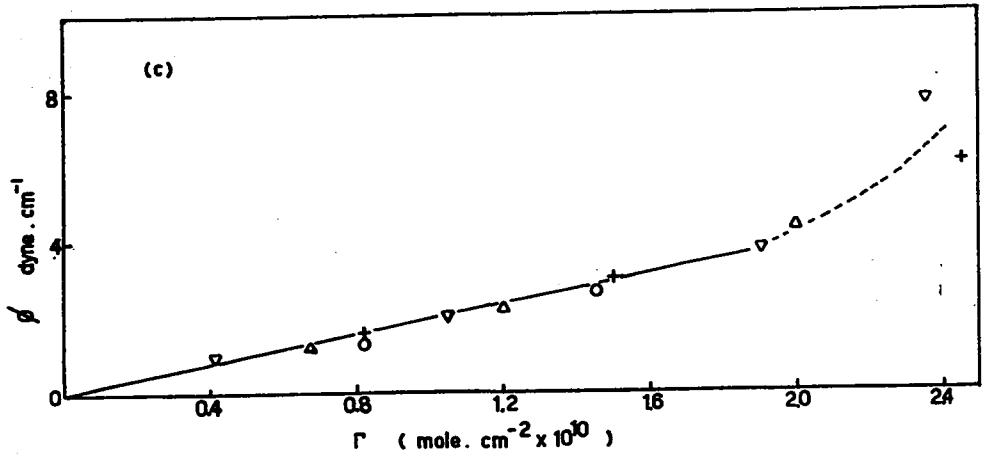
(c)
ϕ dyne. cm⁻¹
Γ (mole. cm⁻² x 10¹⁰)

ϕ vs Γ plots appear in the region 0.6 - 1.1 x 10^{-10} mole. cm.$^{-2}$ and the surface coverages at which these inflections occur depend on the electrode charge density.

At constant composition of the surface phase (i.e. under isoplethic or isosteric conditions), it is noticeable (Figure 16a) that the surface pressure is very dependent on the surface charge density, i.e. ϕ increases for a given Γ value as q_M becomes more positive. The effect may be connected with orientation of the > CO group with consequent dipole repulsion in the ad-layer.

In the third set of plots of this series (Figure 16c), where a "three-component" solvent (i.e. 20% water-methanol + pinacol) was used, no charge dependence of the surface pressure and no change in slope of the ϕ - Γ relation is observed over the range of surface concentrations studied.

The graphs of ϕ vs Γ (Figure 16b) for acetophenone adsorption from the methanol-water mixture, represent a behaviour which is intermediate between the two extreme cases just discussed. On changing the solvent system from methanol to 20% water-methanol mixture, there remain the vestiges of a slight kink at Γ = 1.0 x 10^{-10} mole. cm.$^{-2}$ and a small dependence of ϕ at given constant Γ values on surface charge. Again this may reflect orientation effects (see Figure 14).

A final comparison that is useful to make is that between the ϕ - Γ plots for acetophenone and pinacol in the same solvent system, methanol-water (see Figures 16b, d). Except for the high concentration region where surface pressures are a little larger in the acetophenone case, there is a great deal of similarity between the behaviour of the two solutes even though their nature and bulk concentration ranges are very different. Isosteres from Figure 16d in the case of pinacol show a dependence of surface pressure on

charge which, although not large, is the reverse of that found for the other adsorption processes considered so far.

4.5.2 Esin-Markov Effect for Acetophenone and its Pinacol

Acetophenone when adsorbed from pure methanol (Figure 14) showed a negative shift of $(E_b - E)_{p.z.c.}$ at low concentrations followed by a positive shift at concentrations above 1M. A similar type of behaviour is recorded (Figure 10) for pyridine adsorption from perchlorate solutions at the p.z.c. For solutions of acetophenone in the 20% water-methanol mixture the shape of the $\Delta E_{p.z.c.}$ vs log C plot is not changed significantly by the addition of 0.1M pinacol, although the presence of the latter lowers the values of $\Delta E_{p.z.c.}$ for the higher concentration region by about 10 mV. In contrast to the acetophenone adsorption, the adsorption of pinacol results in a negative shift of $(E_b - E)_{p.z.c.}$ for all concentrations studied. The solubility of the pinacol was the limiting factor in extending the investigation to higher concentrations.

4.6 ADSORPTION OF NAPHTHALENE

The purpose of this aspect of the work was to evaluate the change of p.z.c. (if any) attendent upon the adsorption of a completely non-polar molecule from a dipolar solvent and thus obtain an indication of solvent orientation.

The data shown in Figure 17 have been plotted on the basis of the Helmholtz electrostatic formula (Eq. 2) and indicate consistency between the theoretical concept concerning the development of a surface dipole potential and the experimental results. The values of $(E_b - E)_{e.c.m.}$ are all positive and therefore the adsorption behaviour is apparently similar to that of acetophenone, pyridine and pinacol from dilute methanolic, dilute aqueous and methanolic-

Figure 17

Variation of potential of zero charge with surface concentration (Γ) of naphthalene in methanolic 1M H_2SO_4.

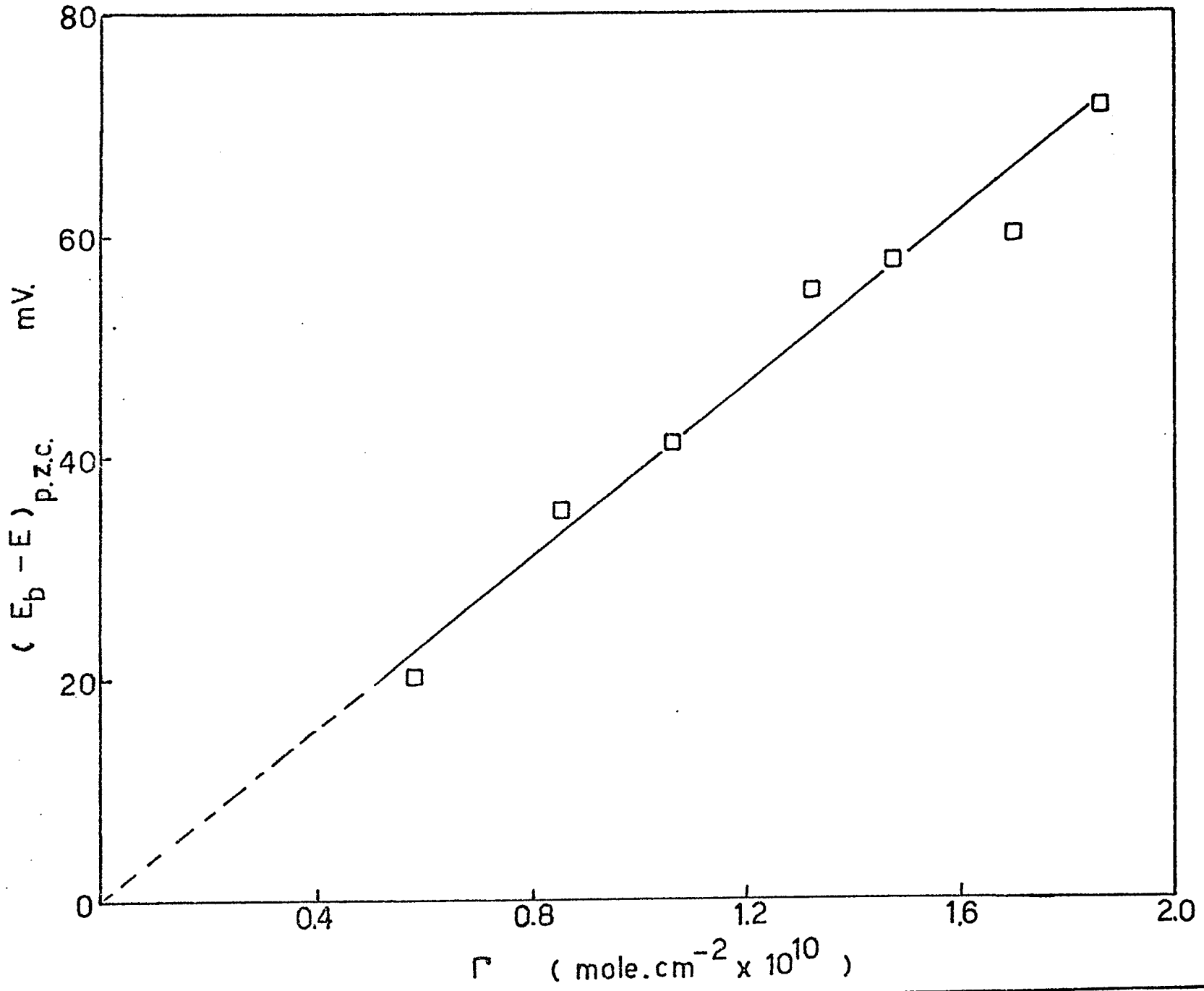
80
60
40
20
0
mV.
$(E_b - E)_{p.z.c.}$
0.4
0.8
1.2
1.6
2.0
Γ (mole.cm^{-2} x 10^{10})

aqueous solutions, respectively. In the latter case, $(E_b - E)_{e.c.m.}$ is also positive at all bulk concentrations.

The ϕ - Γ relationship for naphthalene adsorption from methanol (Figure 18) is rather surprising in that the plots at constant q_M are nearly superimposable on the corresponding plots for the acetophenone-methanol system (Figure 16) but not on those for pinacol (Figure 16d) which is a little more similar to naphthalene in structure. Both systems contained 1M H_2SO_4 as the supporting electrolyte. Keeping in mind, however, that a greater similarity was observed between the behaviour of acetophenone and pinacol when adsorbed from the same solvent (Figures 16b, d) than between the effects shown by acetophenone adsorbed from different solvents (Figures 16a, b, c), the above result may not be so surprising.

In conclusion, the ϕ - Γ plots appear to be of prime importance in the study of adsorption at the mercury electrode-solution interface in respect to the roles played by the solvent and the supporting electrolyte. This statement is borne out by the fact that the shapes of these plots are quite sensitive to the nature of the solvent and the electrolyte but relatively insensitive to the type of adsorbate present.

Figure 18

Variation of surface pressure (ϕ) with surface concentrations (Γ) of naphthalene in methanolic 1M H_2SO_4.

q_M	μ coul. cm.$^{-2}$
12	○
8	△
4	+
0	□
-4	■

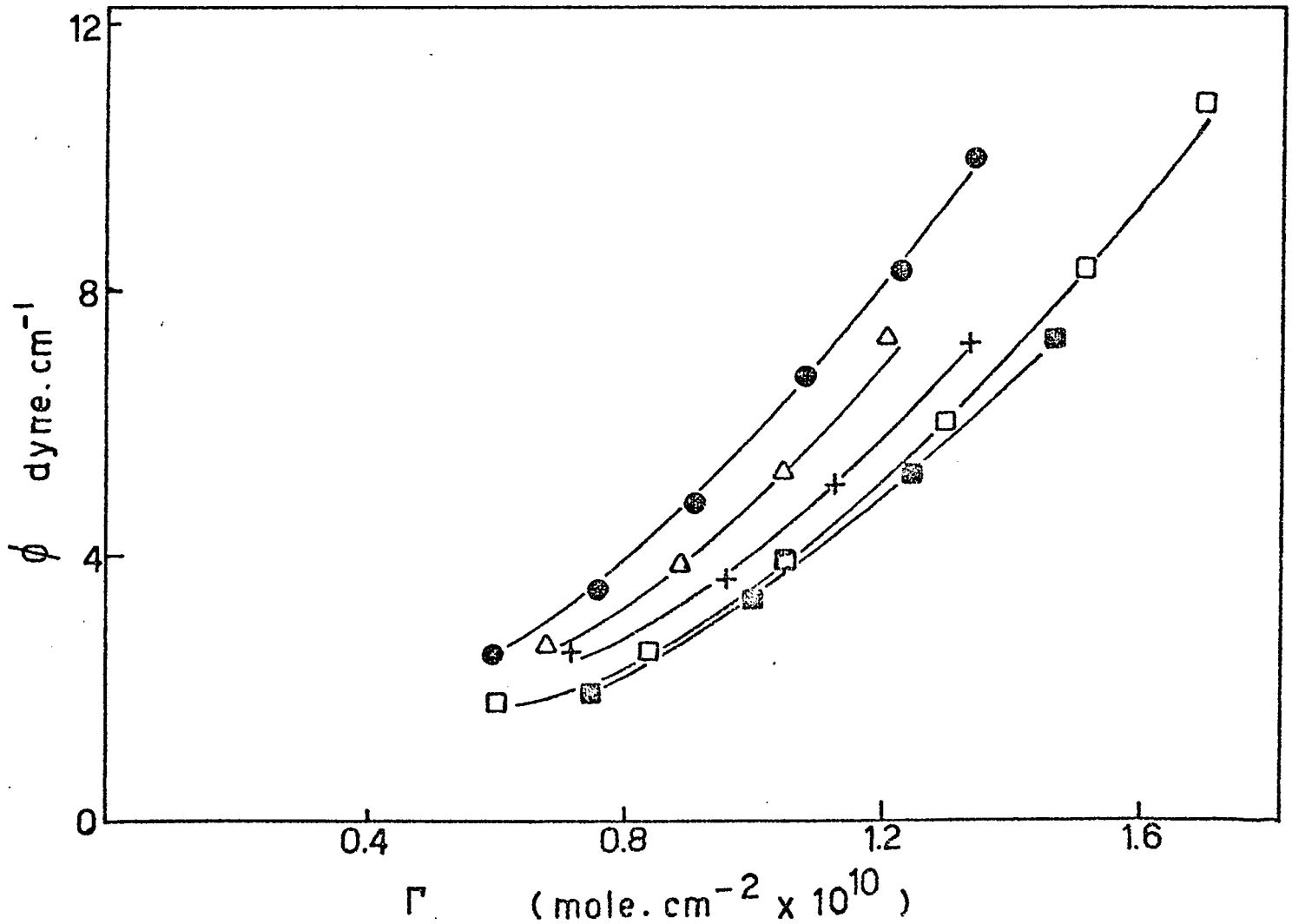
12
8
4
0
ϕ dyne.cm^{-1}
0.4
0.8
1.2
1.6
Γ (mole.cm^{-2} x 10^{10})

CHAPTER V

DISCUSSION

5.1 TYPES OF ISOTHERMS

As shown in § 1.5, an adsorption isotherm is a convenient way of expressing the condition of thermodynamic equilibrium between bulk and surface phases in terms of the surface and bulk concentrations, using a free energy quantity which can usually be interpreted independently in terms of particle-surface and particle-particle interactions. The adsorption isotherm is thus a basic relation in interphase equilibria.

5.1.1 Isotherms of the Langmuir Type

(a) Interactions at the Interface

The simple Langmuir isotherm can be written in the form

$$\frac{\Theta}{1 - \Theta} = K.C \qquad (54)$$

or in terms of Γ

$$\frac{\Gamma}{\Gamma_m - \Gamma} = K.C \qquad (55)$$

(see eqn. 40) where K is the adsorption coefficient related to the standard free energy of adsorption ΔG° by the equation

$$- RT \ln K = \Delta G^\circ \qquad (56)$$

As well as being applicable to solid surfaces at which fixed site adsorption occurs, this isotherm is also applicable at solution surfaces only when (i) the adsorbing particle is of the same size[77, 24]

as the solvent particle and when (ii) no lateral surface interactions occur between the solute (adsorbate) molecules. If the latter interactions are negligible in the adsorption processes, then ΔG^{o} is the sum of two terms: (i) the enthalpy of adsorption, ΔH^{o}, which is associated with the difference between the interaction energies of the solute and solvent with the (mercury) surface and the surrounding adsorbed solvent and (ii) an energy term $T\Delta S^{o}$ associated with the change of entropy for the substitutional adsorption process of the type referred to above where adsorbed solvent is replaced by adsorbate.

When lateral interactions are involved in the interphase, ΔH^{o} will be dependent on the coverage. In addition, many previous workers have neglected to consider structural factors which may affect $\Delta S^{o}_{rot, vib, trans}$ contributions. In the present work, such effects have been shown to be of considerable importance (§ 5.4.1).

It should be pointed out that in a recent review by Parsons[77], the term on the L.H.S. of eqn. 54 was considered to represent the "particle-particle interactions". This representation appears to be incorrect since the term in question is obtained in the statistical and kinetic derivations of the Langmuir isotherm in which it is assumed that the heat of adsorption is independent of coverage. This assumption implies that particle-particle interactions must necessarily be absent. Secondly, it can readily be seen that for any fixed value of Θ the term $\Theta/(1 - \Theta)$ does not vary with the magnitude of the interaction forces and thus it cannot be associated with particle-particle interactions, except as these limitingly determine the effective size of the adsorbate particles and hence the value of Γ_{max} corresponding to $\Theta = 1$.

The non-ideality effects in the surface phase can, in the first approximation, be represented in terms of the lateral interaction energy in the interphase as a linear function of Θ^{n} where n is

dependent on the type of adsorbate-adsorbate interaction (e.g. charge-charge or dipole-dipole). Equation 54 then takes a form similar to that of the Frumkin isotherm, viz.

$$\frac{\Theta}{1 - \Theta} \cdot \exp[r\Theta^n] = K.C \qquad (57)$$

where r is an interaction parameter containing the factor 1/RT. $\exp[r\Theta^n]$ can, in effect, be regarded as an activity coefficient term f so that

$$\frac{f\Theta}{1 - \Theta} = C.\exp[-\Delta G^o/RT] \qquad (58)$$

As in the electrolyte solution case, where unit activity is taken as the standard state, here it becomes convenient to evaluate ΔG^o for $f\Theta/1-\Theta = 1$, i.e. at $\Theta = 1/(1+f)$ as the standard state for the surface phase. Usually f is not directly known, so an apparent value of ΔG^o must be evaluated from eqn. (54) and extrapolated w.r.t. Θ to $\Theta = 0$, thus eliminating f in eqn. (58).

Following the procedures adopted in earlier publications[66, 78], ΔG^o has been obtained in the present work as a function of $\Gamma^{3/2}$ to test in the first place whether or not dipole repulsion effects mainly determine the non-ideality of the surface layer (see § 5.3).

(b) Molecular Areas in the Surface Phase

In cases where the ratio of the molecular areas of solvent and solute in the ad-layer differs appreciably from unity, the relative area factor may be as significant as the interaction effect and $f(\Gamma)$ of eqn. (40) will then be of the Flory-Huggins[79, 80] form $\Theta/[x(1 - \Theta)^x]$. In such a case, where x is the molecular size ratio of adsorbate and adsorbed solvent, it is of interest to compare

the results for ΔG^{o} or K which would be derived from the Langmuir (L) and the Flory-Huggins (F. H.) type isotherms for a given determined coverage in equilibrium with adsorbate at a fixed bulk concentration C in the solution. Writing the F. H. isotherm as a function of Θ in the form

$$\frac{\Theta}{x(1-\Theta)^{x}} = K_{F.H.} \cdot C \qquad (59)$$

it is seen immediately that

$$K_{L}/K_{F.H.} = x(1 - \Theta)^{x-1} \qquad (60)$$

or

$$\frac{1}{RT}(\Delta G^{o}_{F.H} - \Delta G^{o}_{L}) = \ln x + (x - 1)\ln(1 - \Theta) \qquad (61)$$

$(\Delta G^{o}_{F.H} - \Delta G^{o}_{L})/2.30\ RT$ is shown as a function of Θ in Figure 19 for various values of x from 1 (Langmuir case) to 6, i. e. over the range applicable to adsorption of pyridine from water (x = 3 - 4) considered in the present work. It is evident that at appreciable coverages (Θ > 0.5 - 0.7), the relative area factor can introduce changes in the evaluated ΔG^{o} quantity which are comparable with the magnitude of ΔG^{o} commonly obtained (ca. -2 to -6 Kcal. mole^{-1}) for substitutional molecular adsorption at mercury. However, at Θ = 0.25 the ΔG^{o} values derived from both isotherms are almost identical.

5.1.2 "Gaseous" Surface Phase

a) Properties of the "Gaseous" Interphase

A variety of isotherms based on the equation of state for "gaseous" surface films have been used to represent the adsorption process at the mercury-solution interface. The equations of state for such films are as follows:

Figure 19

Values of the difference of ΔG^{o} for an adsorption process as calculated in terms of a Flory-Huggins and a Langmuir adsorption isotherm for a given value of coverage Θ of an adsorbate in equilibrium with the adsorbate in solution at a fixed concentration.

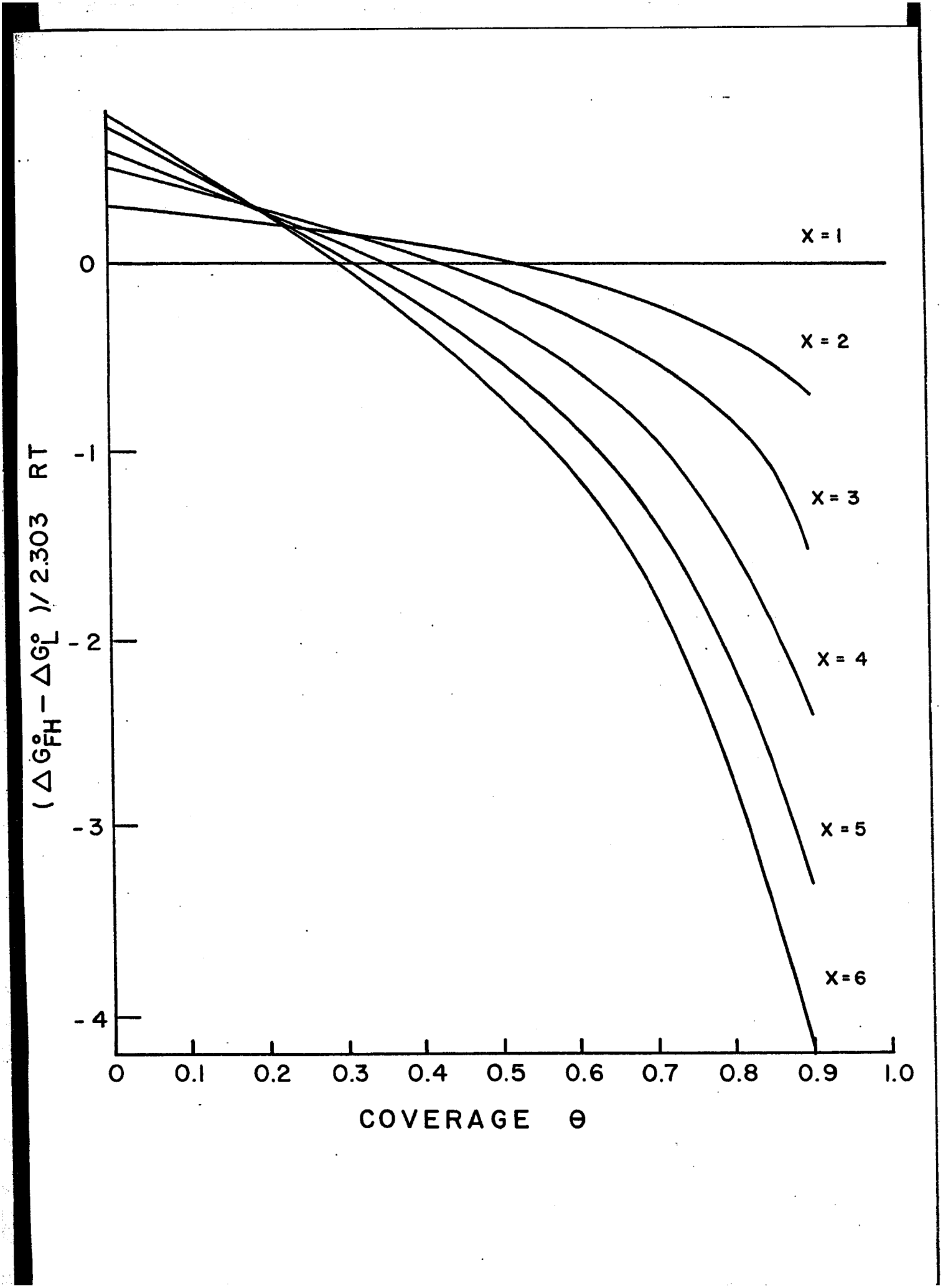
X = 1
X = 2
X = 3
X = 4
X = 5
X = 6
0
-1
-2
-3
-4
0
0.1
0.2
0.3
0.4
0.5
0.6
0.7
0.8
0.9
1.0
COVERAGE θ
(ΔG°FH − ΔG°L) / 2.303 RT

Henry's Law $$\phi = RT\Gamma \quad ; \tag{62}$$

Volmer $$\phi = \frac{RT\Gamma}{1 - b\Gamma} \tag{63}$$

where 'b' is the co-area of the adsorbate molecule;

Virial $$\phi = RT\Gamma + g\Gamma^2 \tag{64}$$

where g is an interaction parameter;

van der Waals $$\phi = \frac{RT\Gamma}{1 - b\Gamma} + g\Gamma^2 \tag{65}$$

(For tables of equations of state and the corresponding isotherms see ref's. 49, 34, and 27. The relationship between the equation of state and the corresponding isotherm is illustrated in § 1.5 and ref. 27).

In the above treatments of the adsorption process, the adsorption force is considered to be non-localised, so that the adsorbed particle is free to move across the surface in an essentially uniform force field. This situation applies ideally to mercury. The equation of state which corresponds to Henry's Law (eqn. (62)) is one in which molecular areas and particle-particle interactions are not taken into account. When these two effects are introduced separately into the simple model, the Volmer and virial equations of state are obtained, respectively. The van der Waals surface equation of state is obtained when the molecular area and the particle-particle interactions of the solute molecules are both included in the description.

b) Evaluation of Thermodynamic Quantities from the Volmer Equation

If a gaseous interphase exists between two bulk phases, then the critical properties for the surface phase must differ from those of the bulk phases. Although there have been no direct investigations on the temperature dependence of the 2-dimensional condensation phenomenon of adsorbates at the air-water interface, it appears evident that a critical temperature exists, above which no discontinuous condensation in the surface phase can take place, e. g. at the air-water interface, the fatty acids with chain lengths of up to 12 carbon atoms all exhibit gaseous behaviour over the complete surface pressure range[117], an indication that the study was conducted above the critical temperature. Substances of longer chain length showed the existence of two phases in the surface layer. However, experiments[118, 119] have shown, that at the gas-solid interface, 2-dimensional phase transformations similar to those occurring in unimolecular layers on water can occur, and 2-dimensional critical temperatures ($T_{c,2}$) have been recorded for CO adsorbed on steel[118] (93°K) and n-heptane adsorbed on ferric oxide[119] (29°C).

The 2-dimensional van der Waal's equation (eqn. (65)) which can be written in the form

$$(\phi + \frac{g}{A^2})(A - b) = RT \qquad (65a)$$

where $A = 1/\Gamma$, enables the critical data to be expressed in terms of the constants g and b in the same way as can be done for the 3-dimensional case. At the critical point

$$\frac{d\phi}{dA} = 0 \qquad \text{and} \qquad \frac{d^2\phi}{dA^2} = 0$$

and therefore the critical values are

$$\phi_{c,2} = \frac{g}{27b^2} ,$$

$$A_{c,2} = 3b$$

and $$T_{c,2} = \frac{g}{27Rb} \qquad (65b)$$

It has been shown by de Boer[115] that if a' and b' are the 3-dimensional van der Waal's constants, then by a simple treatment it can be shown that

$$b = \frac{3b'}{4d}$$

and $$g = \frac{3a'}{8d}$$

where the adsorbate particle is a sphere of diameter d.

The normal 3-dimensional critical temperature, T_c, is given by

$$T_c = \frac{8a'}{27Rb'}$$

and thus

$$T_{c,2} = \frac{1}{2} T_c \qquad (65c)$$

i.e., a gaseous surface film can arise at temperatures and pressures at which a 3-dimensional bulk phase would normally be condensed.

It should be noted that g is positive for attractive interactions between the adsorbate particles and thus $T_{c,2}$ depends on the type and magnitude of the interactions involved (eqn. (65b)). If the interactions are small then $T_{c,2}$ will be low and a gaseous

surface phase will be more likely to result. Attractive interactions could be decreased by a greater alignment of dipoles in the surface phase than in the bulk phase.

A method for evaluating the free energy of adsorption in the supposed absence of solute-solute interactions has been developed in this work. The treatment is analogous to that first proposed by Kemball and Rideal[81] for the adsorption of vapours on mercury.

The surface phase is considered to have a thickness (cf. Guggenheim[110]) of 6 Å and thus the two-dimensional surface concentration can be converted to a three-dimensional concentration. The standard states of both the surface and bulk phases can thus be taken as 1M. However, it should be kept in mind that the standard state of the surface phase is dependent on the surface layer thickness which is usually chosen on the basis of molecular size of the adsorbate but is independent of temperature.

Let C_s be the concentration of the solute in the standard state in the bulk phase (i.e. 1M) and C_1 be the bulk concentration which would be in equilibrium with a standard state concentration of 1M in the surface layer where the adsorption forces are operating.

The free energy change associated with the adsorption, taking into account the two standard states is given by

$$\Delta G = -RT \ln \frac{C_s}{C_1} \qquad (66)$$

From the above, it is seen that the adsorption of the molecules from the bulk phase at the equilibrium concentration C_1 to the standard adsorbed state, is, by definition, not accompanied by a change in free energy since for the condition of equilibrium

$$G_{ads.} = G_{solute(bulk)}$$

From the Gibbs adsorption equation (see eqn. 6), expressed in terms of surface pressure,

$$\Gamma = \frac{C}{RT} \left(\frac{\partial \phi}{\partial C}\right) \tag{67}$$

and thus, for the standard state of the adsorbed phase,

$$C_1 = RT \quad \Gamma_s \left(\frac{\partial C}{\partial \phi}\right) \tag{68}$$

and therefore from eqn. (66)

$$-\Delta G = RT \ln\left[\frac{C_s}{RT \ \Gamma_s} \left(\frac{\partial \phi}{\partial C}\right)\right] \tag{69}$$

Noting that C_s is in units of mole.l^{-1} and Γ_{s_o} is in moles per cm.^{2} in the standard adsorbed layer of thickness 6 Å, then

$$-\Delta G = RT \ln\left(\frac{10^{11}}{6.RT} \left(\frac{\partial \phi}{\partial C}\right)\right) \tag{70}$$

$$= RT\left(k - \ln T + \ln \frac{\partial \phi}{\partial C}\right) \tag{71}$$

where $k = \ln 10^{11}/6R$ is a constant, the magnitude of which is dependent on the value taken for the thickness of the adsorbed layer.

In this work, as in that of Kemball and Rideal[81], the ϕ vs C (or ϕ vs - gas pressure[81]) plots were not linear even at the lowest surface coverages. Now since eqn. (71) is only applicable when the adsorbed film behaves ideally, the initial value of $\partial\phi/\partial C$ is required. Graphical procedures for determining the slope of the ϕ vs C plot as ϕ approaches zero are difficult to carry out with precision, since the graph is curved and the percentage error in ϕ at small values of ϕ is usually quite large.

Experimentally, it has been found convenient to select an isotherm that will represent the ϕ vs C relationship over a large portion of the concentration range and to extrapolate to obtain $(\partial\phi/\partial C)_{\phi=0}$.

The Volmer equation of state was used in the following method for obtaining the free energy of adsorption when the surface phase was considered ideal.

Writing equation (63) in the form

$$\frac{\phi}{\Gamma} = \phi b + RT \tag{72}$$

and substituting for Γ from eqn. (67)

$$\phi RT \frac{\partial \ln C}{\partial \phi} = \phi b + RT$$

i.e.

$$\frac{\partial \ln C}{\partial \phi} = \frac{b}{RT} + \frac{1}{\phi}$$

On integrating w.r.t. ϕ, and introducing the integration constant m,

$$\ln C = \frac{b\phi}{RT} + \ln \phi + m$$

or

$$\ln \frac{C}{\phi} = \frac{b\phi}{RT} + m \tag{73}$$

i.e.

$$C = \phi \exp\left[\frac{b\phi}{RT} + m\right]$$

and

$$\frac{\partial C}{\partial \phi} = \exp\left[\frac{b\phi}{RT} + m\right] + \frac{b\phi}{RT} \exp\left[\frac{b\phi}{RT} + m\right]$$

Therefore

$$\lim_{\phi \to 0} \left(\frac{\partial C}{\partial \phi}\right) = e^{m}$$

or

$$\lim_{\phi \to 0} \left(\frac{\partial \phi}{\partial C}\right) = e^{-m} \tag{74}$$

Thus, from eqn. 71, $-\Delta G = RT[k - \ln T - m]$ (75)

Hence the plot of $\ln \frac{C}{\phi}$ vs ϕ (eqn. (73) gives an intercept m which can be used in eqn. (75) for the evaluation of the free energy change which accompanies, at constant temperature, the transference of a mole of solute from the standard dissolved state to a standard adsorbed state.

The entropy of adsorption can be obtained from the variation of ΔG with temperature, i.e.

$$\Delta S = - \frac{\partial \Delta G}{\partial T}$$

$$= R[(k - 1) - \ln T - m - \frac{\partial m}{\partial \ln T}] \qquad (76)$$

and the corresponding enthalpy is

$$\Delta H = RT[1 + \frac{\partial m}{\partial \ln T}] \qquad (77)$$

which is independent of k and the thickness of the surface phase, i.e. ΔH is independent of the standard state chosen.

The parameter 'b' found from the slope of the $\ln C/\phi$ vs ϕ plots is expected to represent twice the molecular area (cf. the van der Waal's b coefficient) when the simple theory of molecules in a dilute gas is assumed but in the work of Kemball and Rideal[81] b was approximately equal to the molecular area found from liquid volume measurements. This latter interpretation of b is more satisfying theoretically since the Volmer equation of state would otherwise indicate that infinite surface pressures would be required to increase the coverage above $\Theta = 0.5$. The relation $b = 1/\Gamma_m$ has been found empirically by Hill[114] and Livingstone[116] and a theoretical explanation has been given by de Boer[115].

It should be noted that eqn. (73), from which the parameters m and b are obtained, relies entirely on the experimentally evaluated quantities ϕ and C and thus errors arising in derived quantities such as Γ are not involved.

Before the methods described above in 5.1.1 and 5.1.2 for thermodynamic analysis of the results are applied to the data obtained in the present work, it is first necessary to examine the question of (a) the way in which the effective surface area of adsorbates may be influenced by their orientation; and (b) how estimated areas can influence the determination of apparent interactions between adsorbate molecules in the interphase. These problems will be discussed below in §§5.2 and 5.3.

5.2 ORIENTATION EFFECTS

5.2.1 Effect of Orientation on Potential at Constant Charge

The two regions sometimes found in the $(E_b - E)_{p.z.c.}$ vs Γ plots (e.g. see Figure 9) for the adsorption of neutral polar molecules have previously been interpreted in terms of the orientation of the adsorbate molecules (see § 4.4) and the junction of the lines in such plots has been regarded as indicating the coverage at which complete reorientation of the adsorbate molecules occurs.

This interpretation should be modified since the linear regions of the $\Delta E_{p.z.c.}$ vs Γ plots for the adsorption of neutral polar molecules at high coverages seldom extrapolate to $\Delta E_{p.z.c.} = 0$ at zero coverage. If complete reorientation did occur then the dotted line of Figure 9(a) would represent the results. The experimental data which can be represented by the solid line of Figure 9(a) indicates that reorientation does not occur with increasing coverage, ($\Gamma > \Gamma_a$) but, on the contrary, a surface concentration of molecules Γ_a with dipoles lying horizontally in the surface remains constant over the high coverage region. The increased slope (where $\Gamma > \Gamma_a$) must be due to additional adsorbate molecules entering the surface phase with their dipoles aligned and oriented perpendicular to the surface. Mathematically the condition can be expressed in the following way.

For $\Gamma < \Gamma_a$

$$\Delta E_{p.z.c.} = \frac{4\pi\mu_1}{\varepsilon_1}\Gamma$$

and for $\Gamma > \Gamma_a$

$$\Delta E_{p.z.c.} = \frac{4\pi\mu_1}{\varepsilon_1}\Gamma_a + \frac{4\pi\mu_2}{\varepsilon_2}(\Gamma - \Gamma_a)$$

In Figure 9, the effects of the surface concentration of pyridine (adsorbed from aqueous $NaClO_4$ solutions) and the temperature on the p.z.c. can be seen. The value of Γ_a defined above decreased with increasing temperature, a situation which could indicate that the π-bonding of the pyridine molecules with the surface is unfavourable at higher temperatures and thus the adsorption of vertically oriented pyridine molecules can begin at lower surface concentrations.

It is important to note that in the high coverage region $[\partial(\Delta E_{p.z.c.})/\partial\Gamma]$ is, to a first approximation, independent of temperature so that it is unlikely (as discussed above) that reorientation with increasing coverage takes place. However, there is a large variation of $(\Delta E_{p.z.c.})_{\Gamma > \Gamma_a}$ with temperature and this is probably due to the dependence on the temperature, of the surface concentration (Γ_a) of pyridine molecules lying in the flat position on the surface.

5.2.2 Effect of Orientation on Effective Molecular Area

The accurate evaluation of the free energy of adsorption using the Langmuir model relies on the accuracy of the determination or estimation of the parameter Γ_m. It is to be noted, however, that the value to be assigned to Γ_m will usually be dependent on

orientation in the case of the neutral organic molecules. Under conditions of varying Γ_m ($1/\Gamma_m$ = molecular area), the analysis becomes quite difficult and usually, in previous work, a representative constant value of the molecular area has been simply chosen to be used over the entire ranges of concentration and charge studied in the experiment. In certain cases, this procedure is obviously of questionable validity, particularly when, with changing surface charge or temperature, changing orientation of the adsorbate occurs.

Two methods have been used to obtain suitable values of Γ_m for the systems under investigation. A knowledge of the bond angles and the interatomic distances in the adsorbate molecules, in addition to information about the van der Waals radii for the atomic species present, allows an estimate of the molecular area to be made once the orientation has been decided upon. Secondly, at high bulk concentrations where Γ tends to become constant and independent of the bulk concentration, that value of Γ can be taken as being equivalent to Γ_m. However, difficulties arise in this experimental method since the maximum value of Γ is usually charge (or potential) dependent (approximate Γ_m values calculated from ref. 67 for pyridine adsorbed from 1M KCl solution are given in Table I).

A third method for obtaining the molecular area is to equate the value of 'b', the co-area parameter in the Volmer equation (§ 5.1.2), with the required area. Fourthly, at low surface coverages where solute-solute interactions in the surface phase are negligible, the Langmuir equation can be rearranged as follows.

$$\frac{\Theta}{1 - \Theta} = K.C$$

i.e.

$$\frac{\Gamma}{\Gamma_m - \Gamma} = K.C$$

TABLE I

MOLECULAR AREA OF PYRIDINE

Electrolyte	1M KCl; 25°			0.03M $NaClO_4$; 20°	
q_M	Ref. 85	L	V	L	V
12	58	128	58	-	28
10	54	106	52.7	90.5	32.5
8	50	89	43	97	38
6	47	74.5	-	95	41.5
4	43	64	31	74	44.5
2	39.5	52	-	65	42.5
0	35	46.5	22	55	40.5
-2	31	44	-	51	38.0
-4	30	-	-	44	34.0
-6	29	-	-	42.5	35.5

Ref. 85: maximum value of Γ obtained at high bulk concentrations.

(L) From Langmuir eqn., $\frac{C}{\Gamma} = \frac{1}{\Gamma_m K} + \frac{C}{\Gamma_m}$

(V) From Volmer eqn., $\ln C/\phi = b\phi/RT + m$

Upon inverting and rearranging,

$$\frac{C}{\Gamma} = \frac{1}{K\,\Gamma_m} + \frac{C}{\Gamma_m} \qquad (78)$$

A plot of C/Γ vs C hence gives a linear relation* with a slope equivalent to the molecular area, and the quotient of the slope and intercept enables K to be evaluated. This procedure is also valid when the Flory-Huggins isotherm is used in the region of low surface concentration. However, the complete evaluation of the parameters x, Γ_m and $K_{F.H.}$ cannot be made. From eqn. (59)

$$\frac{\Theta}{(1-\Theta)^x} = xK_{F.H.}.C$$

and for $\Theta \ll 1$

$$\frac{\Theta}{1-x\Theta} \doteq xK_{F.H.}.C$$

so that

$$\frac{1}{\Theta} - x = \frac{1}{xK_{F.H.}.C}$$

i.e. $$\frac{C}{\Gamma} = \frac{1}{xK_{F.H.}\,\Gamma_m} + \frac{C.x}{\Gamma_m} \qquad (78a)$$

As in the Langmuir case, linearity results in the plot of C/Γ vs C.

The latter two methods are not usually employed for finding Γ_m when equation 54 is used for analysing the data. A

---

*Linear relations will not, however, usually be observed if significant intermolecular attractive or repulsive forces arise between the adsorbate molecule leading to a dependence of K or the equivalent "standard" free energy of adsorption on Γ / Γ_m.

comparison of the values obtained for the molecular area of pyridine by the various methods outlined above is presented in Table I. The Langmuir results show a marked difference from those obtained using the Volmer equation and this may be accounted for in part in the following way. As suggested in § 5.1.2, the molecular area of the adsorbate can be equated with b, the co-area parameter of the Volmer equation of state. It remains to be shown that the value of b is half that of $(1/\ \Gamma_m)_L$ derived from the Langmuir equation (eqn. 78).

The Volmer isotherm (eqn. 45) can be expressed in terms of Γ as follows

$$K.C = \frac{RT\,\Gamma}{1 - b}\ \exp\left[\frac{b\,\Gamma}{1 - b}\right]$$

or

$$C = \frac{K'}{A - b}\ \exp\left[\frac{b}{A - b}\right]$$

where K' is a constant. For large values of A

$$C = \frac{K'}{A - b}\ \left(1 + \frac{b}{A - b}\right)$$

which may be transformed into

$$C = \frac{K'}{A - [2b - b^2/A]}\ .$$

This expression is of the same form as the Langmuir adsorption isotherm where

$$(1/\ \Gamma_m)_L = 2b - b^2/A$$

so that, when A is sufficiently large,

$$(1/\ \Gamma_m)_L = 2b$$

a result which is supported by empirical evidence (Table I). It should be stressed at this point, however, that if data satisfy the Volmer

equation of state then linearity in the C/Γ vs C plots (see eqn. (78)) will only arise when A is sufficiently large (as discussed above). This matter will be discussed further in § 5.3f. A fuller discussion of the variation of the molecular area with surface charge density and surface concentration must be delayed until the subject of the solute-solute interactions in the adsorbed phase (§ 5.3) has been examined.

5.3 THE APPARENT SOLUTE-SOLUTE INTERACTION

In this section it will be shown that the "solute-solute" interaction for the neutral molecules of the adsorbate could in many cases be considered negligible when solvents with large intermolecular bonding energies are used in the systems studied. If this hypothesis proves to be correct, then its consequences will change considerably those ideas held previously[66] concerning the coverage-dependent energy term in the Frumkin isotherm (eqn. 57) for the adsorption of neutral molecules where 'n' has the value of 3/2 and where a fixed Γ_m is chosen for the analysis of the whole range of results. The hypothesis mentioned above could be justified on several grounds:

a) The free energy of adsorption should be dependent on the orientation of the adsorbate under conditions of fixed surface charge density. From this assumption it would be expected that the plot ΔG^o vs Γ (or Θ or $\Theta^{3/2}$) should have a definite inflexion at the same coverage at which the inflexion in the $(E_b - E)_{p.z.c.}$ vs Γ plot is found. In all cases, except for the adsorption of 2-chloropyridine from aqueous N KCl solution in ref. 66, inflexions were not observed on the ΔG^o vs $\Theta^{3/2}$ plots which could correspond in coverage to the sharply drawn inflexions of the $\Delta E_{p.z.c.}$ vs Γ plots. The same conclusions can be drawn from the present work.

b) The second piece of evidence arises in regard to the coverage dependence of the free energy of adsorption of naphthalene (Figure 39), the molecules of which are entirely non-polar. No repulsion forces would be expected between the adsorbed molecules of naphthalene; on the contrary, attractive forces of the van der Waals type would be more probable and ΔG^{o} would be expected to increase negatively with coverage whereas the opposite effect is actually observed. Therefore the variation of ΔG^{o} with coverage is not dependent necessarily on the solute-solute interaction in the ad-layer.

c) Thirdly, there is evidence from the temperature dependence of the free energy of adsorption of pyridine from aqueous $NaClO_4$ solutions (§ 5.4.1a) that the water structure in the ad-layer is extremely important and is probably the controlling factor in the adsorption process, i.e. the change in $T\Delta S^{o}$ (associated with the solvent structure) with coverage may be more influential in ΔG^{o} than the enthalpy associated with the adsorbate-adsorbate interaction.

d) The picture given above of the solvent playing an important role in the adsorption process is supported by the results shown in §§ 4.5.1 and 4.6. The $\emptyset$ - Γ plots for the adsorption of acetophenone from various solvents were found to be different, but different solutes, such as acetophenone and pinacol, adsorbed from the same solvent, 20% water-methanol, gave similar plots, as did the solutes acetophenone and naphthalene from the same solvent, pure methanol. (These effects seen in Figures 16 and 18.).

e) Theoretically the 3/2 power in the repulsion energy term should only be appropriate at low coverages where the length of the dipole (ℓ) is much smaller than the distance between the dipoles $(2r)$[83]. If the lower acceptable limit of the ratio r/ℓ is say 2, and ℓ is approximately the diameter of the molecule, then the upper limit of the coverage for which $\Theta^{3/2}$ is acceptable as a representation

of the dipole-dipole interaction, is $\Theta = 0.25$. However, when the dipole moment is very large and localised in a small segment of the molecule, the $\Theta^{3/2}$ relation may then be theoretically applicable up to higher coverages. The changes in the slopes of the $\Delta G^{o}_{p.z.c.}$ vs Γ and $(E_b - E)_{p.z.c.}$ vs Γ plots were observed to occur at the same Γ for 2-chloropyridine[66] and this behaviour was recorded in (a) above as being exceptional. The molecule of 2-chloropyridine had the largest dipole moment of all those considered and the magnitude of the moment cannot be accounted for by direct vector addition of the bond (or group) moments. Cumper and Vogel[82] have shown that when induction factors are taken into account, the calculated dipole moment was in closer agreement with the experimental value. Thus the dipole length is small (separation distance of N and Cl) and the moment is large. These properties of 2-chloropyridine would theoretically justify the inclusion of intermolecular interaction energy of the adsorbate in the controversial interaction energy term ($\Gamma\ \Theta^{n}$) of equation (57).

f) The apparent coverage dependence of the Langmuir-type standard free energy of adsorption (ΔG^{o}_{L}), which is often found in the analysis of experimental data, can be explained on grounds other than those of interaction effects.

The Langmuir isotherm

$$\frac{\Theta}{1 - \Theta} = C.\exp[-\Delta G^{o}_{L}/RT]$$

can be compared to the Volmer isotherm written in a similar form

$$\frac{\Theta}{1 - \Theta} = C.\exp\left(\frac{\Theta}{1 - \Theta}\right)\exp[-\Delta G^{o}_{v}/RT]$$

(cf. eqn. 45). Haydon and Taylor[120] have made comparisons between these two isotherms for the adsorption of neutral molecules at the oil-water interface.

If the surface phase is gaseous and the Volmer isotherm is applicable in describing the adsorption behaviour, then ΔG_v^o will be constant and ΔG_L^o will be a function of Θ as indicated in the equation

$$\Delta G_L^o = \Delta G_v^o - \frac{RT\Theta}{1 - \Theta}$$

which is readily derived from the two equations above.

In fact, for small values of Θ,

$$\frac{\Theta}{1 - \Theta} \doteq \Theta(1 + \Theta)$$

$$= \Theta + \Theta^2$$

which could be comparable with $\Theta^{3/2}$ in the range of Θ applicable to experimental results. Thus the application of the Langmuir treatment to a gaseous surface phase can result in a free energy of adsorption being derived which is dependent on coverage.

In conclusion, it can be shown that if the charge-dependent Γ_m values found experimentally by the second method outlined in § 5.2.2 (i.e. from the plateau on the Γ vs log C plots), are used in the calculation of the free energy of adsorption in any one system, the variation of ΔG^o with coverage will be quite small (see Figure 39 for q = +12). When, however, a single Γ_m value (which corresponds to a particular value of surface charge q'_M) is chosen for the whole system, the slope of the ΔG^o vs Γ plot will be small for q'_M but will increase for other values of q_M as $|q'_M - q_M|$ increases. Thus, instead of employing a fixed surface molecular area for the adsorbate at all surface charge densities, it should be possible, and in some cases may be necessary, to consider Γ_m as a variable parameter. Since Γ_m may also be dependent on the surface concentration, the Langmuir equation becomes less suitable for evaluating the free energy of adsorption.

Since the evidence here, or in any other work hitherto published, is not sufficiently conclusive for determing whether a fixed or a variable Γ_m should be used in the evaluation of the free energy of adsorption, the traditional method (using a fixed value of Γ_m) will be employed but the evaluation of the adsorption process using a variable Γ_m will in some cases be carried out for comparison.

5.4 STUDY OF THE ADSORPTION OF PYRIDINE AT VARIOUS TEMPERATURES: ENTHALPY AND ENTROPY EFFECTS

5.4.1 Interpretation in terms of the Langmuir Type Isotherm

In the present discussion of the adsorption of pyridine from aqueous 0.03 M $NaClO_4$ solutions, the results will be evaluated in terms of ΔG^o, ΔH^o and ΔS^o derived for isosteric conditions at constant q_M^* (and constant supporting electrolyte activity) using the ξ function employed in various publications of Parsons[20] and others[15,58]. The Gibbs equation also gives the excess entropy (see eqn. (3)). It is evident (cf.[58]) that $-d\gamma/dT$ does not simply give σ unless the chemical potential(s) of the components i and n in solution are kept constant at constant E. In practice, this is difficult to achieve and implies, for example, that for a neutral adsorbate such as pyridine, the partial vapor pressure at various temperatures must be kept constant by adjustments of the concentration or by appropriate interpolations. Alternatively if $-d\mu_i/dT$ is known (it is the partial molar entropy of the adsorbate in solution), σ can be evaluated[58]. In fact σ will be a complex quantity related to the temperature dependence of the free energy of solute and solvent species, and their interactions, in the interphase. It is for this reason that the entropy (and heat) of the substitutional adsorption process directly evaluated from ΔG^o, calculated for various

*The subscript M has been deleted in § 5.4.1 to conform with the usage in the work now in press[122].

temperatures, is the quantity to which preferred attention is given in the present work.

Plots of ΔG° on the basis of equation (54) (used for evaluation purposes only) are shown* in Figures 20a-c for various temperatures and at various q values. At T = 280.5°K, for example, ΔG° becomes less negative with coverage (plotted as $\Gamma^{3/2}$), the effect increasing as q becomes more positive. The trend shown in the low surface concentration region is thought to be due to the inaccuracy of the computational method (see § 4.1). The results obtained in dilute (0.03N) $NaClO_4$ may be assumed to refer to pyridine molecule adsorption (hydrolysis effects are negligible[84]) in the absence of significant specific adsorption of anions. It is for this reason that they probably differ from the previous results[66] obtained for pyridine adsorption at 298°K which were based on experiments in 1N KCl. The results in that supporting electrolyte were interpreted[66, 15, 85] in terms of relatively sudden orientation of pyridine at a critical Γ dependent on electrode potential, and the behaviour was shown[15] to be dependent on the Cl^- adsorption. It is evident that the present results in the presence of ClO_4^- anions are rather different although formally, over the ΔG° - $\Gamma^{3/2}$ curves, ΔG° is numerically decreasing, corresponding to repulsion or other non-ideality effects, but the apparent repulsion effects (see § 5.3) are evidently least at the most negative q values.

The extent to which the variations of ΔG° calculated from the experimental observations depend on the choice of x in eqn. (59) is shown in Figure 21 for x = 1, 2 and 4. Space-filling models

---

*Although the ΔG° values derived here vary significantly with Γ or Θ, the effects are not very large and might be minimised by choice of somewhat different Γ_m values. The values of $T\Delta S^{\circ}$ and ΔH° derived from $d\Delta G^{\circ}/dT$ are, however, much larger (see below) and are not invalidated by any arbitrariness in the choice of Γ_m (see p.102).

Figure 20

Evaluation of apparent ΔG^{o} values as a function of $\Gamma^{3/2}$ for pyridine adsorption at mercury at various values of q and at several temperatures.

(a) 280.5°K (b) 313°K (c) 353°K

(In [b], the ΔG^{o} data were evaluated for two values of the saturation coverage Γ_{m}).

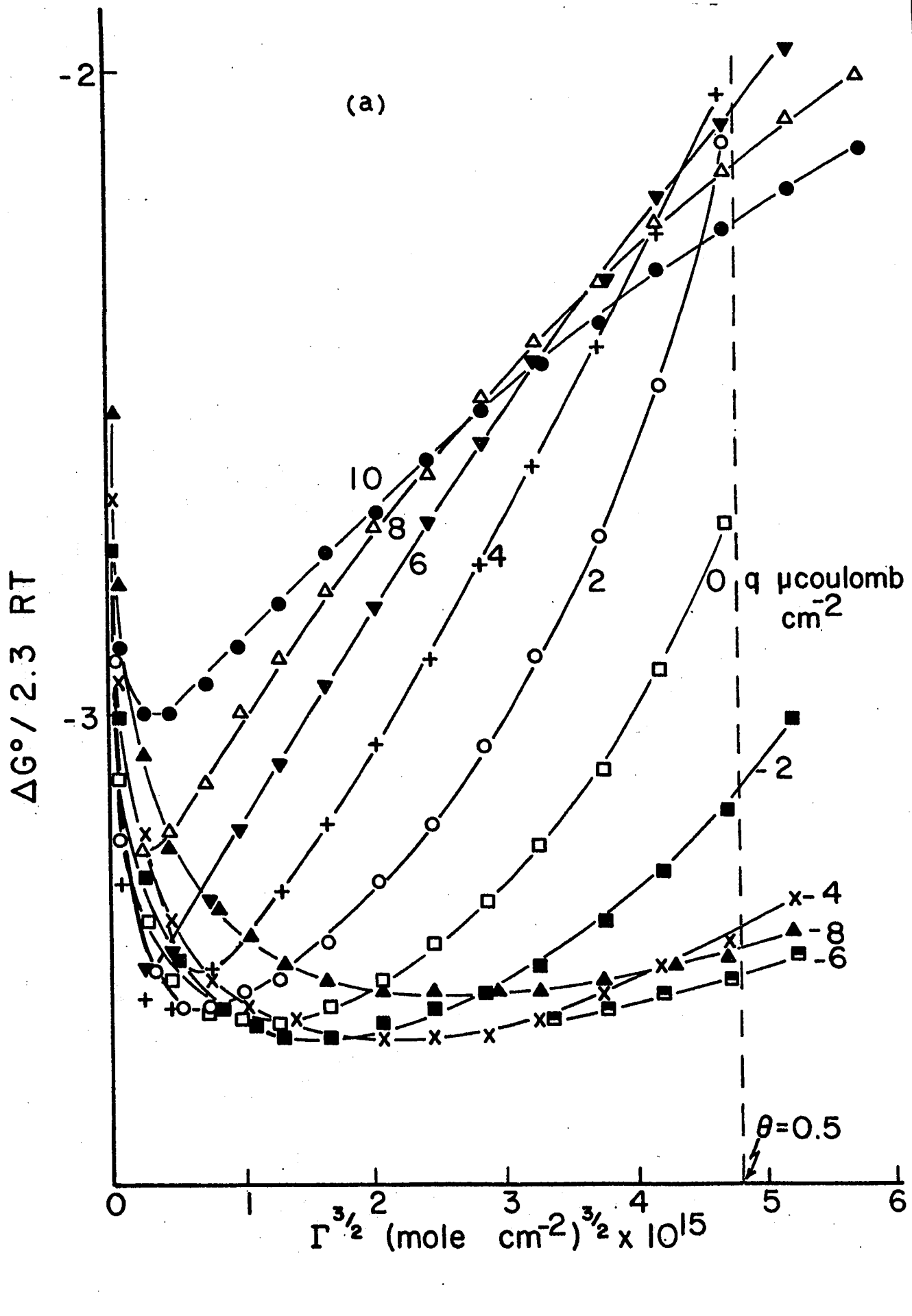
(a)
-2
-3
ΔG° / 2.3 RT
10
8
6
4
2
0
-2
-4
-8
-6
q μcoulomb cm⁻²
θ=0.5
0
1
2
3
4
5
6
Γ^3/2 (mole cm⁻²)^3/2 x 10^15

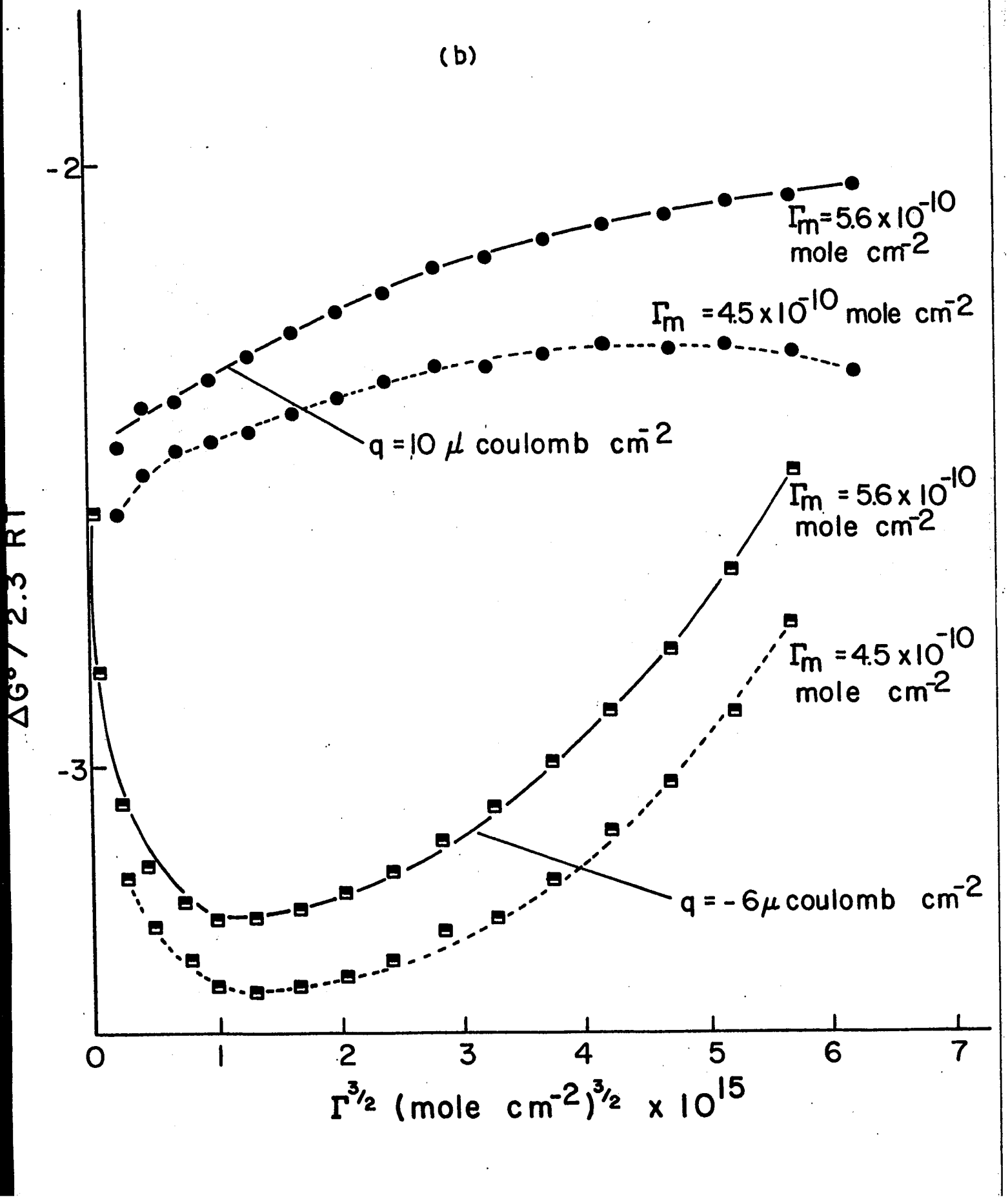
(b)
-2
-3
$\Delta G^\circ / 2.3\ RT$
$\Gamma_m = 5.6 \times 10^{-10}$ mole cm^{-2}
$\Gamma_m = 4.5 \times 10^{-10}$ mole cm^{-2}
q = 10 μ coulomb cm^{-2}
$\Gamma_m = 5.6 \times 10^{-10}$ mole cm^{-2}
$\Gamma_m = 4.5 \times 10^{-10}$ mole cm^{-2}
q = - 6μ coulomb cm^{-2}
0
1
2
3
4
5
6
7
$\Gamma^{3/2}$ (mole cm^{-2})$^{3/2}$ x 10^{15}

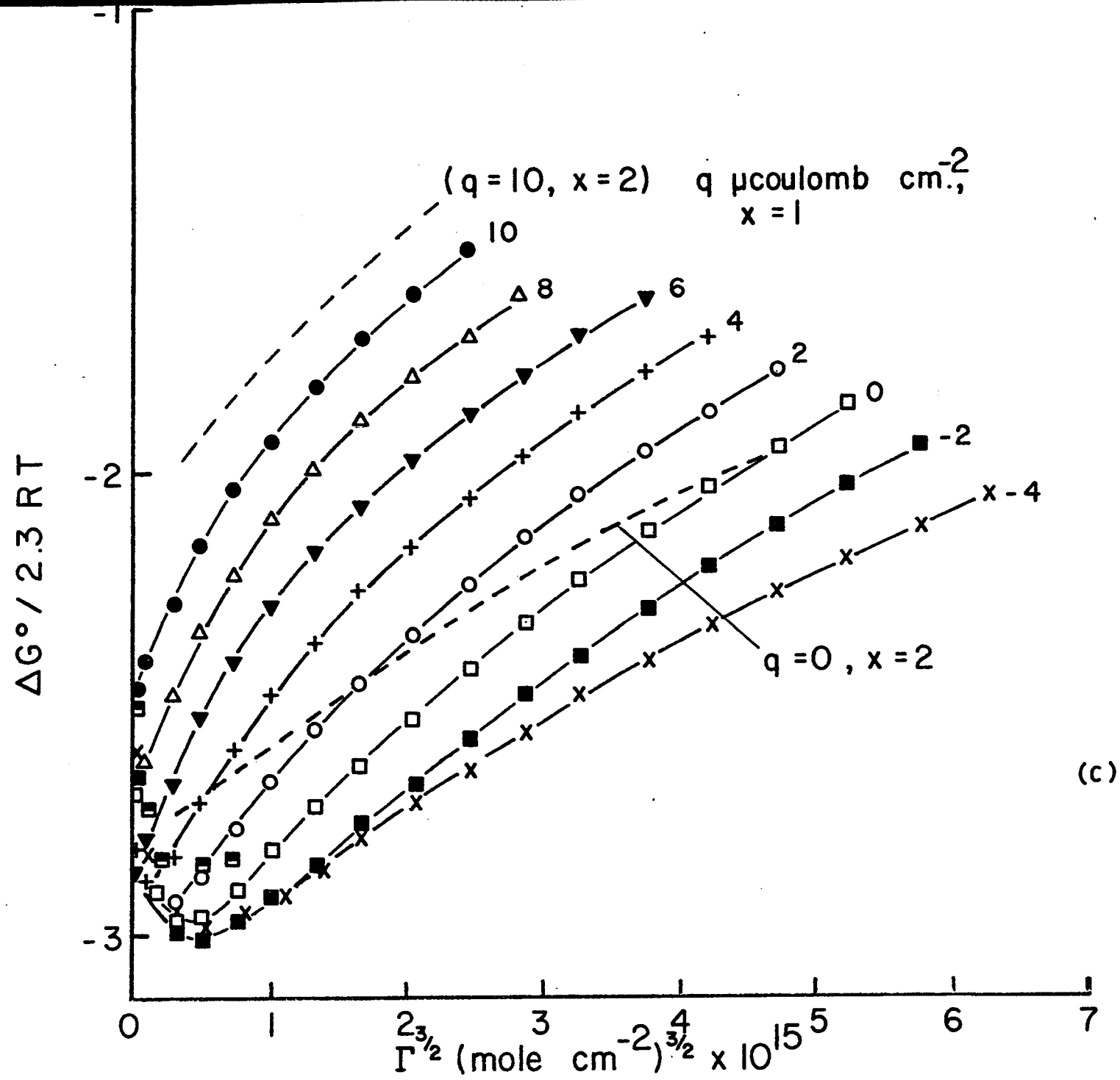
(q = 10, x = 2) q μcoulomb cm⁻²,
x = 1
10
8
6
4
2
0
-2
x -4
q = 0 , x = 2
ΔG° / 2.3 RT
-1
-2
-3
0
1
2
3
4
5
6
7
Γ^3/2 (mole cm^-2)^3/2 x 10^15
(c)

Figure 21

Calculations of ΔG° from the experimental results on the basis of the Flory-Huggins isotherm with various x values (eqn. 59).

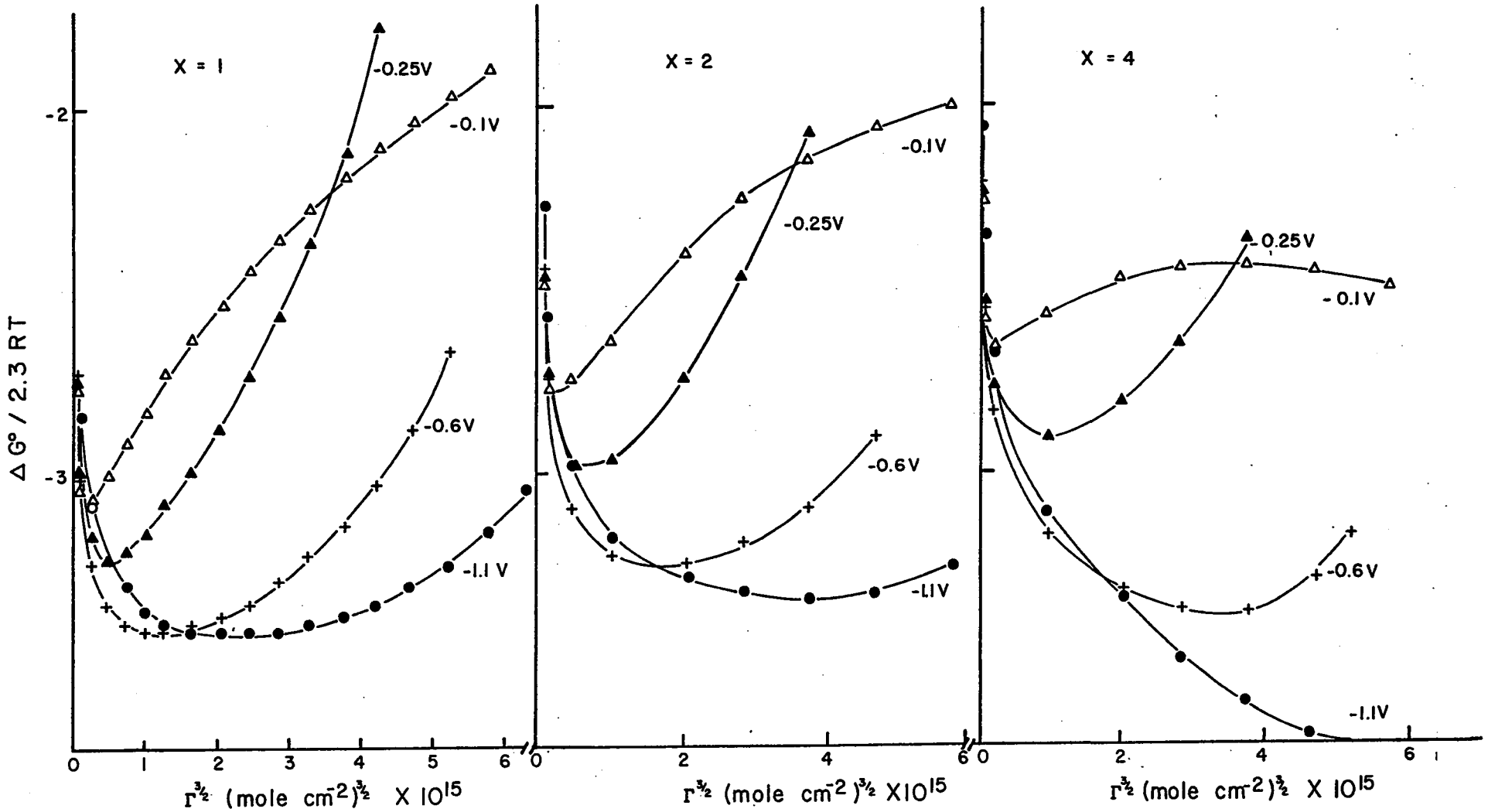
X = 1
X = 2
X = 4
-0.25V
-0.1V
-0.6V
-1.1V
-2
-3
ΔG° / 2.3 RT
0
1
2
3
4
5
6
r^3/2 (mole cm^-2)^3/2 X 10^15

indicate x will be between 2 and 4, depending on the rotational freedom. Increasing x has the effect of lowering the ΔG^{o} values calculated for the larger coverages.

A variation of ΔG^{o} with Γ need not, of course, be ascribed only to repulsion effects (see §§. 5.1, 5.2, 5.3). The role of solvent structural effects in relation to the adsorbate(solute)-solvent interaction in the ad-layer, similar to those which occur in aqueous solutions of soluble organic molecules[86,87], must be considered. It is in regard to such effects that the studies over a range of temperatures are particularly informative in so far as entropies of substitutional adsorption can be evaluated for appropriate isosteric and constant charge conditions. Before referring to such results, however, it is of interest to illustrate how ΔG^{o}, evaluated for various constant Γ values, is dependent on q (Figure 22).

Basically, ΔG^{o} has maximum values of ca. -4.5 kcal. $mole^{-1}$ for various Γ and these maxima occur at q values which become more negative with increasing Γ. ΔG^{o} for neutral molecules usually[35] has a parabolic form with respect to q (except at high $\pm$ q where orientation saturation polarization becomes dominant). There is evidently (Figure 22) a shift of the ΔG^{o} - q relationship towards higher q values as Γ increases so that at given q values, ΔG^{o} tends to become less negative with increasing Γ except where the curves cross over towards the more negative q values. Over most of the curves, a higher negative value of q is required for ΔG^{o} to attain a given value as Γ increases; it is suggested that this reflects (a) the competition arising from orientation polarization of water dipoles and pyridine molecules in the interphase, and the resulting hydrogen bonding which can arise at the N-center when it is oriented away from the electrode at more negative q; (b) the change in two-dimensional structure-breaking in the water ad-layer comprising

Figure 22

Variation of ΔG^{o} for pyridine adsorption at mercury calculated for various Γ values as a function of surface charge q (for x = 1).

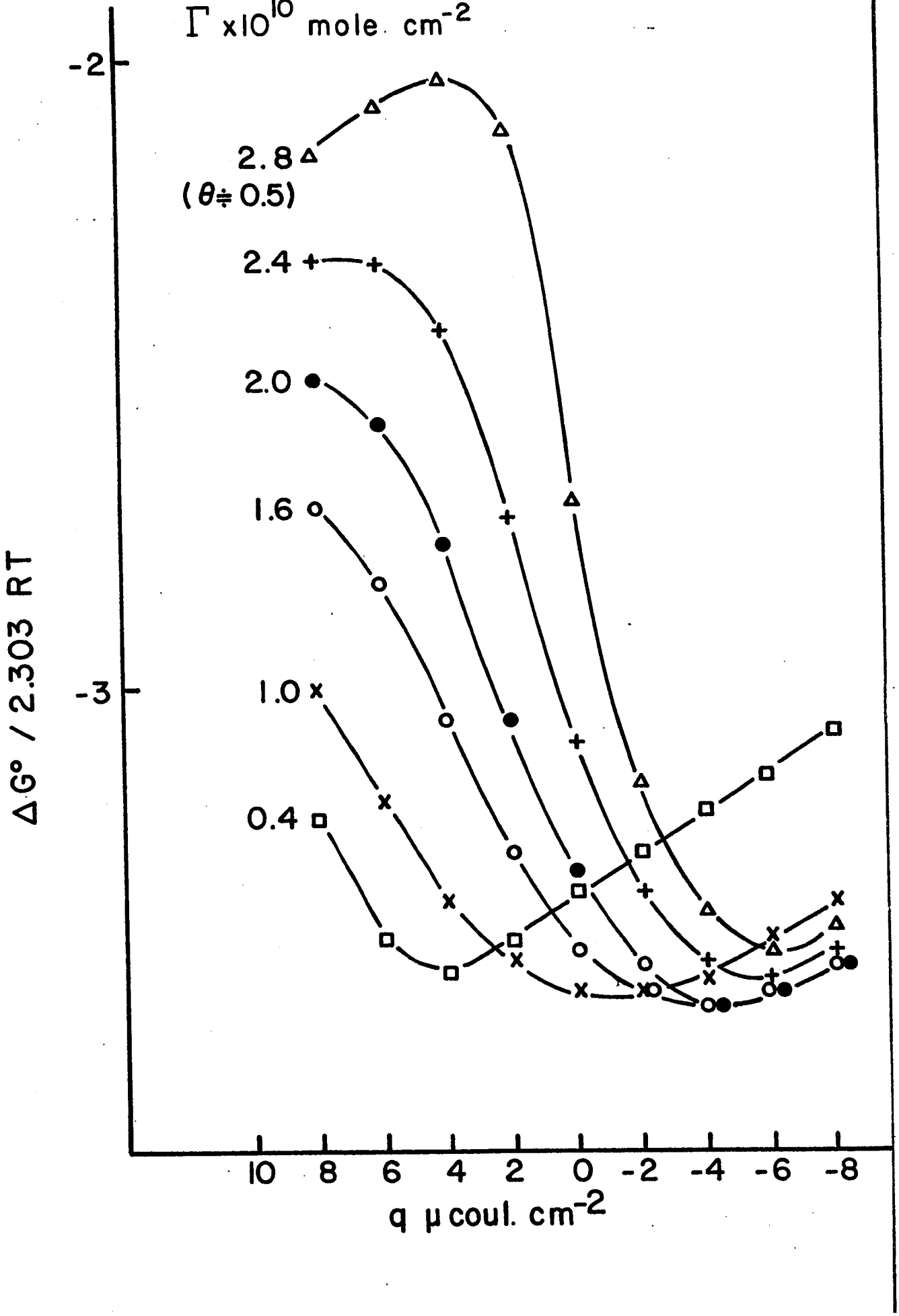
Γ x10^10 mole. cm^-2
-2
-3
2.8
(θ≒0.5)
2.4
2.0
1.6
1.0
0.4
ΔG° / 2.303 RT
10 8 6 4 2 0 -2 -4 -6 -8
q μ coul. cm^-2

the interphase as the surface excess of pyridine is increased and (c) the displacement of anions as q is made more negative, an effect which has been shown previously to depend on the pyridine adsorption[15] in so far as at higher pyridine coverage, the anion specific adsorption (Cl^- in that case) is enhanced at a given potential.

a) The heats and entropies of adsorption

Here isosteric entropies of adsorption were evaluated at constant charge from plots of ΔG° vs T and ΔH° was obtained from ΔG° with the derived values of ΔS°. Previously, for ions[71], isotensile thermodynamic functions for adsorption were evaluated, but the isosteric quantities will reflect better any effects of changing interaction effects with charge at given degrees of coverage. The standard heats and entropies of adsorption are shown in Figure 23 and 24 as a function of q. The striking feature of these results is that ΔS° for given Γ values increases towards a maximum positive value (cf.[84]) as q varies from +8 to ca. -4 μ coulomb cm^{-2} and then tends to decrease while ΔH° has a corresponding variation with q. Similarly, the isotensile entropy of adsorption of I^- is largest near q = 0[71]. Behaviour related to these effects is more difficult to discern in the ΔG° plots and indeed there is a substantial compensation between ΔH° and ΔS° or $T\Delta S^\circ$ tending to make ΔG° a function rather less sensitive to q (cf. the analogous case of ionization constants in relation to structure of organic acids and bases). This type of compensation is familiar in ionic solutions[88, 89] and has recently been demonstrated[90] in the thermodynamics of binding of acetylcholine competitors at the enzyme acetylcholinesterase. The compensation plot relating ΔH° and ΔS° for pyridine adsorption at Hg at 313°K is shown in Figure 25 and covers a wide range of ΔS° values (for various Γ and q values) with a slope of ca. 300°K close to the value

Figure 23

Isosteric heats of adsorption of pyridine plotted as function of charge q for various coverages.

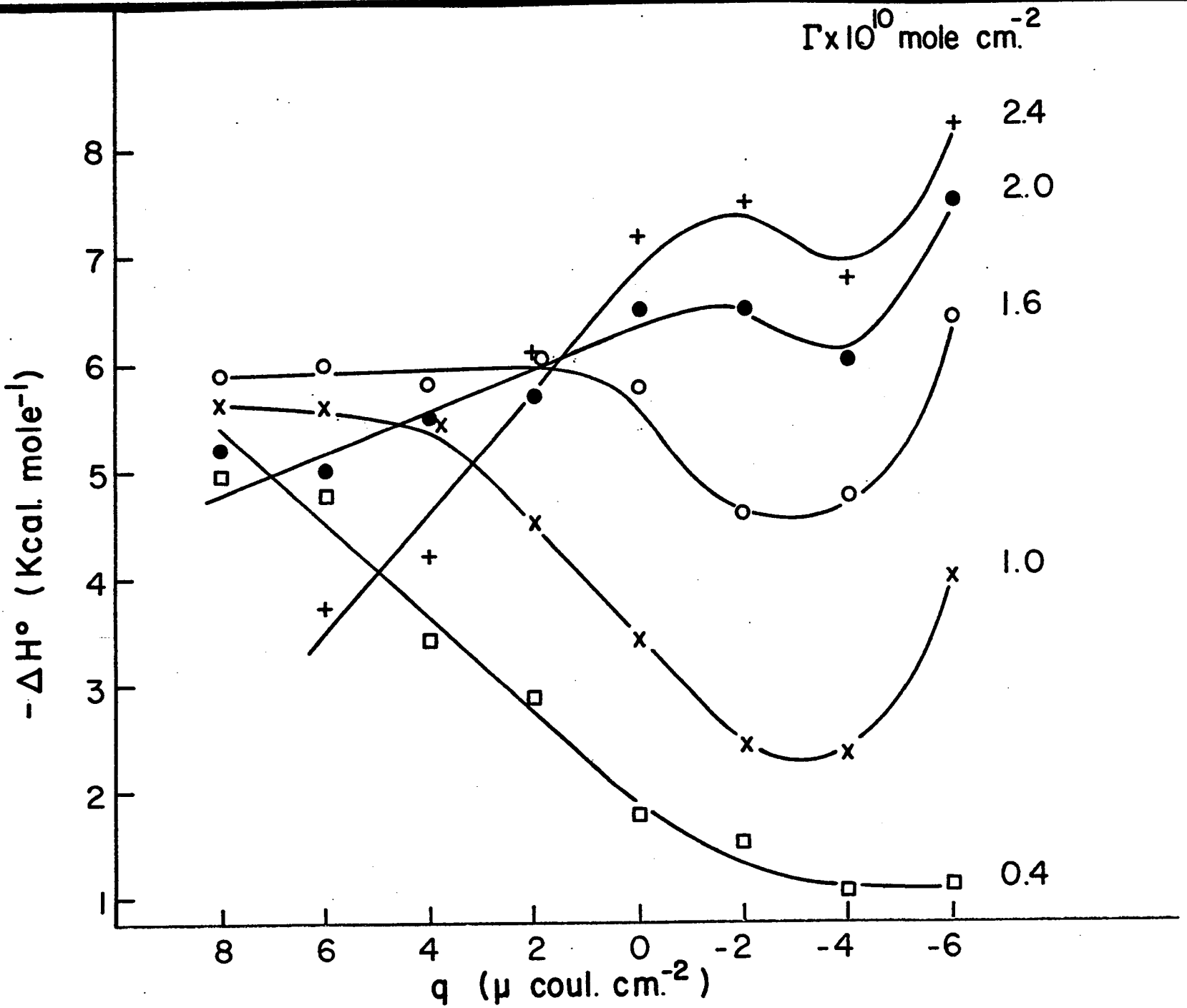
Γx10^10 mole cm.^-2
2.4
2.0
1.6
1.0
0.4
-ΔH° (Kcal. mole^-1)
8
7
6
5
4
3
2
1
8
6
4
2
0
-2
-4
-6
q (μ coul. cm.^-2)

Figure 24

Isosteric standard entropies of adsorption of pyridine plotted as a function of charge for various coverages.

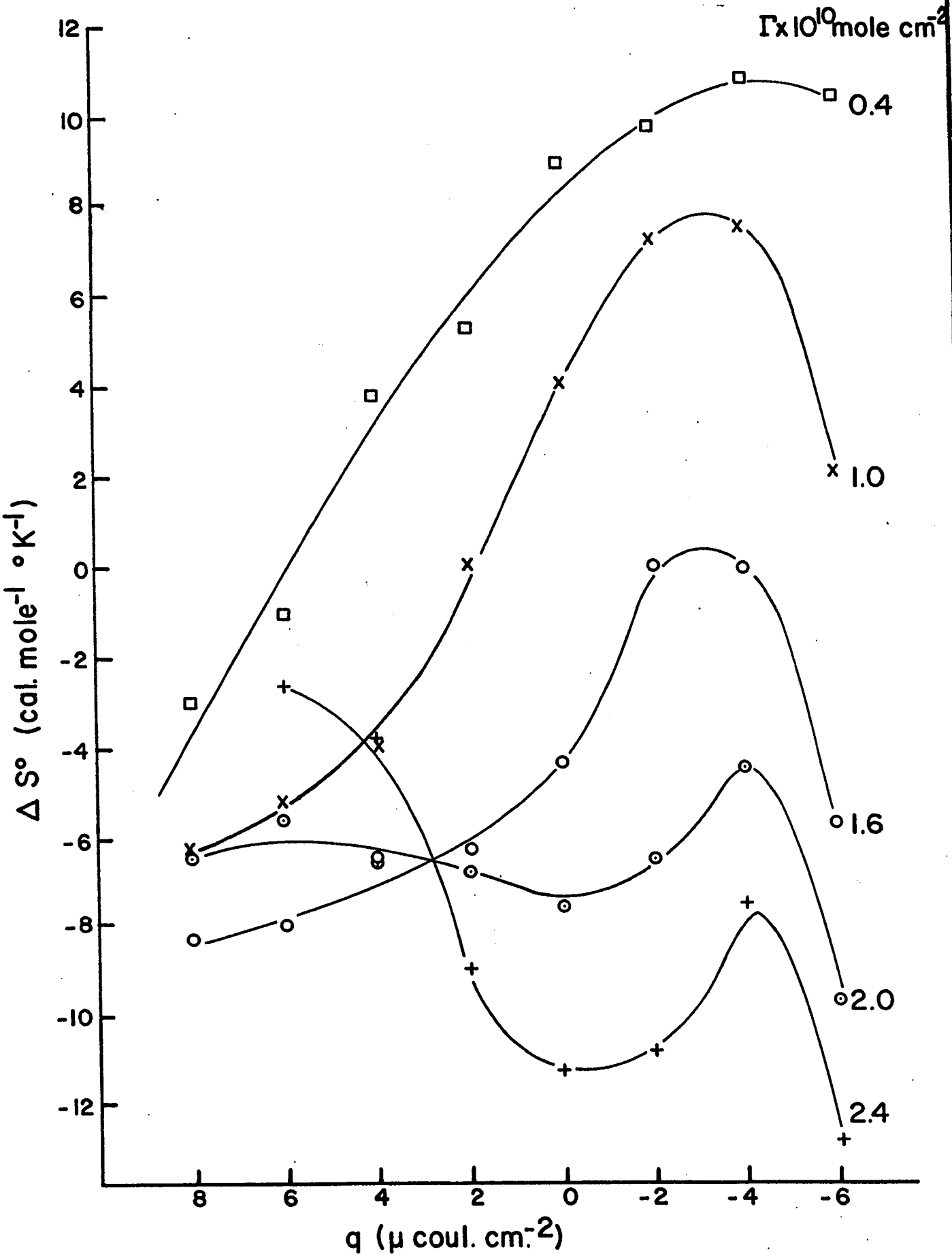
Γx10^10 mole cm^-2
0.4
1.0
1.6
2.0
2.4
Δ S° (cal. mole^-1 °K^-1)
q (μ coul. cm^-2)
12
10
8
6
4
2
0
-2
-4
-6
-8
-10
-12
8
6
4
2
0
-2
-4
-6

Figure 25

Compensation effect between heat and standard entropy of adsorption of pyridine at mercury for various q and Γ values.

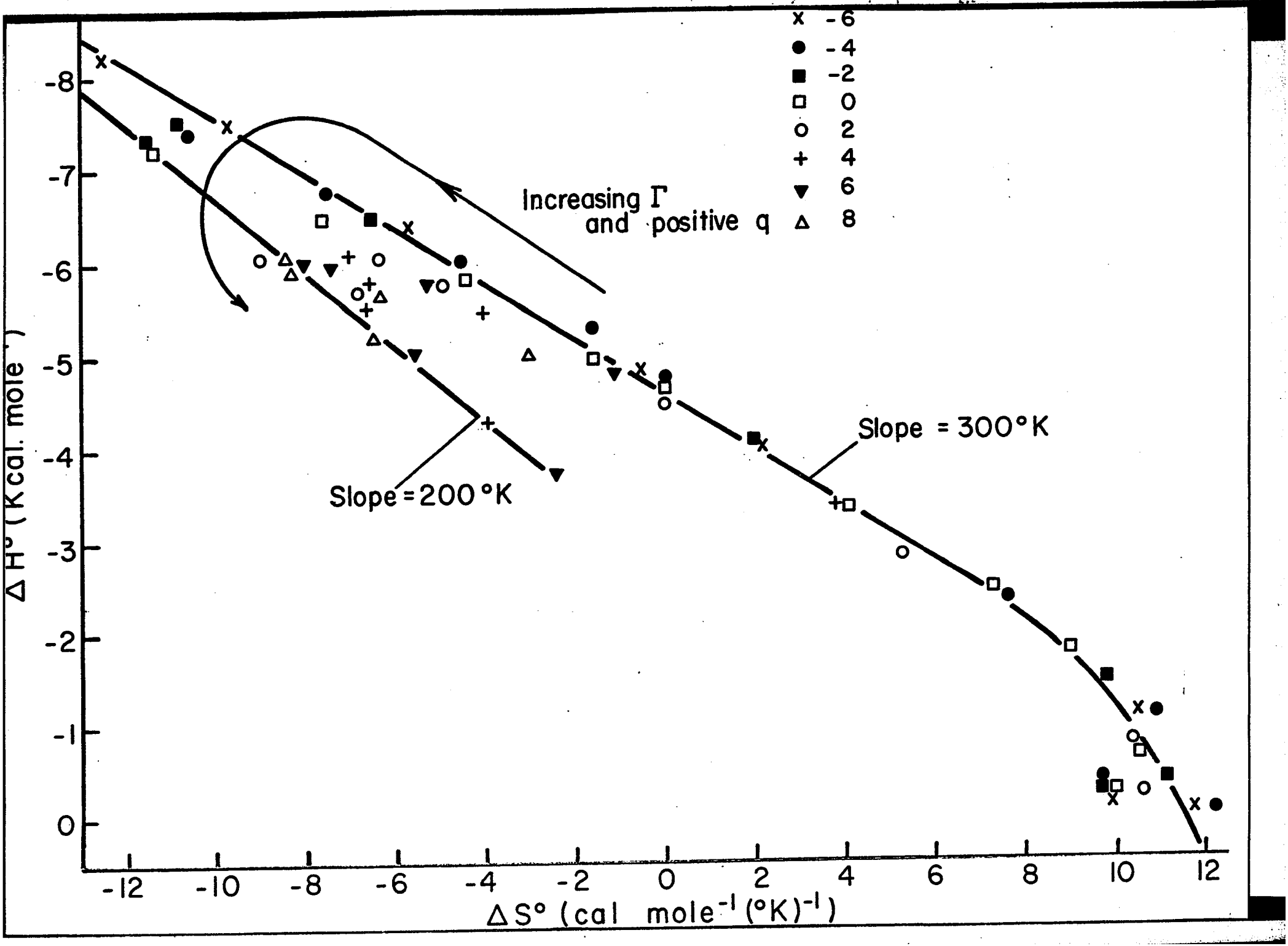
x -6
● -4
■ -2
□ 0
o 2
+ 4
▼ 6
△ 8
Increasing Γ
and positive q
Slope = 300°K
Slope = 200°K
ΔH° (Kcal. mole⁻¹)
ΔS° (cal mole⁻¹ (°K)⁻¹)
-8
-7
-6
-5
-4
-3
-2
-1
0
-12
-10
-8
-6
-4
-2
0
2
4
6
8
10
12

obtained for binding of various competitors at the enzyme mentioned above[90] and for hydration of ions[89]. At high values of Γ and for the more positive values of q, the degree of compensation is less (Figure 24) and the relation has a slope of ca. 200°K. This is probably connected with the reversal of orientation of pyridine together with the presence of ClO_4^- ions in the ad-layer which enhance structure-breaking effects in the interphase. In general, as is shown below, the best compensation between entropy and energy terms is achieved when interaction-dependent librations are involved. Configurational entropy changes are usually insufficient[91] to account for the large changes of entropy often associated with substantial energies of interaction (cf. the case of ionic solutions[89]).

Although pyridine is more strongly adsorbed at a given concentration on the negative branch of the electrocapillary curve so that ΔG° values are relatively more negative at the negative q values, ΔH° in fact tends to become less negative as -q increases except at higher Γ values where it tends to remain more constant (Figure 23). The unfavourable trend in ΔH° is compensated by an opposite trend in $-T\Delta S^\circ$. At low coverage, the positive ΔS° reflects, the author believes, release of structured, low entropy water at the surface with a consequent net positive entropy change in the adsorption process, an effect which has been observed previously[84] at solid electrodes. This implies that the water layer at Hg tends to be most structured in the region of q = -3 to -6 μ coulomb cm.$^{-2}$ (Figure 24). This may not seem consistent with the maximum observed[58] in the derived excess entropy σ of the interphase in NaF solution at ca. q = -8 μ coulombs cm.$^{-2}$, but σ is a complex quantity involving both the electrostatically adsorbed ions, their hydration shells and the water itself in the interphase, and cannot be directly related to the entropy of the water layer or to the entropies of adsorption calculated here[63].

That the water in the interphase may be maximally structured near the potential of zero charge might be inferred by analogy with the effect of large organic hydrophobic groups in promoting structure in water solutions[92]. Mercury probably has little specific interaction with water molecules, (except perhaps residually at positive q with the lone pair electrons on oxygen, cf. the weak HgII complex with dioxane) but its metallic nature will allow an effective continuation of the dipole (hydrogen bond) interactions amongst the water molecules "through" the interface on account of the dipole images and their interactions with the parent charge distributions on the solution side.

As in the ΔG^{o} plots (Figure 20), ΔS^{o} depends appreciably on the coverage, becoming less positive for ΔS^{o} values calculated for higher Γ values (Figure 26a). This suggests that at higher Γ values in Figure 26), the water layer is already disorganized so that less entropy is released per mole of pyridine adsorbed under such conditions and the apparent standard entropy of adsorption, like the corresponding ΔG^{o}, varies with the equilibrium Γ value from which the ΔG^{o}, and hence the ΔS^{o} value, has been calculated. The dependence of ΔH^{o} on coverage is shown in Figure 26b.

At higher negative or positive q values, the ΔS^{o} values decrease presumably due to (a) the field effect on water orientation leading to structure-breaking effects analogous to those associated with electrostriction which arise at small ions, so that substitutional adsorption no longer leads to anomalous positive entropy changes; and (b) orientation of the pyridine itself (cf.[66,15]) at high fields. At positive q values, the tendency for ClO_4^- ions increasingly to enter the interphase may assist the structure-breaking effect of the electrode field itself and enhance the tendency for ΔS^{o} to become more negative.

Figure 26

(a) Dependence of ΔS^{o} on coverage (Γ) and

(b) Dependence of ΔH^{o} on coverage (Γ) for the adsorption of pyridine from aqueous 0.03M $NaClO_4$.

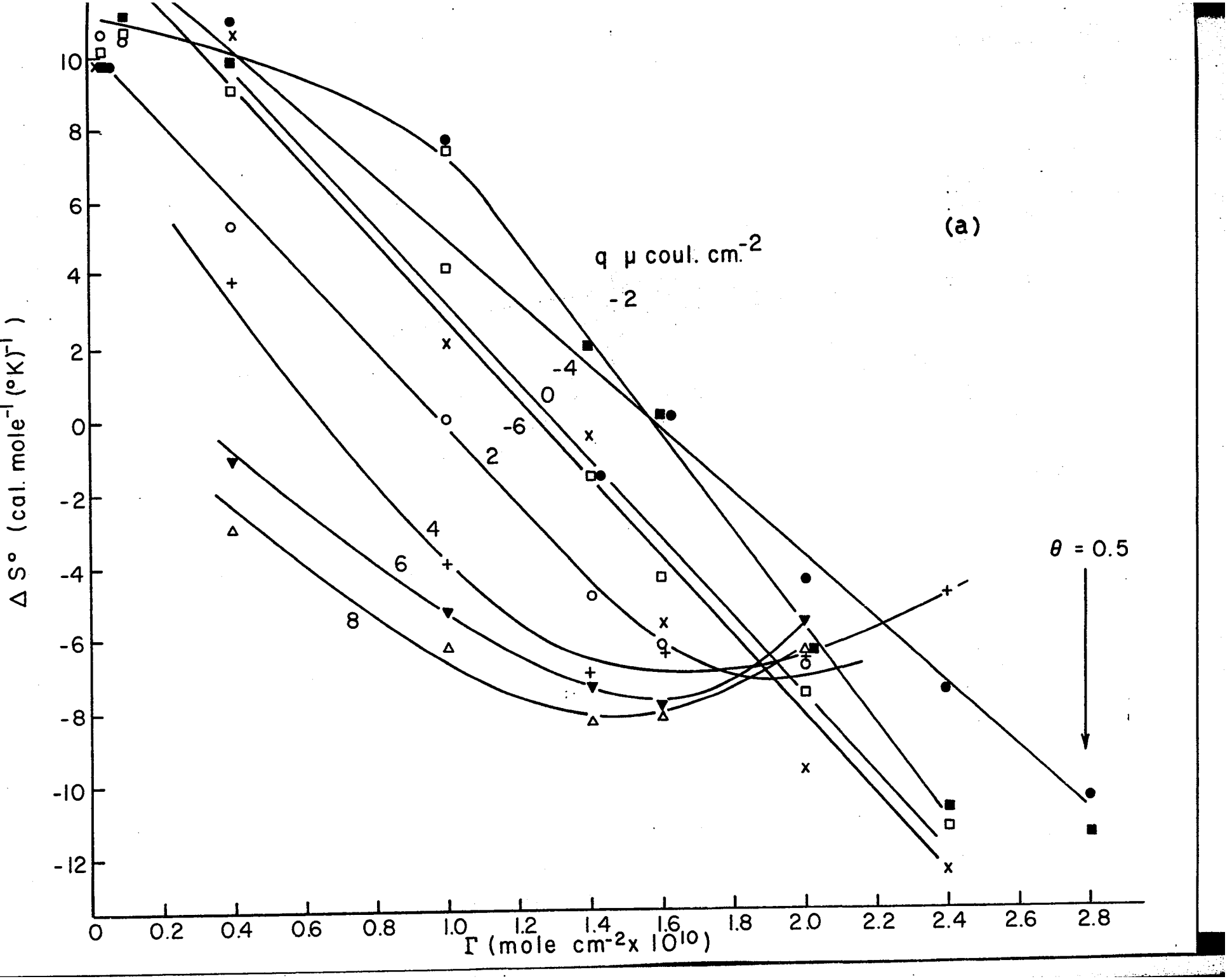
(a)
q μ coul. cm.$^{-2}$
-2
-4
0
-6
2
4
6
8
θ = 0.5
ΔS° (cal. mole^{-1} (°K)$^{-1}$)
Γ (mole cm^{-2} x 10^{10})
10
8
6
4
2
0
-2
-4
-6
-8
-10
-12
0
0.2
0.4
0.6
0.8
1.0
1.2
1.4
1.6
1.8
2.0
2.2
2.4
2.6
2.8

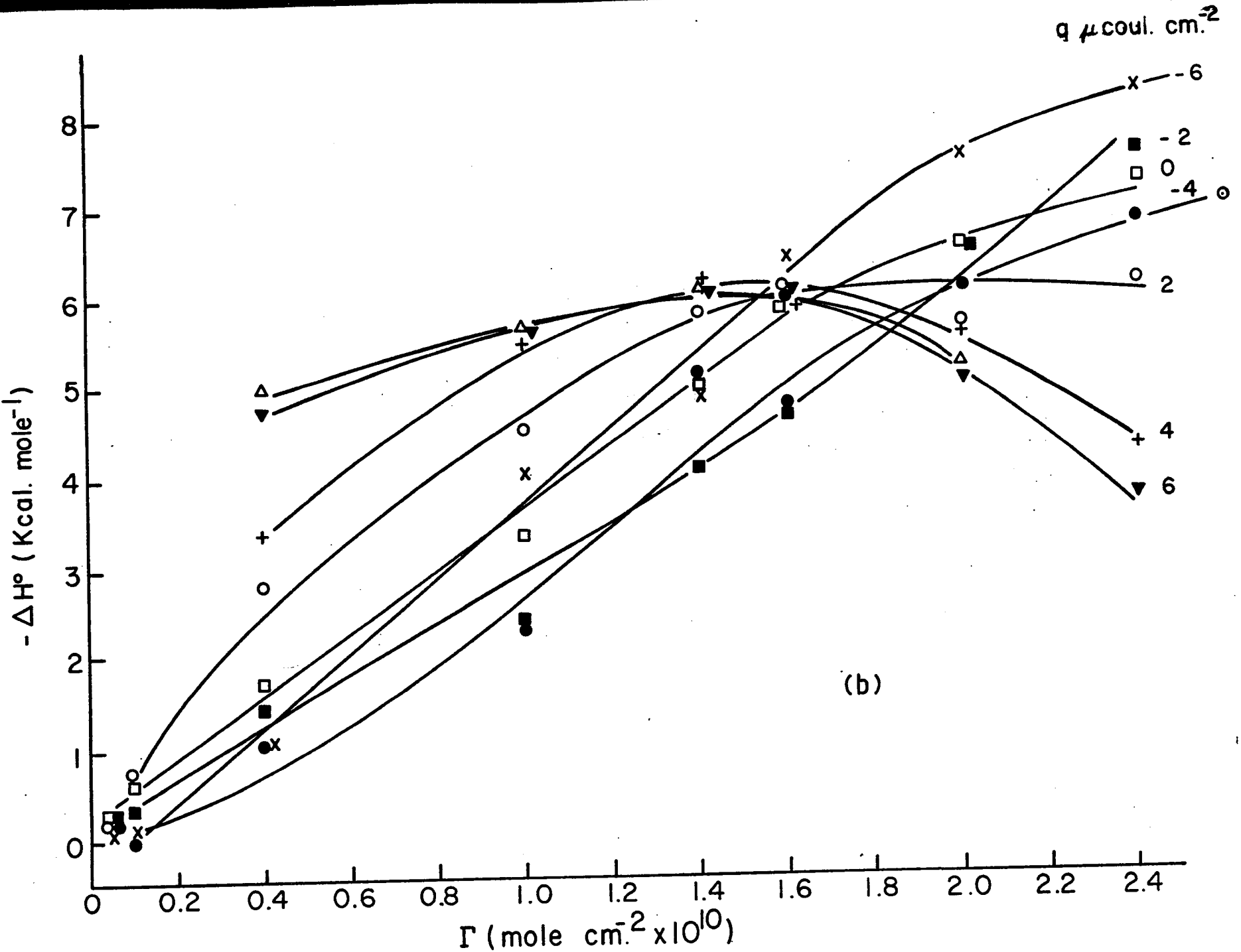
q μcoul. cm.-2
x -6
■ -2
□ 0
⊙ -4
○ 2
+ 4
▼ 6
(b)
- ΔH° (Kcal. mole-1)
Γ (mole cm.-2 x 10^10)
0
1
2
3
4
5
6
7
8
0.2
0.4
0.6
0.8
1.0
1.2
1.4
1.6
1.8
2.0
2.2
2.4

b) Components of the Entropy of the Water Layer

It is of interest to examine to what extent the electrostatic and configurational entropy of water in the interphase could vary with electrode surface charge, and then to examine if such solvent adsorption effects could account for part of the substitutional entropy changes found in the present thermodynamic study of pyridine adsorption.

(i) Configurational effects: solvent dipole orientation can be considered in terms of the model of Bockris, Devanathan and Müller[40] in which dipoles are regarded as being in an up ($\uparrow$) and down ($\downarrow$) direction with respect to the surface (see §1.4.2(ii)(c)). This will give rise to a molar configurational entropy of mixing S_c of the two orientational states

$$S_c = - R[\Theta_{\downarrow} \ln \Theta_{\downarrow} + \Theta_{\uparrow} \ln \Theta_{\uparrow}] \qquad (79)$$

where the Θ terms are the surface fractions (and hence relative coverages) of dipoles oriented in $\uparrow$ or $\downarrow$ directions. In eqn. (79), interaction effects (see below) have not been considered. The orientation of dipoles will be determined by their interaction with the electrode field X and by their mutual interactions[40]. The resulting distribution function (cf.[33]) for interacting dipoles is given by eqn. (37).

In terms of the relative coverages Θ, eqn. (37) is

$$(2\Theta_{\downarrow}) - 1 = \tanh[-\frac{E.c}{kT}(2\Theta_{\uparrow} - 1) + \frac{\mu X}{kT}] \qquad (80)$$

which is evaluated below for various values of the interaction factor $f_i = E.c/kT$ and the electrostatic field-dipole interaction term $\mu X/kT$. The configurational entropy of the layer of molecules with mixed orientations then follows from eqn. (79). $\Theta^{\uparrow}$ and $\Theta^{\downarrow}$ may be

related to q through[93] X given by $X = -4\pi q/\varepsilon$ where ε, the effective dielectric constant of the surface layer, may be taken as ca. 6[94,95] (actually ε will be f(q) at low values of q but we take the reasonable value of 6 discussed previously). The results are shown in Figure 27.

The problem considered here is seen to be closely related to that involved in the calculation of magnetization in a lattice of magnetic dipoles. While interaction effects have been included here in the orientation distribution function, the usual Bragg-Williams approximation has been followed in assuming that the interactions do not appreciably influence the configurational entropy. This is not an entirely satisfactory assumption in any problem in lattice statistics (except in the quasi-ideal case of regular solutions) but corrections for non-random mixing[91] when interaction effects are significant, are in fact relatively small and to a first order approximation, are of the order:

$$-R\left(\frac{\Theta_{\uparrow} + \Theta_{\downarrow}}{4c}\right)^2 \cdot \left(\frac{E.c}{kT}\right)^2$$

i.e. the non-randomness introduced by interaction contributes, as expected, a negative term in the entropy of mixing. For $\Theta_{\uparrow} = \Theta_{\downarrow}$ near q = o, the maximum value of this entropy correction amounts to only -0.5 e.u. for $\frac{2E}{kT} = 5$ say.

(ii) Librational entropy: In an electric field, a dipole tends to become oriented but this orientation is rarely complete and the degree of orientation is determined by the field-dipole interaction energy factor $\mu X/kT$. The dipole executes librative motion in the field and the partition function for the libration mode is[96,89]

$$f_L = \frac{8\pi^2 (8\pi^3 I_1 I_2 I_3 k^3 T^3)^{1/2}}{\sigma h^3} \cdot \frac{\sinh[E_e/kT]}{E_e/kT} \qquad (81)$$

Figure 27

Configurational and librational entropy of oriented water molecules in the electrode interphase in relation to the orientation distribution function (lower Figure) plotted in terms of the orienting field X and corresponding charge $\dot{+}$ q.

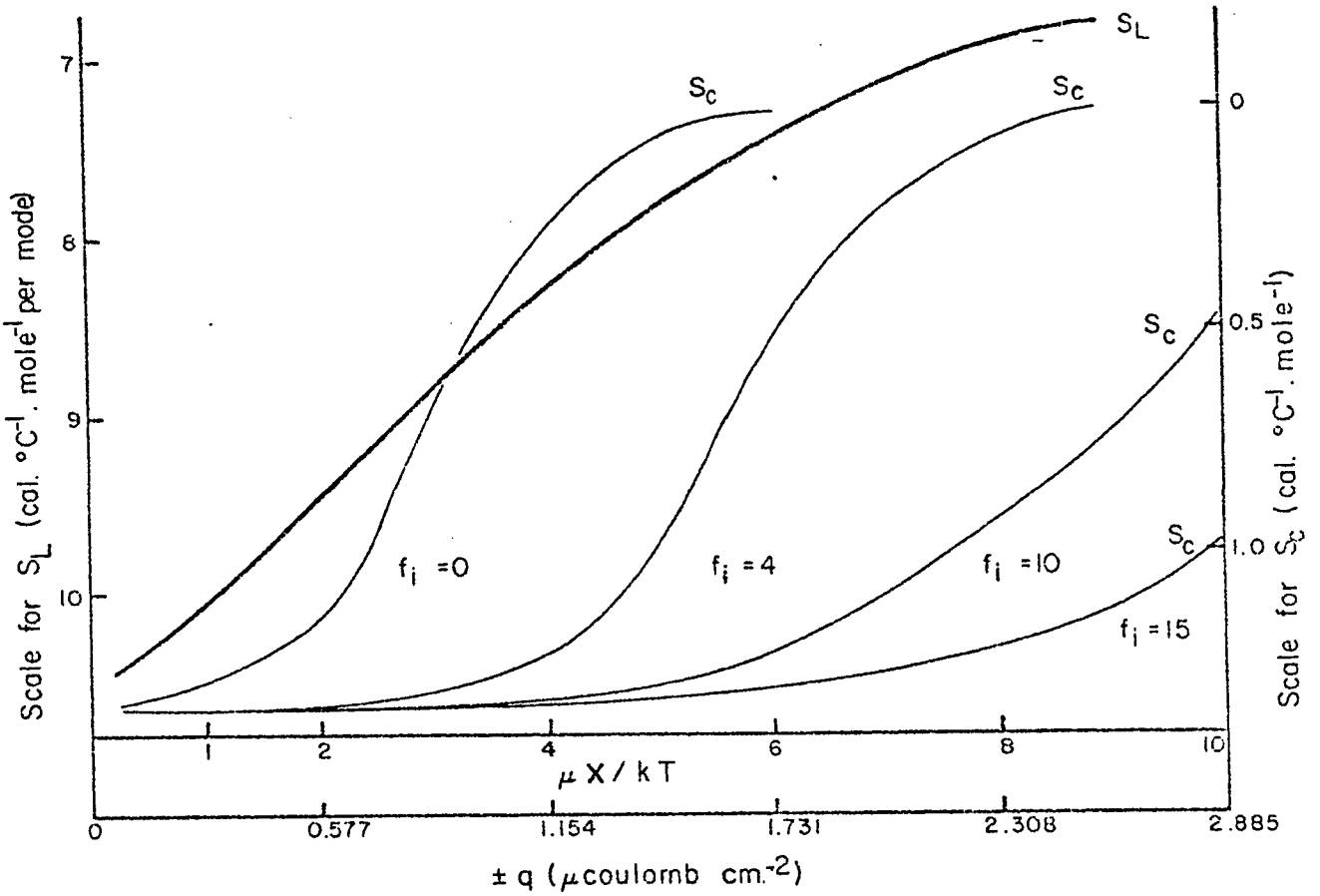
S_L
S_c
S_c
S_c
S_c
f_i =0
f_i =4
f_i =10
f_i =15
Scale for S_L (cal. °C^{-1}. mole^{-1} per mode)
Scale for S_c (cal. °C^{-1}. mole^{-1})
7
6
9
10
0
0.5
1.0
1
2
4
6
8
10
μ X / kT
0
0.577
1.154
1.731
2.308
2.885
± q (μcoulomb cm.$^{-2}$)

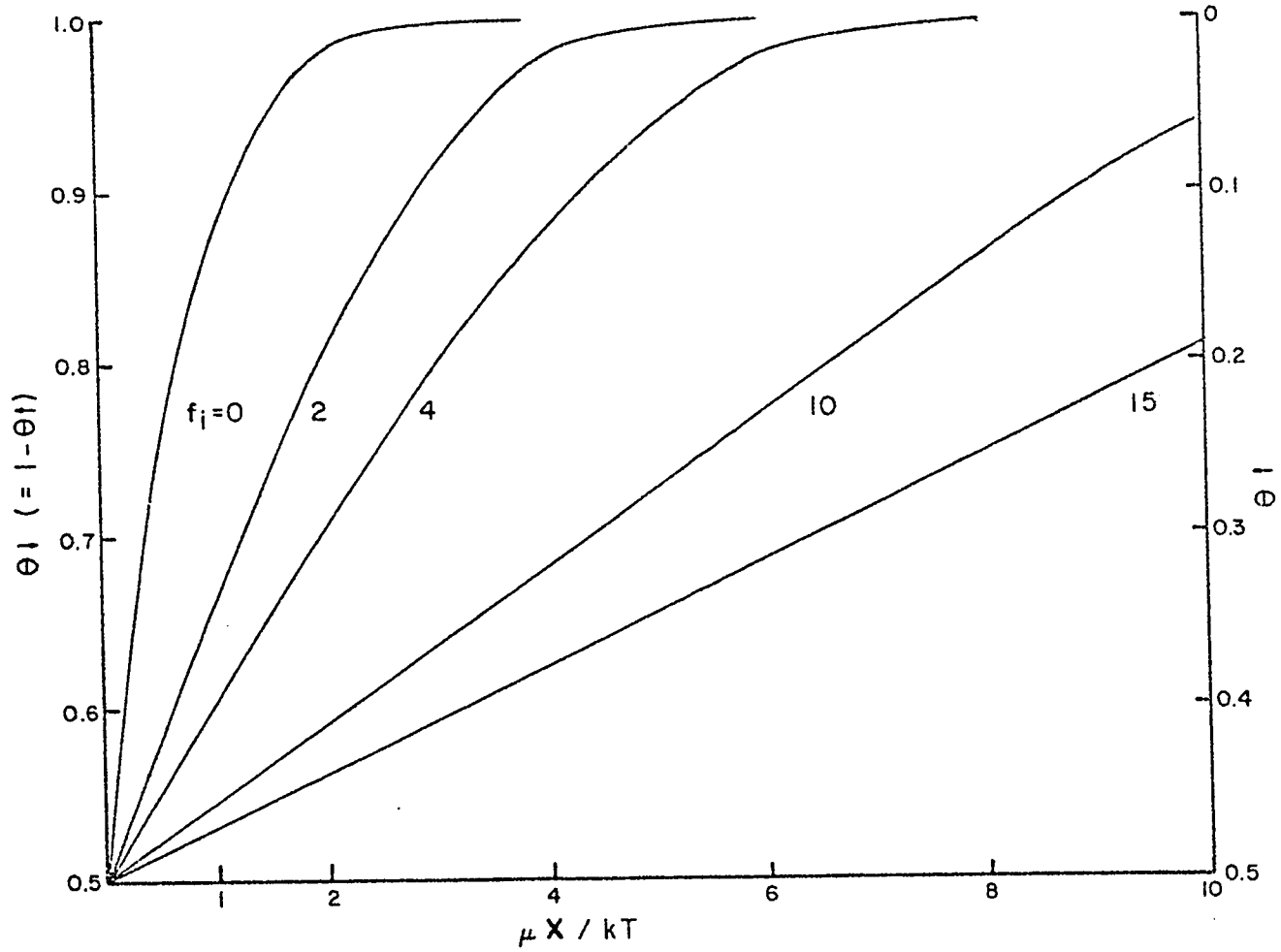
θ 1 (= 1-θ1)
θ 1
f_i=0
2
4
10
15
1.0
0.9
0.8
0.7
0.6
0.5
0
0.1
0.2
0.3
0.4
0.5
1
2
4
6
8
10
μ X / kT

where E_e is the electrostatic field-dipole interaction energy and I's are the principal moments of inertia of the water dipole. The entropy associated with the librational energy states in the field is then

$$\frac{S_L}{R} = \ln \frac{8\pi^2 (8\pi^3 I_1 I_2 I_3 k^3 T^3)^{1/2}}{\sigma h^3} - \ln E_e/kT + \ln \sinh[E_e/kT] - \frac{E_e}{kT} \coth[\frac{E_e}{kT}] + 5/2 \quad (82)$$

S_L was evaluated for various values of the inner Helmholtz field $X = -4\pi q/\varepsilon$ with μ_{H_2O} taken as 1.87 D (a larger value could be taken corresponding to the water molecule associated in the water structure; this would result in given S_L values arising at somewhat lower values of field X or charge q). S_L as a function of $\pm$ q is shown in Figure 27 for one librational mode. The variation of entropy with q is appreciable and larger than that of S_c with q. It is also approximately linear with E_e thus providing a basis for compensation between energy and entropy terms.

(iii) Vibrations: It can generally be assumed that the internal vibrations of H_2O molecules are little affected by the field exept indirectly by hydrogen bond bending or breaking effects. In any case, the internal vibrational entropy will be small at room temperature since the bending and stretching vibrational quanta are between 8 and 16 kT. However, near the electrode surface, water dipoles will tend to execute vibrations normal to the surface, as at ions[89]. This effect is difficult to evaluate in terms of the associated entropy but for appreciable q (= 20 μ coulomb cm.$^{-2}$) the magnitude of S_{vib} may be assumed to be similar to that at an ion where the field is of similar magnitude to that at the interface. E. g., for the F^- ion (4 coordinated), S_{vib} of water in the hydration shell is ca. 2.05

cal. mole^{-1}, $^{o}C^{-1}$, while for the I^- ion (6 coordinated) S_{vib} is ca. 3.0 cal. mole^{-1}, $^{o}C^{-1}$ [89].

(iv) Translational effects and entropy of water in the bulk: According to the calculations of Eley and Evans[89], the components of the entropy of water at 25°C in the bulk are:

$$S_{vib} = 5.3; \quad S_{lib} = 6.7; \quad S_{trans} = 12.8 \text{ cal. mole}^{-1}\ ^{o}C^{-1}.$$

per pair of water molecules. We can assume that the translational entropy of water in the interphase is ca. 2/3 of the value in the bulk and will be almost independent of field except in so far as the free area in the interphase may diminish due to electrostriction (cf. ref. [58]).

c) Relation of Pyridine Adsorption

The curves of Figure 24 indicate appreciable positive entropy changes for low coverages and the lower q values. At higher coverages, the entropy changes are negative but exhibit a reproducible maximum around q = -3 to -6 μ coulomb cm.$^{-2}$. The magnitudes of ΔS^{o} for various conditions reflect (i) the entropy of adsorption of pyridine itself and (ii) the entropy associated with displacements of x water molecules (cf. eqn. (59)) previously adsorbed where x will be between 2 and 4 based on inspection of space-filling models.

The entropies of adsorption and their variation with q or Γ are seen to be quite large in comparison with the calculated librational entropy of water in the interphase or in relation to the known entropy of fusion of water (ca. 6 e.u.). If allowance is made, however, for the fact that substitutional adsorption will involve displacement of several water molecules (x = 2 to 4) per pyridine molecule, the observed values of ΔS^{o} seem plausible. They can be accounted for qualitatively in terms of structural effects to be discussed below.

We have seen above that electrostatic effects in the interphase would tend to give rise to both diminishing configurational and librational entropy contributions as $\pm$ q increases. In point of fact, the librational freedom of solvent water may be less on the negative branch than on the positive, by analogy with the lower entropy of hydrate water at anions in comparison with that at cations. It is now seen (cf. Figure 26a) that the observed entropy change for low coverage conditions (Γ = 0.4 and 1.0 x 10^{-10} mole cm. $^{-2}$) is the opposite of what might be expected in terms of the electrostatic entropy of water in the interphase as a function of q (Figure 27). It is for this reason that it becomes necessary to suppose that the Hg interface has a structure-promoting effect which minimises the entropy of water in the interphase near the potential of zero charge. This effect may be enhanced by the dipole image interaction which in effect preserves the local structure "across" the interface and indeed the surface excess volume Γ_v tends towards a maximum value near the potential of zero charge[58].

At positive q the ΔS^o values tend to be more negative than at corresponding negative charges. It seems likely that this could be due to the different orientation which pyridine can take up in the interphase, since on the positive branch the N centre will be oriented away from the solvent with which it tends to hydrogen-bond, and thus tend to be more specifically associated with the electron-deficient metal surface. In this connection, it is interesting to note that the excess partial molal entropy of pyridine[97] in aqueous solution, calculated limitingly for infinite dilution, is -12 cal. $^oC^{-1}$ $mole^{-1}$, an unusually low value reflecting presumably strong association with water molecules (cf. the case of ionic solutions[89]). Loss of some of this associated water upon adsorption would cause release of positive entropy. The observation that entropies of

adsorption at positive q are in fact the most negative (at low Γ), seems to indicate retention of some of the hydrogen bonding to water so that a "flat" orientation (rather than one in which the pyridine dipole is oriented towards the metal surface) may be preferred in order to minimize "dehydration".

At higher coverages, structure-breaking by the pyridine itself may become significant, so that the entropy of displacement of water is a less positive quantity and the librational effects calculated above may become more representative of the experimental situation, e.g. for $\Gamma = 2.4 \times 10^{-10}$ mole cm.$^{-2}$. Corresponding variations of enthalpy can arise in a similar way: at appreciable coverage, water in the interphase will be less hydrogen bonded and more easily displaced, so that the process of displacement can become relatively more exothermic; this effect will be enhanced by increasing pyridine-pyridine interactions which can contribute approximately 1.47 kcal. mole^{-1} per pair as may be estimated from the known heat of vaporisation of pure pyridine (8.8 kcal. mole^{-1}), assuming 12-coordination in a close-packed liquid lattice.

Analogously, with regard to the variation of the heats of adsorption at low Γ with charge, ΔH tends to become (Figure 23) appreciably less negative with decreasing q; this effect could also be interpreted in terms of increasing difficulty of substitutional adsorption requiring H-bond breaking in the structured and H-bonded water layer as q decreases since the electrostatic energy difference of pyridine and water dipoles, due to field-dipole interactions, can only amount to ca. 1 kcal. over this range of q (see below). At higher Γ values, an opposite trend is seen and ΔH^{o} becomes more exothermic with decreasing q; with a sufficient population of the ad-layer with pyridine, the structural effects associated with the water layer will be less important so that the pyridine reorientation effect can become dominant, i.e. the tendency for the adsorption

energy of pyridine to be smaller at positive than at negative q owing to the diminution of H-bonding which the N-centre would suffer if oriented away from the solvent must be considered. Contrary to earlier expectations[66], the ΔH^{o} is quite negative at the most positive q values where the N-centre of pyridine is presumably oriented more towards the mercury and is thus less H-bonded. The disadvantage with respect to H-bonding which the molecule would experience when in this orientation may be compensated by electron overlap (specific adsorption) with the positive Hg surface under these conditions (cf. the stability of thiourea at Hg[98], the existence of ammonia, amine and amide complexes with Hg II and the π-orbital interaction of pyridine with positive surfaces[66]). On the other hand, at appreciable q values (+4, +6 μ coulomb cm.$^{-2}$), ΔH^{o} changes relatively little with Γ ; this may indicate that pyridine is oriented in a "flat" manner at the electrode and carries with it locally at least one H_2O molecule which at the same time is able to interact with the charged metal surface. This is consistent with the argument made previously regarding ΔS^{o} and "dehydration" effects.

Electrostatic calculations of the energy of polarisation of pyridine (dipole-field and electronic polarisation energy) at various fields in comparison with that of 2 or 3 water molecules which it would replace, indicates that water would tend to remain preferentially adsorbed even up to high $\pm$ q. Again, a purely electrostatic treatment of the problem seems qualitatively inadequate so that structural effects involving hydrogen bonding may be as important in the enthalpies of adsorption as in the entropies. The close compensation between the entropy and enthalpy terms lends confirmation to the supposition that the adsorption characteristics of pyridine at mercury are closely and specifically connected with the behaviour of water adsorbed in the interphase.

5.4.2 Interpretation of Temperature Effects in Terms of the Volmer Isotherm

It is most probable that physically adsorbed neutral molecules at a mercury-solution interface will have reasonable freedom of translation relative to the mercury surface. Sulphur containing compounds with the S atom in a sterically unhindered position could be capable of bonding more firmly with the mercury[111,112] and thus immobility w.r.t. a given mercury atom[123] could arise in these exceptional cases. However, all adsorption processes studied in this work were found to be reversible and fast (< 1 sec) and thus physical electrostatic adsorption was involved (see § 1.1.1).

In the method outlined in § 5.1.2, use was made of the Volmer equation of state for expressing the behaviour of the surface phase in terms of a two-dimensional gaseous film. It should be noted that linearity in the ln C/ϕ vs ϕ plot (eqn. (73)) indicates the absence of adsorbate-adsorbate interactions and examples of this type of behaviour support the hypothesis presented in § 5.3, concerning negligible "solute-solute" interaction effects.

As in the Langmuir model (§ 5.4.1), the ΔG value refers to a substitutional adsorption process. The value of ΔS represents the loss (or gain) of one degree of translational freedom (perpendicular to the surface) which is replaced by a vibration and the possible loss (or gain) of two degrees of rotational freedom of the solute (or solvent). The components of the free energy of adsorption near zero coverage have been described in § 5.1.1.

The surface area b found from the slope of the ln (C/ϕ) vs ϕ plot, unlike the other parameter m (the intercept), does not appear to be theoretically dependent on the solvent size or shape.

The method involving eqn. (73) for obtaining the thermodynamic quantities fails for conditions where the surface excess cannot be equated with the more important quantity, the surface concentration (see § 1.4.1). This is due to the fact that the Gibbs adsorption equation (from which is calculated the surface excess; see, eqn. (66)) is used in the derivation of eqn. (73). However the parameter b can be evaluated from the slope of plots of ϕ/Γ vs ϕ (when they are linear) where Γ is taken as the surface concentration.

For the adsorption of pyridine from aqueous 0.03 M $NaClO_4$ solutions, ΔG approximates to a quadratic function of q_M for constant charge isotherms, and the maximum occurs at ca. -3 μcoul. cm.$^{-2}$ (cf. Figure 22). This behaviour is illustrated in Figure 28 where $-\Delta G$ is plotted against $(q_M - q_M^{max})^2$ and q_M^{max} is the charge at which the free energy for adsorption reaches a maximum.

Whereas the value of ΔG at any one temperature varies by approximately 1 kcal. mole^{-1} over the entire range of q_M investigated, the heat of adsorption (Figure 29a) has a variation of about 3 kcal. mole^{-1}. Thus the entropy of adsorption (Figure 29b) must be a compensating factor in the free energy term as deduced in section 5.4.1(a). The plot of ΔH vs ΔS is shown in Figure 30 and with increasing negative q_M the curve becomes parallel with the corresponding line of Figure 25 (shown dotted in Figure 30) which was obtained by analysing the data in terms of the Langmuir isotherm. However, the values of ΔH obtained in the Volmer type of analysis are approximately 1 kcal. mole^{-1} less than the corresponding values obtained from the Langmuir isotherm if the ΔH values are compared at a given ΔS value in the plots of Figure 30.

Before analysing the heats and entropies of adsorption as functions of q_M, it is perhaps convenient to consider first the b vs q_M

Figure 28

Quadratic dependence of ΔG upon the electrode charge density at various temperatures for the adsorption of pyridine from 0.03M $NaClO_4$.

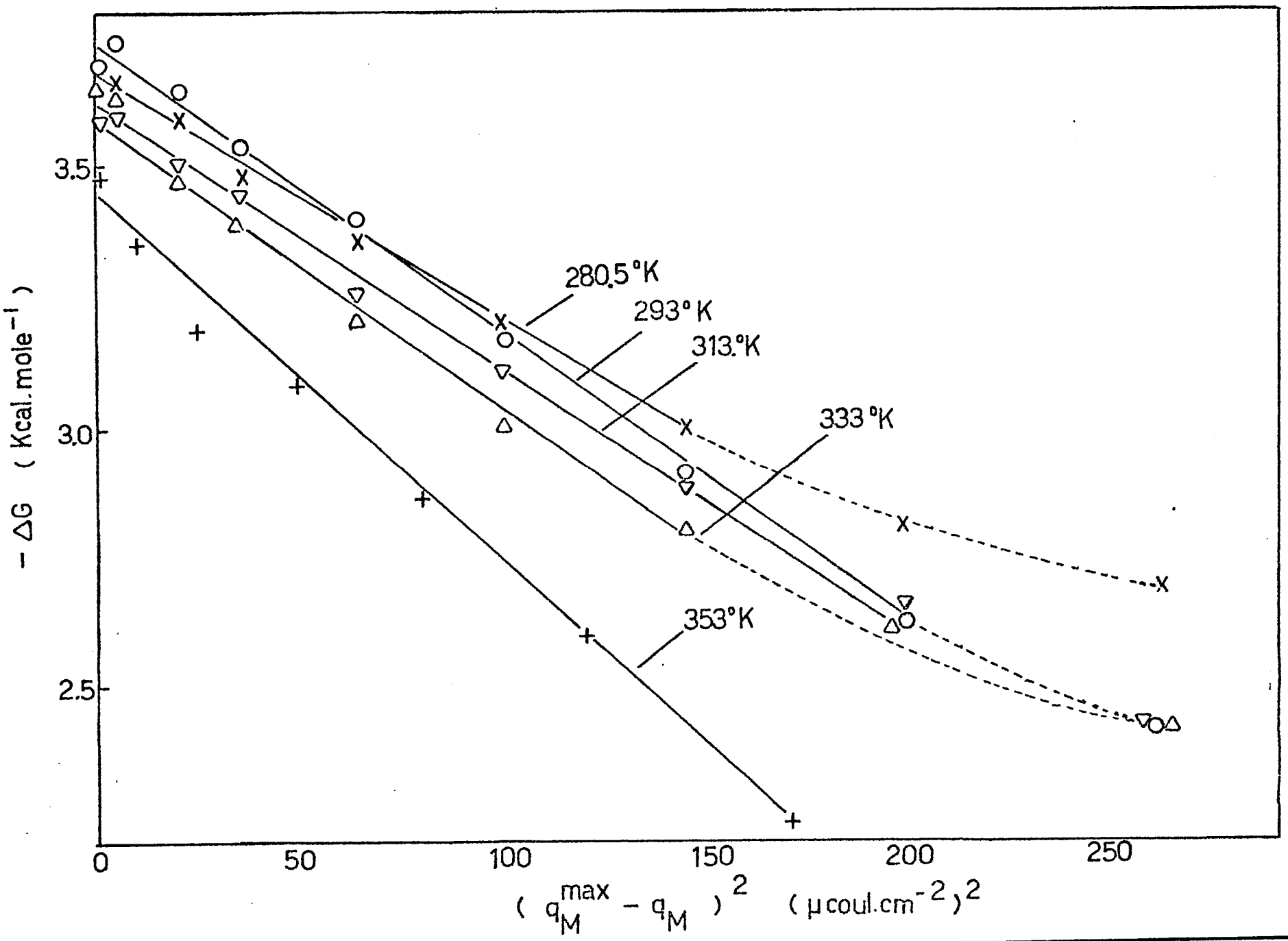
280.5°K
293°K
313°K
333°K
353°K
3.5
3.0
2.5
0
50
100
150
200
250
- ΔG (Kcal.mole⁻¹)
(q_M^max - q_M)² (μcoul.cm⁻²)²

Figure 29

Dependence of (a) heat (ΔH) and (b) entropy of adsorption of pyridine from 0.03M $NaClO_4$ upon the electrode charge density.

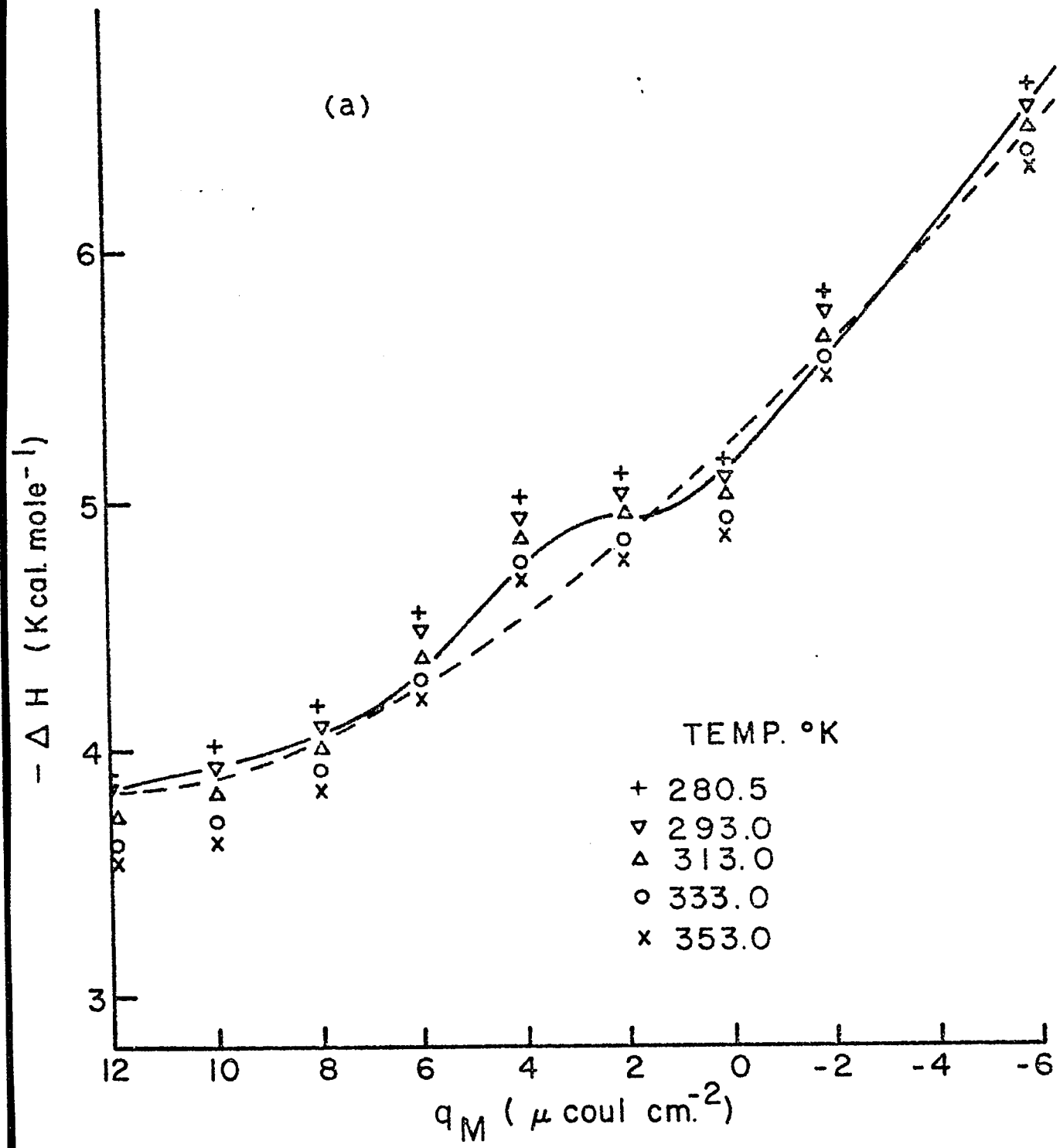
(a)
6
5
4
3
$-\Delta H$ (Kcal. mole^{-1})
TEMP. °K
+ 280.5
▽ 293.0
△ 313.0
o 333.0
x 353.0
12
10
8
6
4
2
0
-2
-4
-6
q_M (μ coul cm.$^{-2}$)

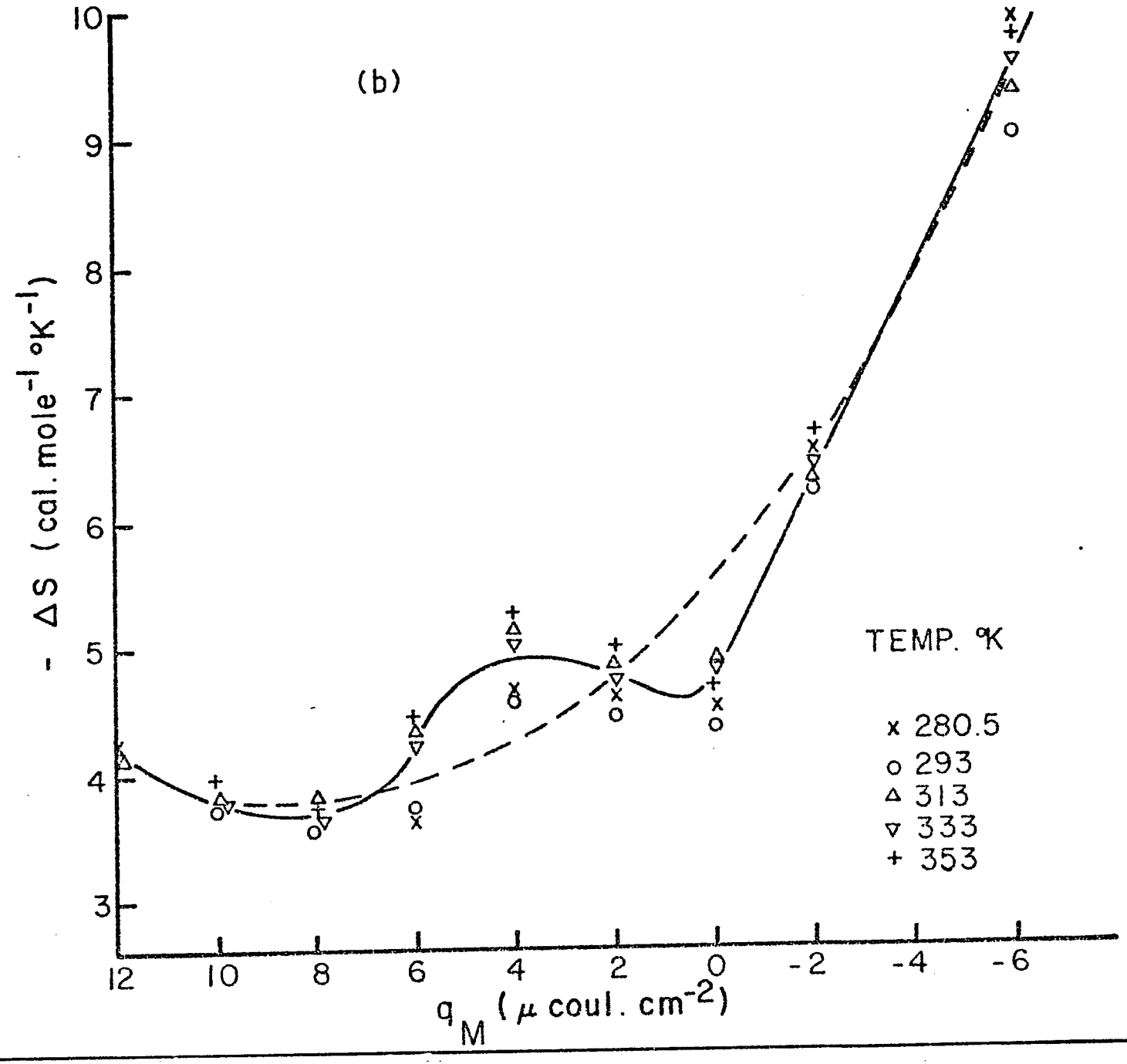
(b)
- ΔS (cal. mole^{-1} °K^{-1})
10
9
8
7
6
5
4
3
12
10
8
6
4
2
0
-2
-4
-6
q_M (μ coul. cm^{-2})
TEMP. °K
x 280.5
o 293
△ 313
▽ 333
+ 353

Figure 30

Compensation effect between heat and entropy of adsorption of pyridine from 0.03M $NaClO_4$.

Dotted line has slope of 300°K and is reproduced from Figure 25.

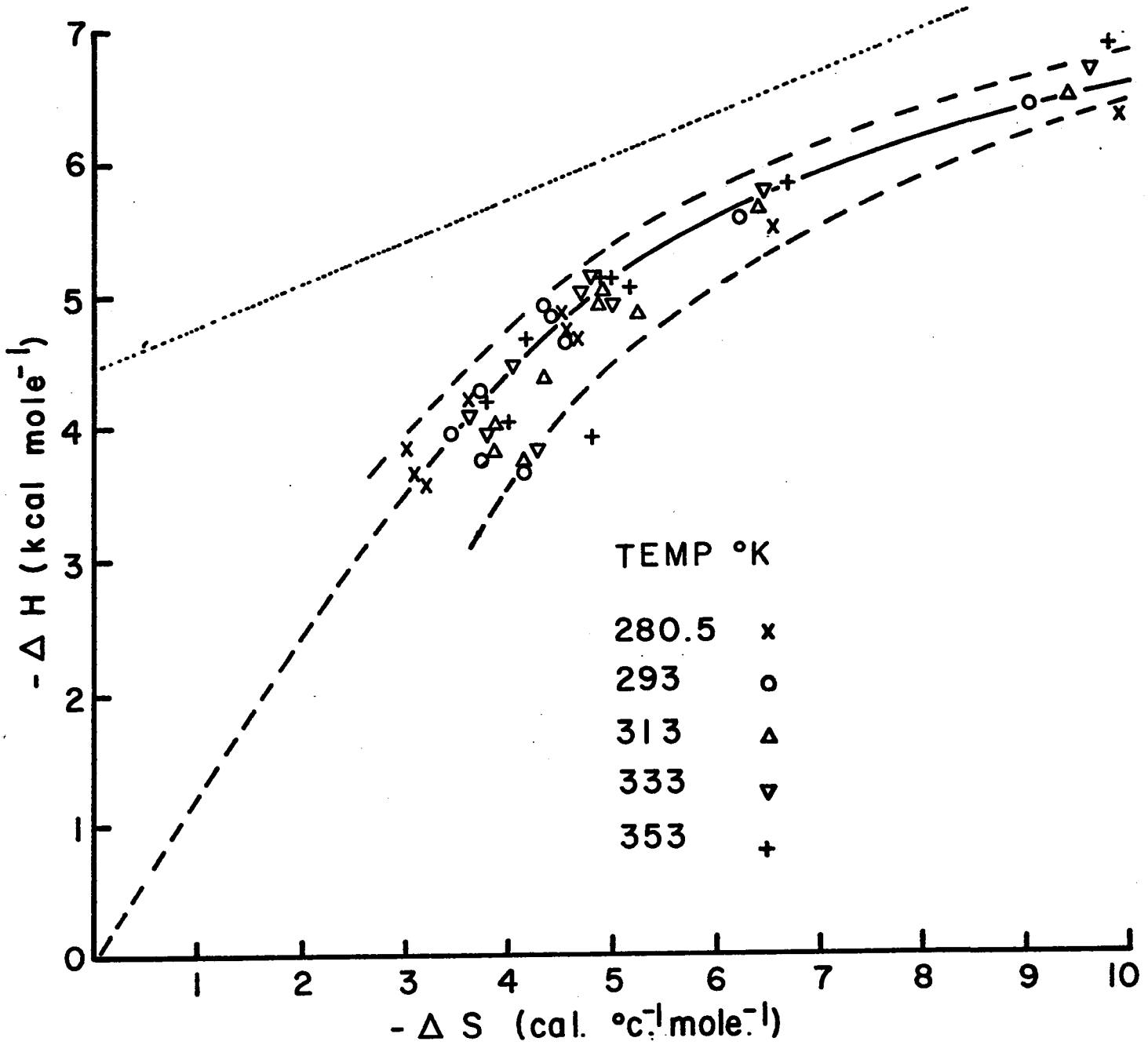
- Δ H (kcal mole⁻¹)
- Δ S (cal. °c⁻¹ mole⁻¹)
0
1
2
3
4
5
6
7
8
9
10
TEMP °K
280.5 x
293 o
313 Δ
333 ▽
353 +

plots of Figure 31. At ca. $q_M = 4$ μcoul. cm.$^{-2}$, b has a well-defined maximum and it is thought that at this charge density the pyridine molecules are π-bonded to the surface in the flat position and thus occupy a maximum area. As q_M increases or decreases from a value of $q_M = 4$ μcoul. cm.$^{-2}$, the value of b decreases from its maximum value indicating a reorientation of the adsorbed solute towards the perpendicular position. With increasing negative q_M, the negative end of the pyridine dipole (N centre) will point more towards the bulk of the solution and is then probably H-bonded to the solvent through the lone pair of electrons on the nitrogen atom. This would be energetically more favourable in the adsorption process than the reverse orientation at charges more positive than the value $q_M = 4$ μcoul. cm.$^{-2}$ where the nitrogen centre is less likely to retain its solvation. The loss or retention of solvation in the adsorption process could well be an important factor in the determination of the adsorbability of the solute (see § 1.3). The variation of ΔH with q_M (Figure 29a), it is believed, reflects these orientation effects. Likewise the entropy of adsorption will be affected by the orientation of the pyridine. At large negative q_M values, where the N atom of pyridine is bound to the solvent, translational freedom will be more hindered and thus ΔS will suffer a decrease. When rotation is confined to the plane of the pyridine ring, as could well be the case at $q_M = 4$ μcoul. cm.$^{-2}$, a small decrease in ΔS should be observed (see hump in Figure 29b and corresponding hump in Figure 29a).

The interpretations of the charge dependence of the heats and entropies of adsorption of pyridine made in this section

are not completely comparable with the conclusions reached from the Langmuir treatment in § 5.4.1, since the corresponding thermodynamic quantities in the latter case (see Figures 23 and 24) are standard quantities which are dependent on coverage, whereas those quantities referred to in this section (see Figure 29a and b) are calculated with respect to an equal distribution of solute between the surface and bulk phases (states), i.e. the Volmer treatment reported here utilizes a method of calculation of such a kind that the derived entropy and heat of adsorption are not associated with an unequal distribution of solute between surface and bulk phases; in the Langmuir case, however, the method of calculation allows the results to be interpreted, in part, in terms of solvent structure and coverage effects in the ad-layer. Therefore the quantities ΔG (§ 5.4.2) and ΔG^{o} (§ 5.4.1) are not associated with exactly the same conditions for the adsorption process; the interpretations of orientation effects and the associated solvation effects described in both treatments are nevertheless very similar.

Figure 31

Variation of co-area (b) of pyridine molecules adsorbed from 0.03M $NaClO_4$ with electrode charge density at various temperatures.

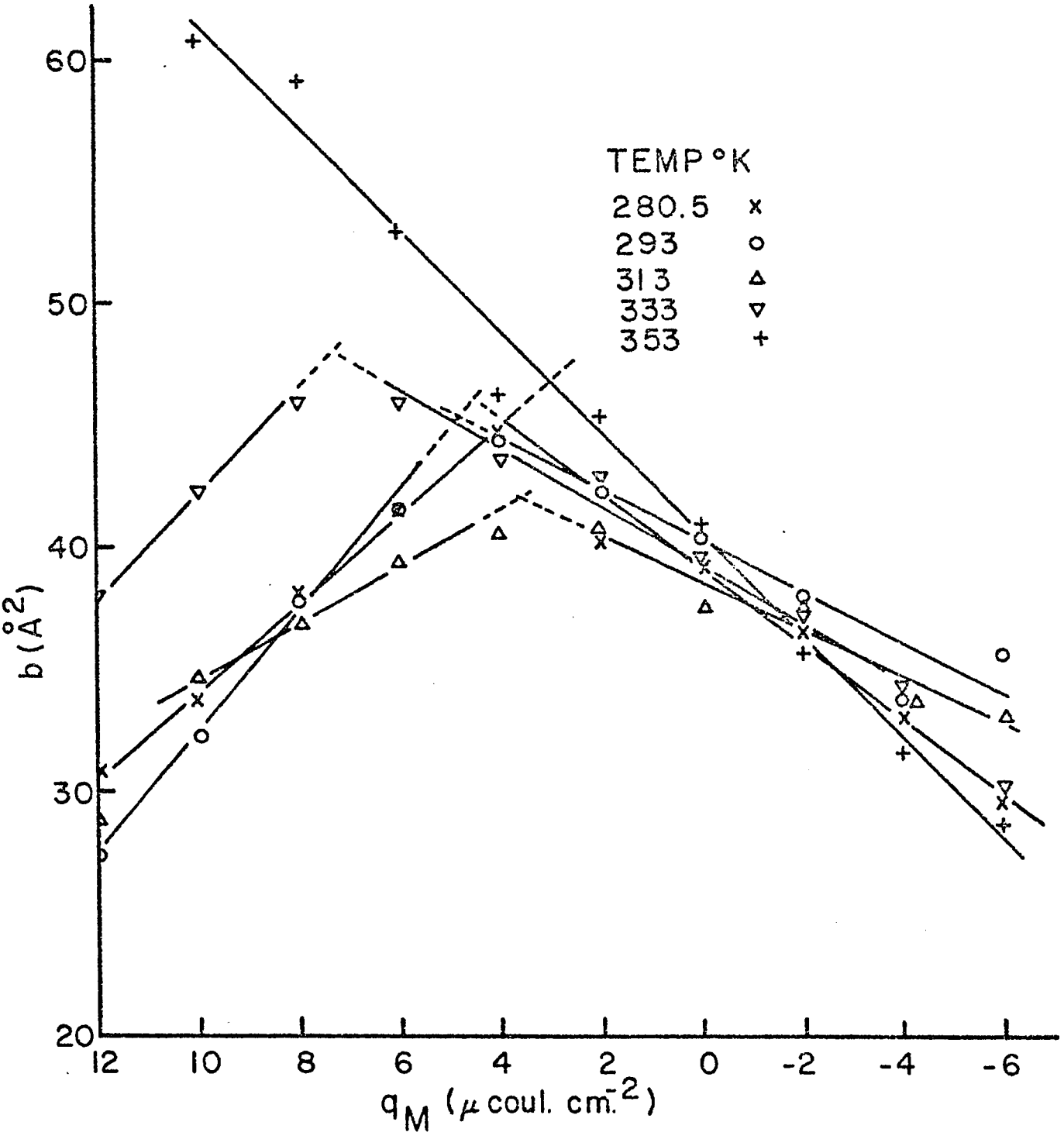
TEMP °K
280.5 x
293 o
313 Δ
333 ▽
353 +
60
50
40
30
20
b (Å2)
12
10
8
6
4
2
0
-2
-4
-6
qM (μ coul. cm-2)

5.5 ANION EFFECT IN THE ADSORPTION OF PYRIDINE

A number of studies have been made of the adsorption of pyridine from aqueous 1M KCl solution[15, 66, 67, 85, 99, 100]. In the present work, a further investigation was made in KCl electrolyte in order to provide a check on the experimental data and the methods employed, and to allow comparisons to be made with the results of a complementary study in which $NaClO_4$ was used as the supporting electrolyte. The results (and interpretations in terms of a Langmuir isotherm study) for the adsorption of pyridine from aqueous 1M KCl were in agreement with those of Barradas, Hamilton and Conway[85].

Comparisons between the results for adsorption of pyridine from aqueous $NaClO_4$ and KCl solutions have been made in § 5.4.1 in terms of the analysis based on the Langmuir isotherm. One further remark that should be made is that the ΔG^{o} values for pyridine adsorption from the $NaClO_4$ solution were, for corresponding q_M's and coverages, approximately 1 kcal. mole^{-1} less negative than in the case where KCl was the supporting electrolyte.

The novel procedure for investigating the adsorption behaviour of neutral adsorbates based on the method adopted by Kemball and Rideal[81] for the study of vapours on mercury, applies exceedingly well to the process of adsorption of pyridine from 1M KCl solution (Figure 32). This arises in part on account of the large surface pressures that arise which can be measured rather accurately. Although the plots of log C/ϕ vs ϕ (Figure 32) at negative values of q_M are not so easily interpreted on the basis of the Volmer model, it is seen that for the positive values of q_M the derived parameters b and m are well-defined (cf. equantion 73).

In Figure 33, b is seen to have a maximum at ca. q_M = 14 μ coul. cm.$^{-2}$ and q_M = 4 μ coul. cm.$^{-2}$ for the cases where the supporting electrolytes are KCl and $NaClO_4$, respectively. The

Figure 32

Plots of log C/Ø vs surface pressure at various electrode charge densities for the adsorption of pyridine from 1M KCl

q_M μ coul. cm.$^{-2}$	
16	x
15	▩
14	▽
12	●
10	◑
8	△
4	+
0	▼
-4	○
-8	□

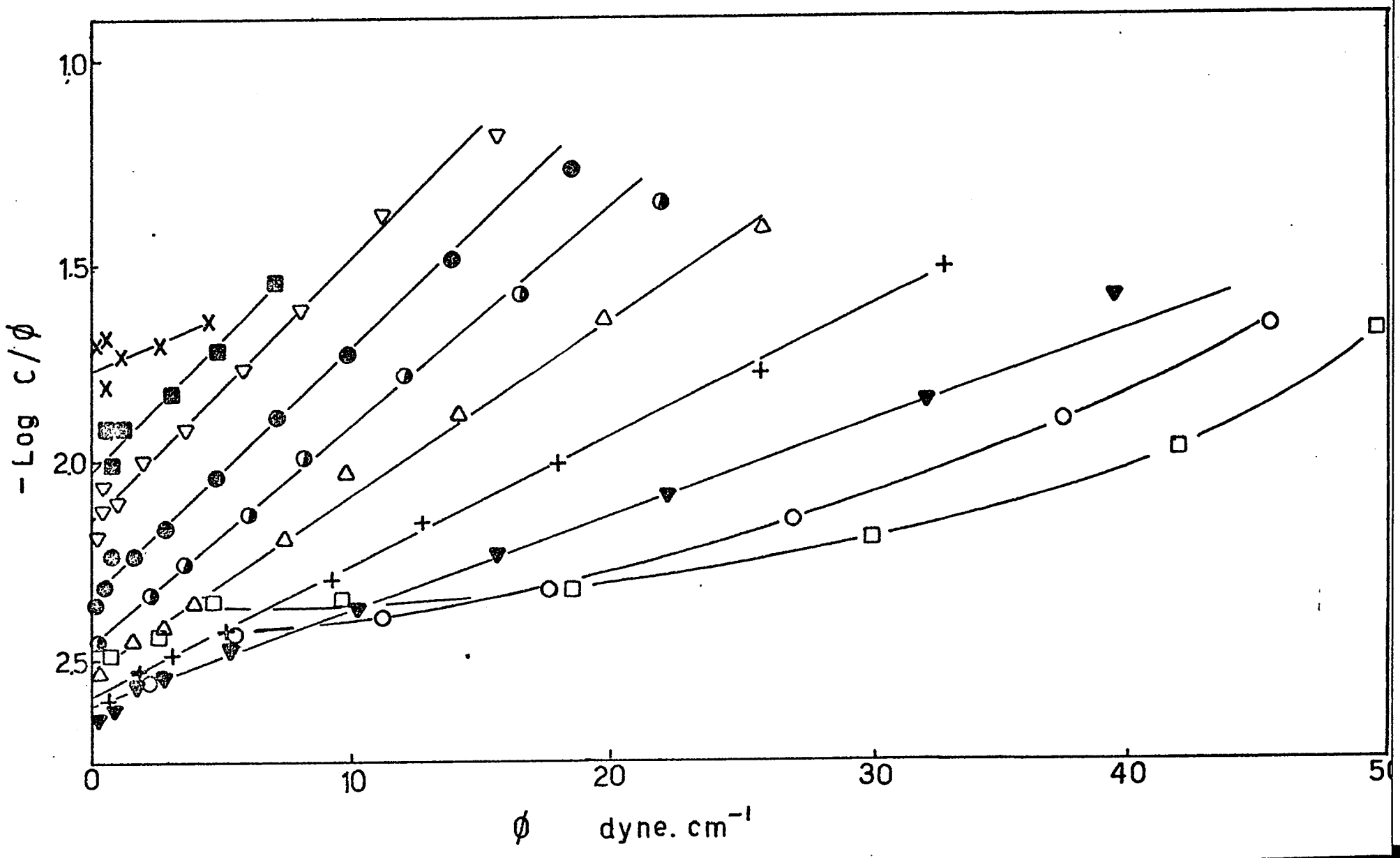
1.0
1.5
2.0
2.5
- Log c/ϕ
0
10
20
30
40
ϕ dyne. cm⁻¹

Figure 33

Dependence of co-area (b) of pyridine upon the electrode charge density and supporting electrolyte.

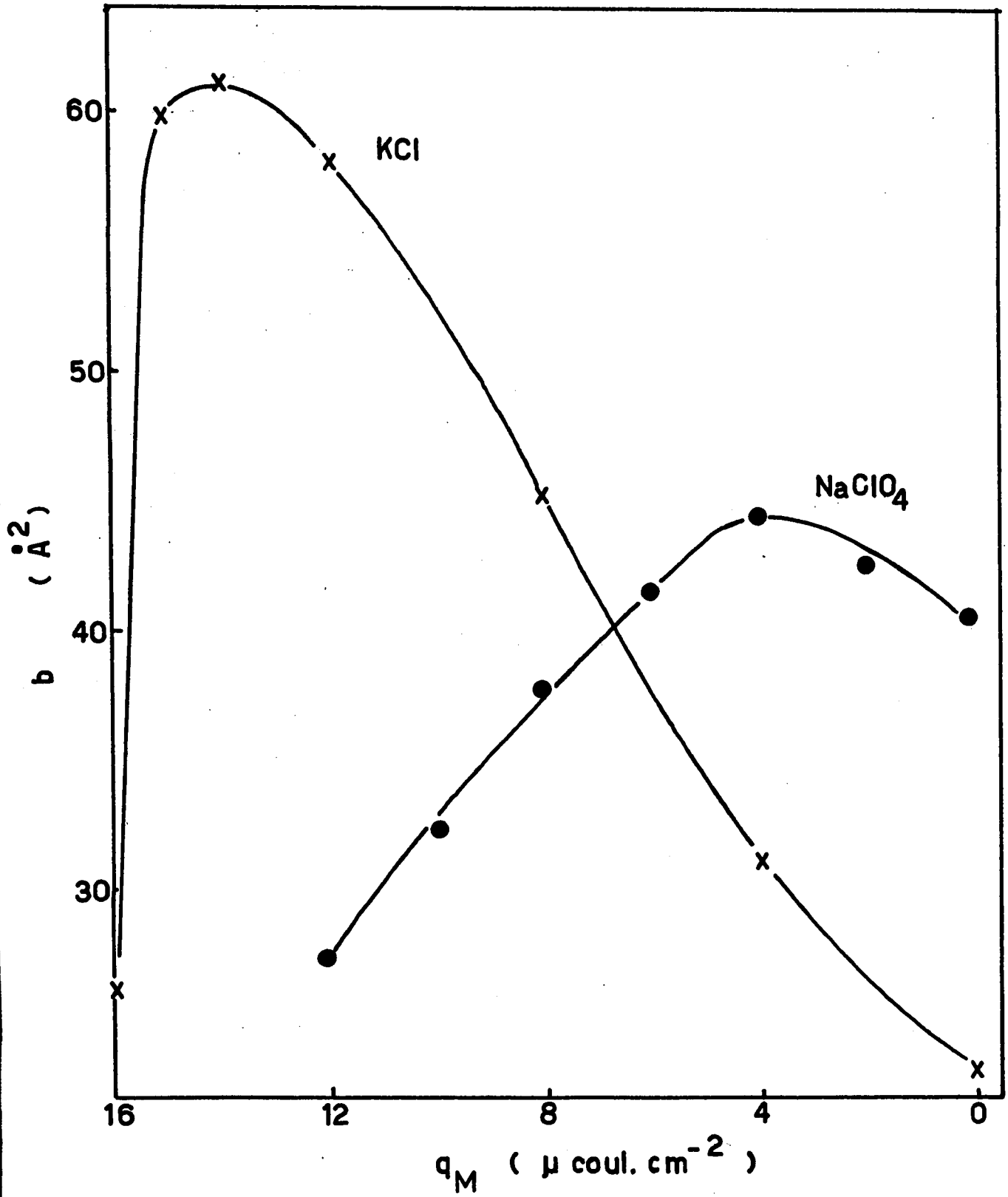
60
50
40
30
b (Å^2)
KCl
NaClO$_4$
16
12
8
4
0
q_M (μ coul. cm^{-2})

presence of the specifically adsorbed chloride ions must be responsible for the differences between the coordinates of the maximum b values. The synergetic adsorption of the pyridine molecule and chloride ion[15] referred to in § 4.4.3 is most easily interpreted in terms of an ion-dipole association where the dipole is aligned towards the centre of the ion. The electrostatic field of the adsorbed chloride ion has probably a greater effect on the orientation of the pyridine molecule than the field resulting from the charged electrode ($X = -4\pi q_M/\varepsilon$). However, at 14 μ coul. cm.$^{-2}$, the electrostatic field of the electrode begins to exert a greater influence on the pyridine dipole than does the field of the ion, so that reorientation can occur at higher positive charges for chloride solutions indicated in the values of b. The maximum value of b (supporting electrolyte $NaClO_4$) is 44 Å^2 which is slightly greater than the value of 40 Å^2 calculated by Barradas and Hamilton[68] but less than the maximum value of b (61 Å^2) found when chloride ions are present. If the ion-dipole pair exists as an entity in the ad-layer then it is not surprising that the maximum value of b (corresponding to the ion-dipole) is greater in the presence of chloride ions. In fact the ionic radius of the Cl^- ion has been given as 1.81Å (i.e. area (Cl^-) = 10.5 Å^2).

The effect of anions on the adsorption behaviour of pyridine expressed in terms of the variation of b as a function of q_M is reflected in the ΔG vs q_M plots (Figure 34). It should be remembered that the values of ΔG are obtained limitingly as ϕ approaches zero (i.e. at infinite dilution of pyridine) so that practically all pyridine molecules in aqueous 1M KCl solutions of very low concentration will be in an ion-dipole pair (Law of mass action). Thus, at large positive values of q_M, the ion-dipole pair will be more easily adsorbed than the neutral molecule (from $NaClO_4$ solutions) and this is reflected on the values of ΔG (Figure 34). At negative surface changes, the free energy of adsorption from $NaClO_4$ solutions

Figure 34

Dependence of free energy of adsorption of pyridine upon the electrode charge density and supporting electrolyte.

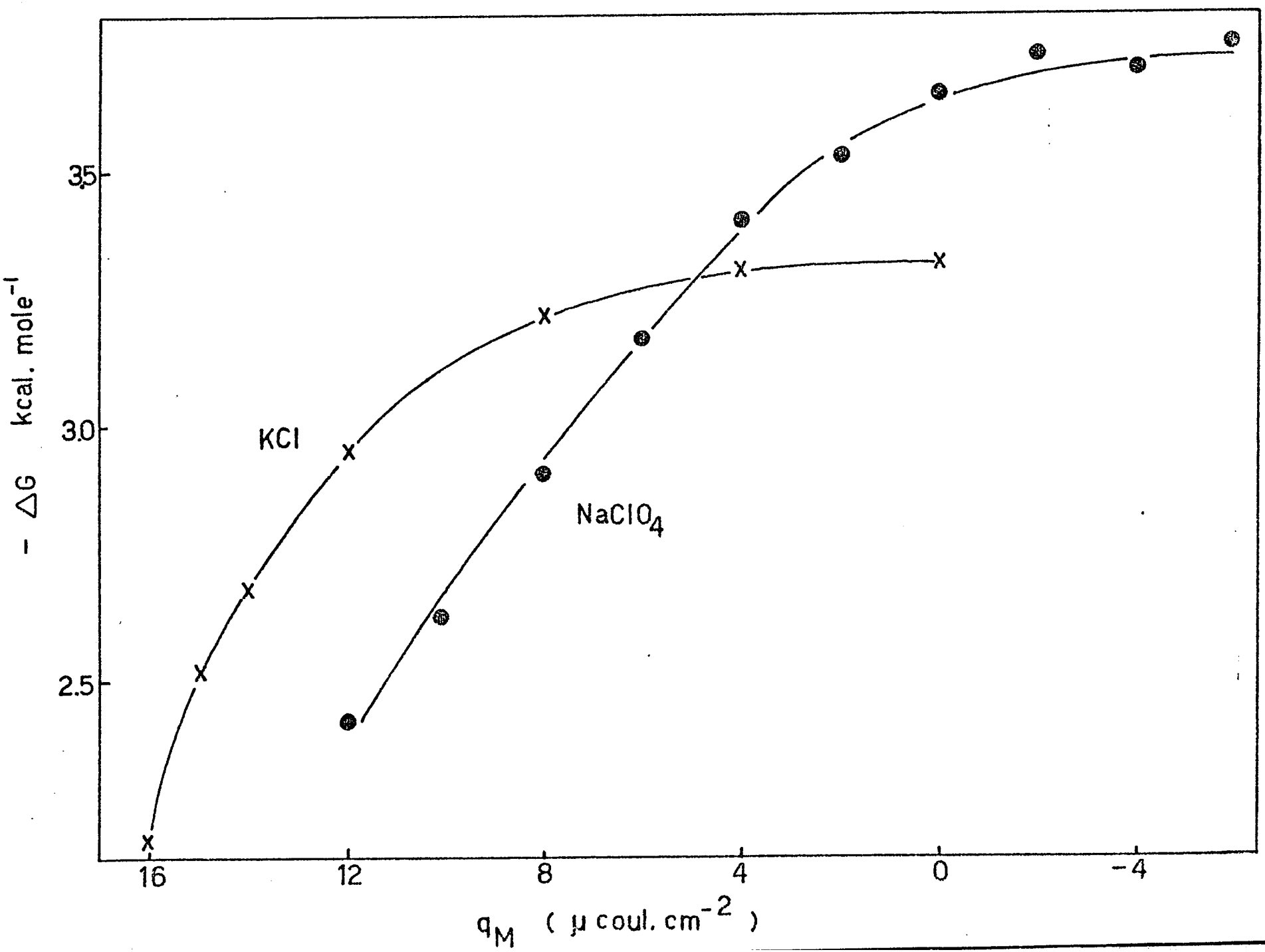
- ΔG kcal. mole⁻¹
3.5
3.0
2.5
KCl
NaClO4
16
12
8
4
0
-4
qM (μ coul. cm⁻²)

is found to be greater since the ion-dipole pair will be repelled from the electrode. Also the ion-dipole pair may be more strongly solvated than the neutral molecule: thus the differences between the values of ΔG^{o} for the two systems do not represent only the differences between the electrode-particle interactions.

5.6 REACTION ORDER AND ADSORPTION IN THE KINETICS OF THE REDUCTION OF ACETOPHENONE

A great volume of work has been carried out, particularly polarographically, on the electrochemical reduction of organic molecules. In many of the studies, the examination of reaction mechanism has been restricted to investigation of (a) the dependence of the half-wave potential on pH; (b) the form of the waves and (c) the nature of reaction products at various pH's and in various solvents. From an electrochemical point of view, current-potential characterization has been rarely carried out and the important kinetic quantity "reaction order" has been little investigated (see § 1.6).

For heterogeneous reactions, the reaction order R is a more complex quantity than in homogeneous reactions and depends on the adsorption isotherm and the reactant coverage. Generally, for an electrochemical rate process, the current density i may be written as

$$i_{V,\Theta} = k\Theta^{n} \exp \alpha VF/RT \qquad (83)$$

where Θ is the surface coverage of the reactant and n is the kinetically significant reaction order. The measured order R is (see eqn. (46))

$$R = n(d \ln \Theta/d \ln C)_{V} \qquad (84)$$

Hence evaluation of true reaction orders requires knowledge of the adsorption isotherm which determines $d \ln \Theta/d \ln C$. In the present

work, experimental evaluation of the derivative d ln Θ/d ln C has been carried out for acetophenone adsorption in relation to kinetic studies performed by another co-worker on the electro-reduction of this molecule at Hg under potentiostatic conditions.

It will be useful first to explore theoretically the dependence of R on Θ or C for some particular isotherms. One of the most widely used isotherms in electrochemical adsorption is that of Frumkin (eqn. 57) where r is an interaction (or heterogeneity[104]) parameter and K is analogous to Langmuir's constant (as $\Theta \rightarrow 0$, the Langmuir isotherm holds in the limit). R as a f(C) for equation 57 is shown in Figure 35b for a generalised case (normalised concentration scale KC); R is seen not to be constant over any appreciable range of C except as $C \rightarrow 0$ ($R \rightarrow n$) or when r is large, whereupon R can attain a low and less varying value. As with other differential quantities derived from isotherms, e.g., the pseudo-capacity[104], the pre-exponential term in eqn. (57) can never by neglected in evaluating R even for larger r values. For multisite adsorption, the analogue of Langmuir's isotherm is

$$\Theta/x(1 - \Theta)^x = KC$$

so that

$$R = n(1 - \Theta)/[1 + (x - 1)\Theta] \qquad (85)$$

which has useful special forms as x = 1, 2 or 3; in all cases, however, $R \rightarrow 0$ as $\Theta \rightarrow 1$. For competitive adsorption of two species 1 and 2, with

$$\Theta_1/(1 - \Theta_1 - \Theta_2) = K_1C_1 \; ; \quad \Theta_2/(1 - \Theta_1 - \Theta_2) = K_2C_2 \; , \qquad (86)$$

$$R = n(1 + K_2C_2)/(K_1C_1 + K_2C_2) \qquad (87)$$

Figure 35

(a) Reaction-order (R/n) derivative plots for Frumkin-type isotherm for various r values including negative ones (attractive interactions).

(b) Reaction order (R/n) from Frumkin-type isotherm with positive r values.

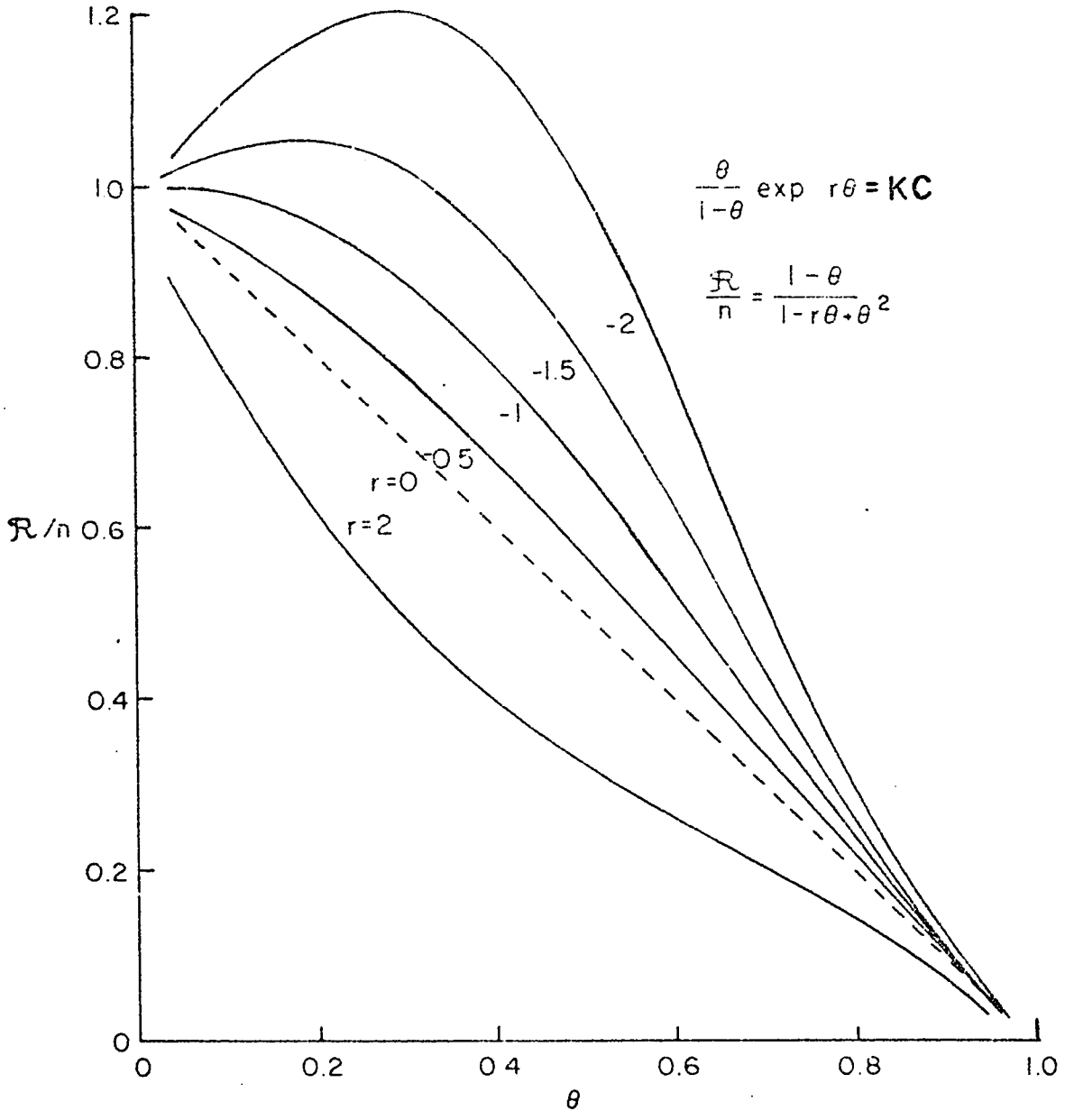
1.2
1.0
0.8
0.6
0.4
0.2
0
ℜ/n
0
0.2
0.4
0.6
0.8
1.0
θ
-2
-1.5
-1
-0.5
r=0
r=2
θ/(1-θ) exp rθ = KC
ℜ/n = (1-θ)/(1-rθ+θ²)

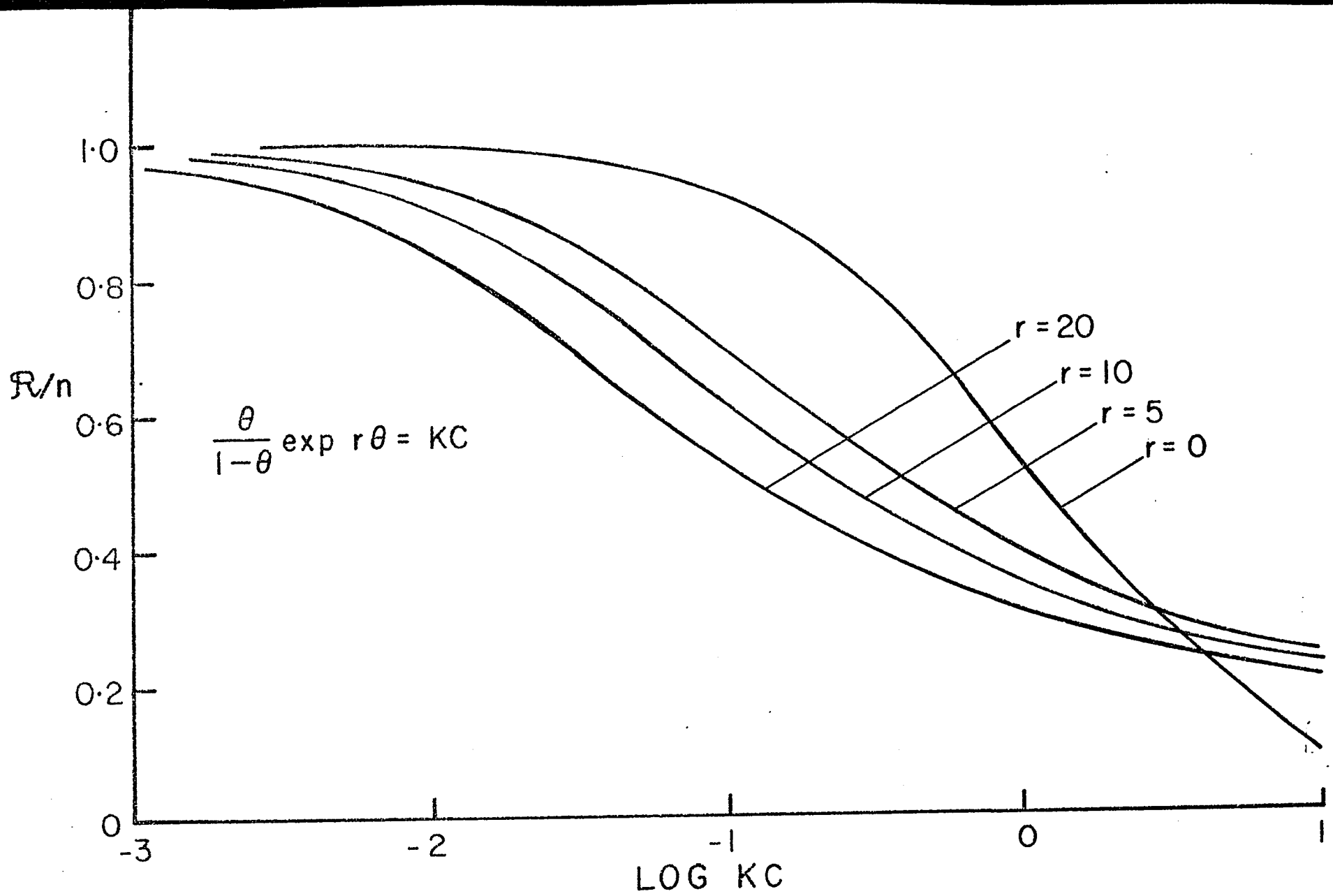
1·0
0·8
0·6
0·4
0·2
0
R/n
θ/(1−θ) exp rθ = KC
r = 20
r = 10
r = 5
r = 0
-3
-2
-1
0
1
LOG KC

An interesting case of eqn. (57) arises when $r < -1$ (attractive interactions); examples are shown in Figure 35a for R/n as $f(\Theta)$. R/n can become > 1 at low Θ but whether this is physically realizable for $r < -4$ is questionable since such conditions can correspond to 2-dimensional phase separation[104] (cf. H in Pd[105]). Evidently, however, for $-r = 1.3 - 1.5$, R/n can remain near unity for an appreciable range of Θ while for $r = 0$ or positive, R/n falls rapidly with Θ already at low Θ. This case has therefore a bearing on the experimental results presented above. However, it will be necessary to examine in more detail the significance of R and n for kinetics proceeding under "Temkin" conditions[106, 59].

From experimental log-log plots of Γ as a function of C, the term $(d \ln \Gamma / d \ln C)_V$ can be evaluated. In combination with the observed apparent orders R (evaluated by another worker in this laboratory) this derivative would give normally the molecularity n of the electrochemical surface reaction. From the present results, the required quantities can be obtained for acetophenone reduction for example at $E_H = -0.4$ and -0.6V. They give apparent values of n which will be called the order of the surface reaction R_s. n is found to be greater than R and increases substantially as $\Gamma \rightarrow \Gamma_m$ (see Table II). It is suggested that the reduction may proceed under "Temkin" (see ref.[33]) conditions and for this case we can show that the quantity $(d \ln \Gamma / d \ln C)_V$ in combination with R will not give the true n value. Thus, for a general rate equation[59] with a coverage-dependent rate constant,

$$v = k\Theta^n \exp(\alpha' nr\Theta) \exp \alpha VF/RT \,, \tag{88}$$

$$\left(\frac{\partial \ln v}{\partial \ln \Theta}\right)_V = n(1 + \alpha' r\Theta) = \left(\frac{\partial \ln i}{\partial \ln \Theta}\right)_V \,, \tag{89}$$

TABLE II

Data for evaluation of apparent surface order R_s and true molecularity n for acetophenone reduction for R = 1.1

log C		-1.9	-1.6	-1.4	-1.2	-1.0	-0.8	-0.6	-0.4	-0.2
$\frac{d \log \Gamma}{d \log C}$	-0.4v	0.9	0.73	0.52	0.435	0.38	0.33	0.32	0.3	0.32
$\frac{d \log \Gamma}{d \log C}$	-0.6v	0	0.75	0.58	0.43	0.38	0.37	0.34	0.32	0.33
$(R_s)_{-0.4v}$		1.22	1.45	2.05	2.45	2.78	3.25	3.36	3.55	3.36
$(R_s)_{-0.6v}$			1.47	1.9	2.54	3.02	3.01	3.25	3.48	3.38
$\Gamma^{3/2} \times 10^{15}$	-0.4v	0.21	0.41	0.62	0.86	1.15	1.5	1.85	2.3	2.8
$\Gamma^{3/2} \times 10^{15}$	-0.6v		0.31	0.49	0.69	0.91	1.19	1.52	1.93	2.4

so that the derivative gives n only as $\Theta \rightarrow 0$. In the general case of finite Θ,

$$n = \left(\frac{d \ln i}{d \ln \Theta}\right)_V / (1 + a'r\Theta), \qquad (90)$$

or in terms of the experimental R quantity, $(d \ln i / d \ln C)_V$,

$$n = \frac{R}{(d \ln \Theta / d \ln c)_V} / (1 + a'r\Theta) = R_s/(1 + a'r\Theta) \qquad (91)$$

Care must therefore be exercised in the interpretation of reaction orders if the reaction proceeds under conditions where interaction and/or heterogeneity effects lead to a dependence of rate constant on coverage (cf. ref.[107]). In the present case, for nearest-neighbour dipole repulsion effects, the interaction term will have approximately the form $r'\Theta^{3/2}$ so that by performing operations similar to those in the general case above,

$$n = R_s/(1 + \frac{3}{2} a'r'\Theta^{3/2}) . \qquad (92)$$

Then R_s will be proportional to $\Gamma^{3/2}$ with an intercept at $\Theta = 0$ of n. This type of plot is shown in Figure 36, based on the experimental evaluation of Γ for acetophenone and evidently the <u>true</u> molecularity of the surface reaction is 1, a value to which the extrapolation of the plots of Figure 36 leads. This evaluation of the true molecularity of the surface reaction used in conjunction with the electrode-kinetic parameters determined in the other electrochemical kinetic work mentioned above, then enables the kinetics and mechanisms of the reduction of acetophenone to be elucidated (see ref.[74] arising from the present work).

From the electrocapillary studies, the free energy of adsorption of the pinacol was found to be greater than that for the acetophenone in the range of potentials that can be employed in electrocapillary studies. However, it was found that the presence of excess pinacol did not significantly affect the rate of reduction of acetophenone. It must therefore be supposed that at the increased

Figure 36

Plots of apparent surface reaction order (R_s) against $r^{3/2}$.

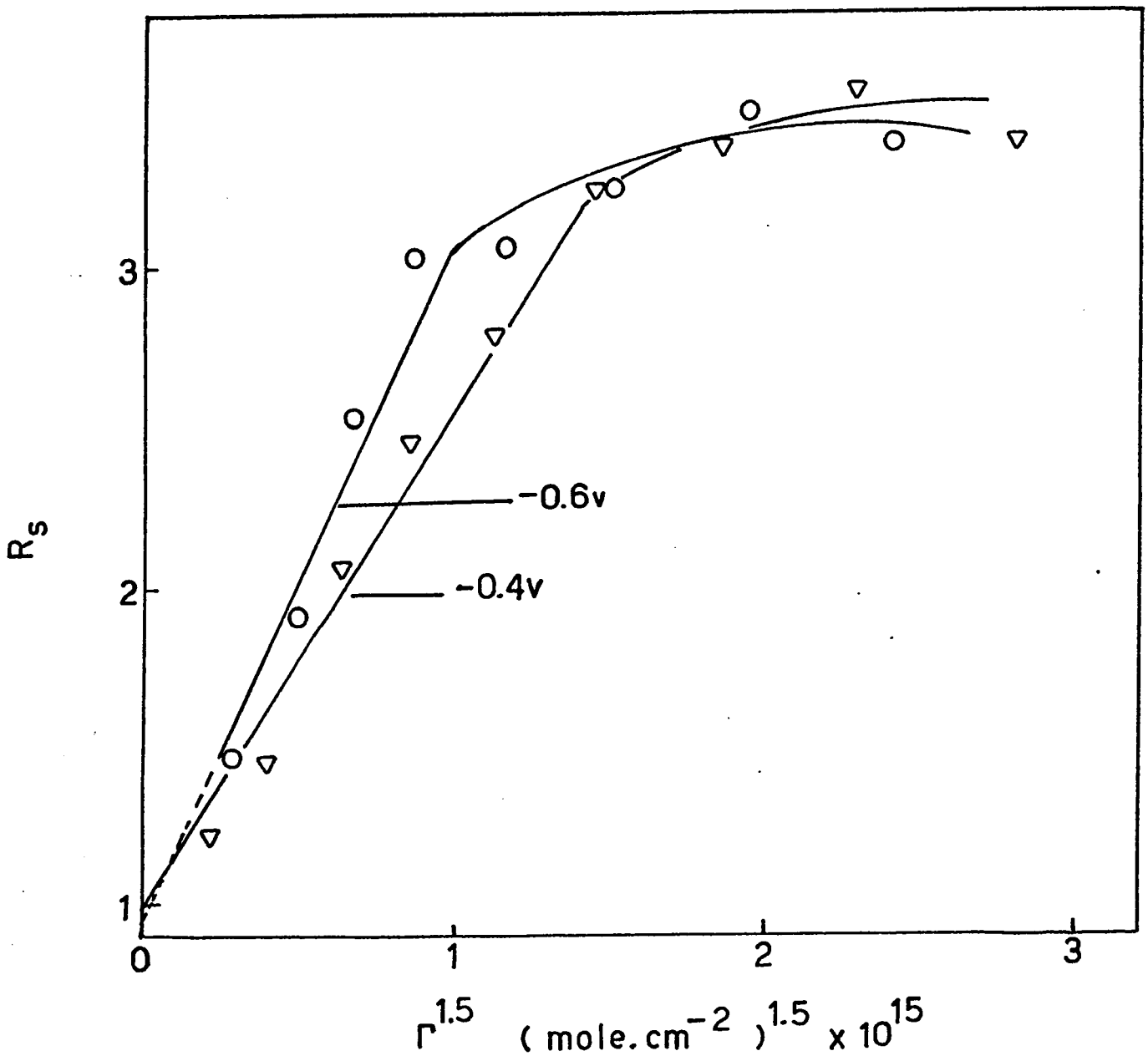
R_S
3
2
1
0
1
2
3
-0.6v
-0.4v
$\Gamma^{1.5}$ (mole.cm^{-2})$^{1.5}$ x 10^{15}

surface charge density, (in the region of potential where reaction occurs) the nearly "non-polar" pinacol is desorbed easily.

5.7 ADSORPTION OF OPTICALLY ACTIVE ISOMERS

Enantiomers usually have the same physical and chemical properties. However physical (chromatography[101]) and chemical (synthesis[102]) methods have been used for the separation of optical isomers.

An experiment which would allow differences in the adsorbability of two enantiomers (DA and LA) at a mercury electrode-solution interface was devised. Since mercury is optically inactive it would be necessary to have an ad-layer of a second optically active solute (say LB) which adsorbs reasonably well to give monolayer coverage but which is easily replaced by DA or LA. Differences between the adsorption characteristics of DA and LA would allow a better understanding of the solute-'solvent' (LB) interactions in the ad-layer to be attained since DA and LA would have the same interaction with the mercury (see § 5.1.1a).

A preliminary experiment was conducted using an aqueous (2N L(+)lactic acid [LB above] + 0.1N H_2SO_4) solution which it was hoped would give the mercury electrode a reasonable coverage of lactic acid. The concentration of lactic acid was kept below 2N since lactide formation becomes prominent at higher concentrations. L(+) and D(-) mandelic acids were the solutes chosen for the adsorption study.

The surface pressures that arise from the adsorption of L(+) and D(-) mandelic acids under identical conditions of bulk concentration and charge are plotted against each other in Figure 37 in which the theoretically expected line $\phi_{DA} = \phi_{LA}$ is also drawn. Two sets of data representing the initial and final time-dependent surface

Figure 37

Comparison of surface pressures of L(+) and D(-) mandelic acids at corresponding electrode potentials and bulk concentrations.

x pressure recorded immediately after meniscus formed inside capillary.

o pressure recorded after one hour.

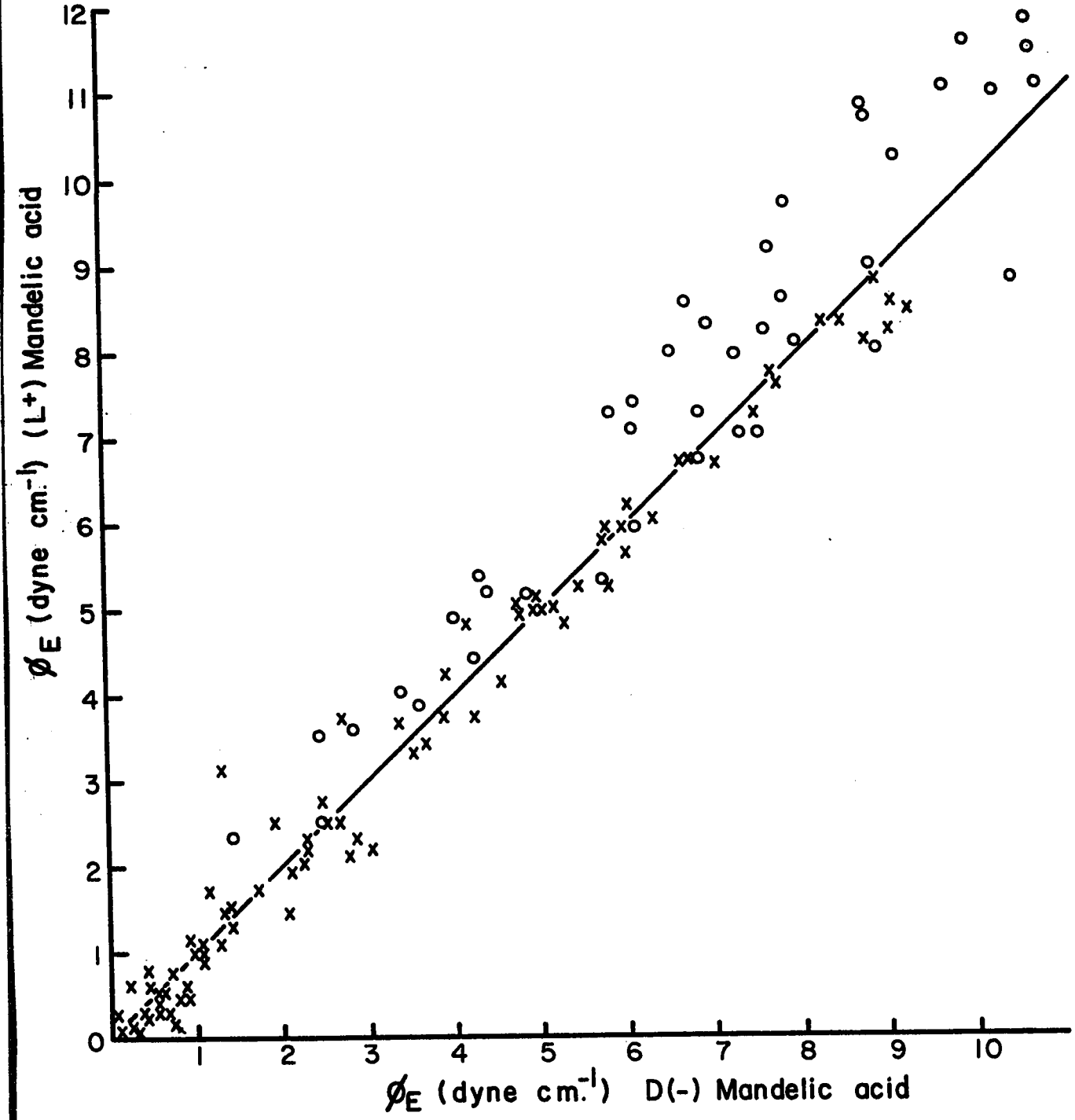
12
11
10
9
8
7
6
5
4
3
2
1
0
ϕ_E (dyne cm.$^{-1}$) (L+) Mandelic acid
1
2
3
4
5
6
7
8
9
10
ϕ_E (dyne cm.$^{-1}$) D(-) Mandelic acid

pressure to reach a final steady state (no time dependence was found in any other study in this work).

Sufficient time was given before each experimental run to allow any esterification processes to reach equilibrium.

It is unlikely that the time-dependence of the surface tension of the electrode is due to the diffusion of the mandelic acid to the interface. It is more probable that the greater concentrations of the mandelic acids in the ad-layer which are quickly obtained disturb the equilibrium between the products and the reactants of the esterification process and thus time is necessary to restore the equilibrium in the surface layer, i.e. the change of surface pressure with time is probably due to the formation of esters. This result was not predictable, however, since the electrocapillary data for the basic solution 2N L(+) lactic acid, which is similar in structure to the mandelic acid, showed no such time dependence of the adsorption process. If the formation of esters, (mandelic lactates or lactic mandelates) is responsible for the time dependence of the surface pressure, then it is not possible to conclude whether the isomeric effects are due to concentration differences (i.e. esterification proceeding to different extents for the different isomers) or to the nature (or properties) of the diasterioisomers in the L(+) lactic acid medium. On the other hand, if the esters formed are mandelic mandelates, then the second of the two reasons just given must apply. The only conclusion that can be drawn from the study at the present time is that optical isomeric differences cause the differences in observed pressures.

It appeared that further investigations along the lines suggested above would be of value although it would be advisable to choose systems of constant chemical nature. Recently an investigation of the adsorption of dibenzoyl tartaric acid (D. B. T. A.) has been

investigated using the drop-time technique with application to the study of the adsorption of enantiomers[103].

D- and L- and DL- D. B. T. A. were adsorbed at the Hg-0.1N HCl solution interface and the electrocapillary curves indicated that at corresponding bulk concentrations, surface pressures due to the racemate were higher than those due to the L- or D- D. B. T. A.

5.8 CONCLUSION

In a recent review[26] it has been stated that the Frumkin equation of state

$$\phi = -kT \Gamma_m(1 - \Gamma / \Gamma_m) + A\Gamma^2 + \ldots \qquad (93)$$

where the second and following terms of the R. H. S. represent lateral interaction effects between the adsorbate solute, would be the most useful representation of the adsorption of a solute at a mercury-solution interface. This representation of the surface layer which is widely accepted is based on the premise that solute-solute interactions are responsible for the variation of the free energy of adsorption with coverage. However, this behaviour may be accounted for in other satisfactory ways. Firstly, the free energy of adsorption at the mercury-solution interface can be shown to be independent of coverage if there is a freedom of choice of Γ_m (§§5.2.2, 5.3). Secondly the ratio of sizes of solute and solvent, when different from unity, gives rise to a coverage dependent free energy of adsorption when the evaluation is based on the Langmuir isotherm (§ 5.1.1b). In addition, discussion (§ 5.3) based on experimental evidence indicates that solute-solute interactions of neutral molecules may be negligible in most cases.

Furthermore, the Frumkin equation of state is, like the Langmuir relation, dependent on a correct estimate of Γ_m (§ 5.2.2 and §5.3) whether it be considered fixed or variable. This is an

unsatisfactory aspect of the treatment, since Γ_m can be influenced by surface concentration and electrode charge density (orientation effects § 5.2), and values are never unambiguous since they may also depend on the method by which the Γ_m is obtained (TableII).

A treatment which is effective in avoiding the above difficulties (i.e. one in which no solute-solute interaction term nor a Γ_m term is involved) is based on the Volmer equation of state. In fact its success in representing the adsorption in the surface layer is demonstrated in the linearity of the ln C/ϕ vs ϕ plots. This model is not only applicable to the adsorption of dipolar neutral molecules but, as shown in Figure 38a, b and c, the results obtained for naphthalene adsorption from methanolic solutions also illustrate the appropriateness of the Volmer type of representation. The values of b obtained from the slope of the ln C/ϕ vs ϕ plots were interpreted as the molecular areas, as was done by Kemball and Rideal[81]. (The Langmuir treatment of the adsorption of naphthalene is graphically represented in Figure 39.)

Although the Volmer model appears to be adaptable to the mercury-solution interphase, the usual procedure using the Langmuir isotherm was also employed and results obtained from this method for the adsorption of pyridine from an aqueous $NaClO_4$ solution indicated that a close compensation arose between the entropy and enthalpy of adsorption under isosteric conditions and tended to make ΔG^o a function relatively insensitive to q_M and Γ. In addition, this aspect of the work showed that the $T\Delta S^o$ term was of such consequence that interpretations of ΔG^o in terms of energies of interactions alone could be misleading. The results of the investigation also indicated that the adsorption characteristics of pyridine at mercury are much more closely and specifically connected with the behaviour of water adsorbed in the interphase than has hitherto been supposed or recognized.

Figure 38

(a) Plots of log C/ϕ vs surface pressure (ϕ) at various electrode charge densities for adsorption of naphthalene.

q_M	μcoul. cm.$^{-2}$
12	○
8	△
4	+
0	□
-4	x

(b) Variation of ΔG with electrode charge density.

(c) Variation of co-area (b) with electrode charge density.

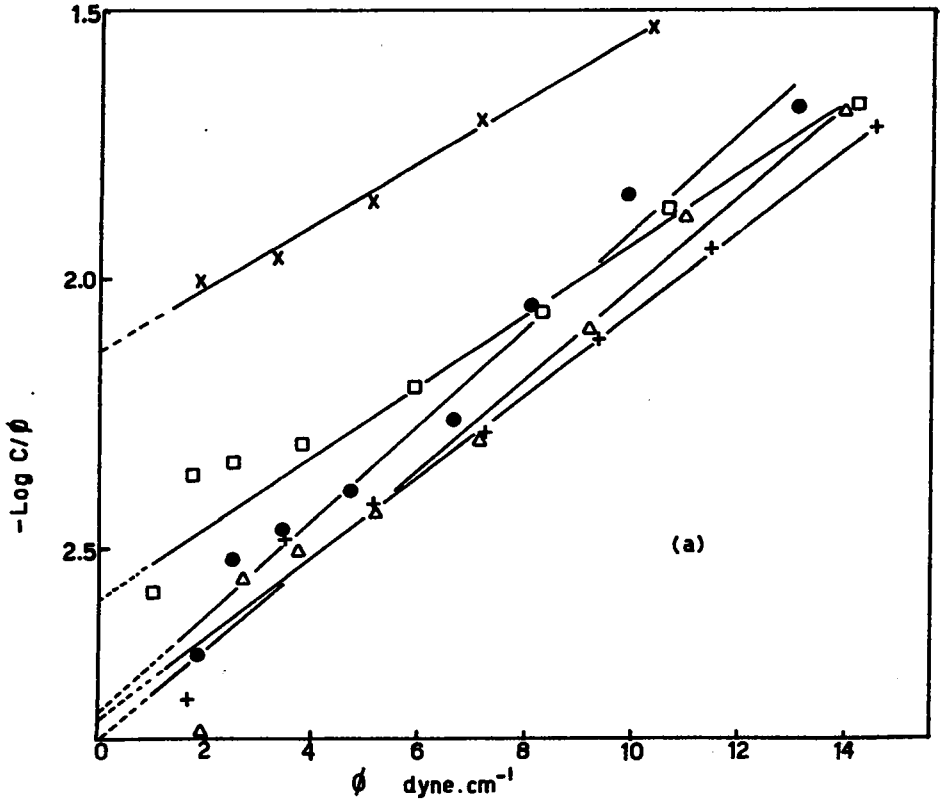
1.5
2.0
2.5
-Log C/ϕ
0
2
4
6
8
10
12
14
ϕ dyne.cm⁻¹
(a)

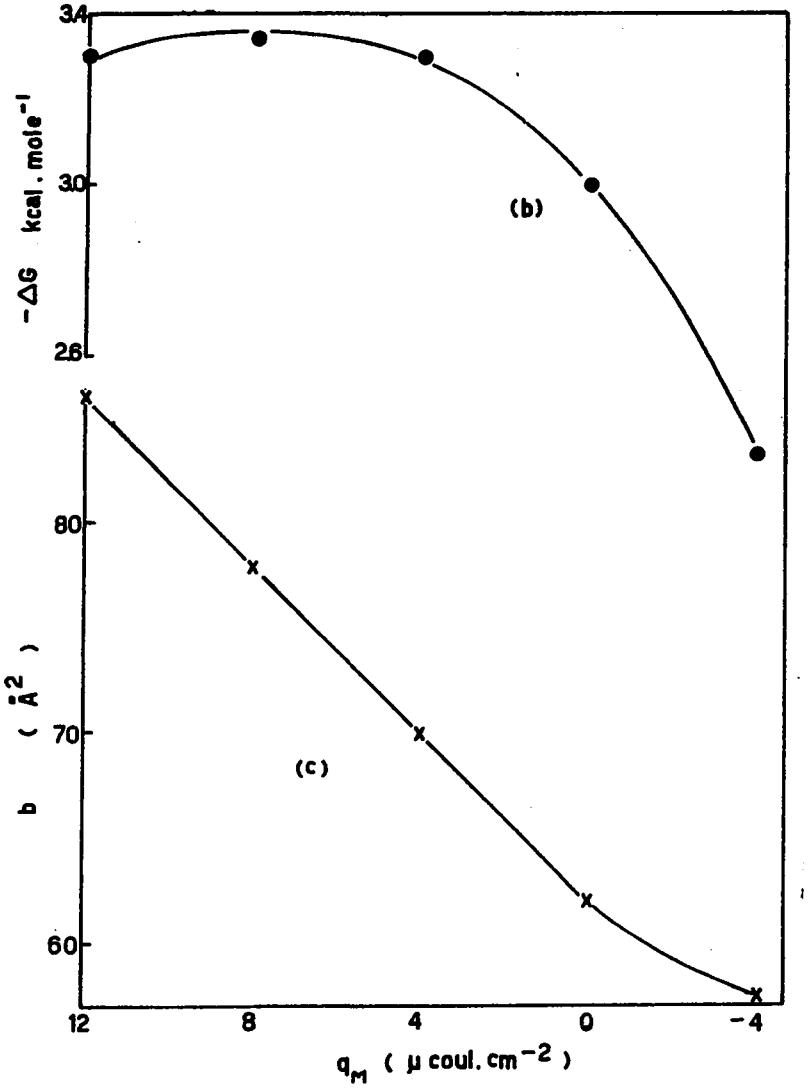
34
30
26
-ΔG kcal. mole⁻¹
(b)
80
70
60
b (Å²)
(c)
12
8
4
0
-4
q_M (μ coul. cm⁻²)

The solvent in the ad-layer was also found to be of greater importance than the solute in determining the adsorption behaviour of acetophenone, its pinacol and naphthalene. This was shown in the ϕ - Γ plots which, for the adsorption of the same solute from various solutions, were found to be different, but which for different solutes adsorbed from the same solvent were, however, more similar (§§ 4.5.1 and 4.6).

The adsorption of acetophenone at the mercury-solution interface was studied in order to enable the true molecularity (n) of the surface reduction of acetophenone to its pinacol to be evaluated. It was not surprising to find that the order of the surface reaction (R_s) was dependent on $\Gamma^{3/2}$ due to interaction effects since the reaction involved the approach of two relatively large localised dipoles (see the behaviour of 2-chloropyridine referred to in § 5.3(a) and (e)).

Finally, in regard to developments of experimental procedure, new techniques were developed to increase the accuracy and convenience of electrocapillary measurements.

Figure 39

Variation of $\Delta G^{o}/RT$ with $\Gamma^{3/2}$ for the adsorption of naphthalene at various electrode charge densities.

$\Gamma_m = 2.4 \times 10^{-10}$ mole cm.$^{-2}$

	q_M μ coul. cm.$^{-2}$
●	12
Δ	8
+	4
□	0
x	-4

○ $\Gamma_m = 1.5 \times 10^{-10}$ mole cm.$^{-2}$; $q_M = 12$ μ coul. cm.$^{-2}$.

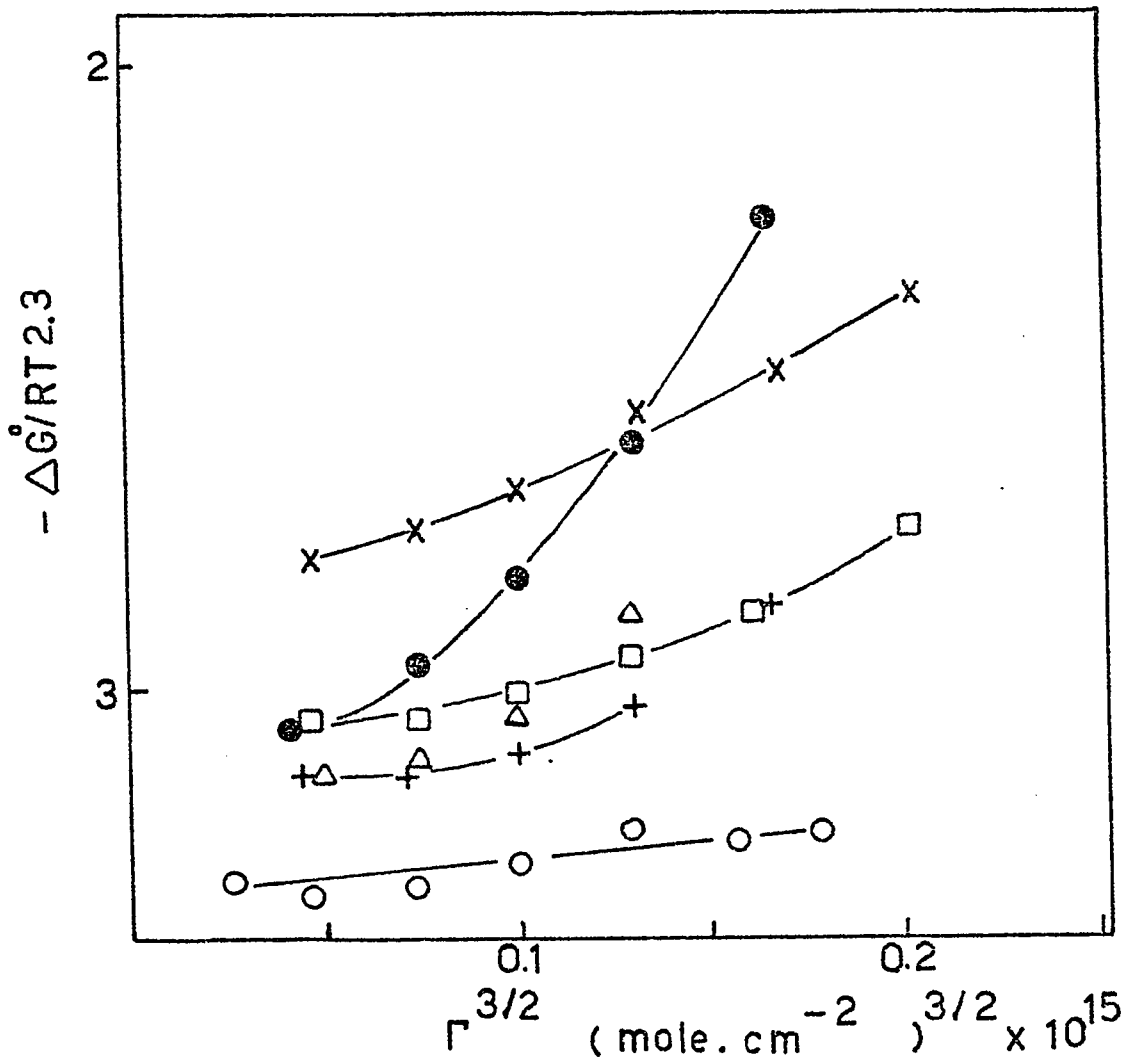
2
3
$-\Delta G^{\circ}/RT\,2.3$
0.1
0.2
$\Gamma^{3/2}$ (mole. cm^{-2})$^{3/2}$ x 10^{15}

CLAIMS TO ORIGINAL RESEARCH

I. New Experimental Results and Theoretical Interpretations

1. Electrochemical isotherms for several neutral aromatic molecules have been determined at the mercury-solution interface in relation to orientation effects associated with the solvent and adsorbate molecules.

2. The standard entropy and heats of adsorption of a neutral organic species (pyridine) have been evaluated in detail.

3. The behaviour of ϕ - Γ plots have been correlated with the nature of the solvent in respect to its structural and polar properties.

4. The generally accepted interpretation of the $\Delta E_{p.z.c.}$ vs Γ graphs which exhibit two distinct linear regions has been modified.

5. Arguments have been advanced suggesting that apparent deviations from ideality can be caused as much by incorrect assignment of the relevant molecular area of the solute to be used in a Langmuir type isotherm as by true solute-solute interaction effects. These deviations can also arise if a Langmuir treatment is applied in a situation where the surface phase is gaseous.

6. A method for the evaluation of the thermodynamic quantities for the adsorption of neutral molecules at

the mercury-solution interface has been developed using a Volmer type isotherm and equation of state.

7. Theoretical interpretations of the effect of anions on the adsorption of pyridine have been presented.

8. The stereospecific behaviour of the optically active isomers, D- and L-mandelic acidsadsorbed into a surface phase previously enriched with L-lactic acid have been investigated.

9. Adsorption isotherms for acetophenone and its pinacol have been obtained in order to provide a direct interpretation of kinetic reaction orders in the electroreduction of acetophenone at mercury. This is the first time kinetics of an electro-organic reaction at Hg has been examined directly in relation to the quantitatively measured adsorption behaviour for reactant and product.

II. New Experimental Techniques

1. A new electrical system has been developed to locate accurately the meniscus in the capillary in capillary electrometer measurements.

2. A new technique is reported for the pressure measurements required in capillary electrometry and utilises a micrometer and the manometer fluid (mercury) in an electrical circuit.

3. A new closed-circuit television microscope system is also reported for direct and facile viewing of the capillary and mercury in capillary electrometer measurements.

REFERENCES

1. J. C. P. Mignolet, "Chemisorption", (Ed. W. E. Garner), p. 118, Butterworths, London (1957).
2. R. V. Culver and F. C. Tompkins, Advanc. Catalys., 11, 67 (1959).
3. J. C. Henniker, Rev. of Mod. Phys., 21, 322 (1949).
4. J. Frenkel, "Kinetic Theory of Liquids", p. 356, Dover Pub. Inc., N. Y. (1955).
5. W. D. Harkins, "The Physical Chemistry of Surface Films," pp. 36-41, Rheinhold Pub. Co., N. Y. (1952).
6. N. H. Fletcher, Phil. Mag., 7, 255 (1962).
7. R. J. Good, J. Phys. Chem., 61, 810 (1957).
8. B. E. Conway, R. G. Barradas and T. Zawidski, J. Phys. Chem., 62, 676 (1958).
9. J. J. Kipling, "Adsorption from Solutions of Non-Electrolytes," Academic Press, London (1965).
10. G. E. Bayle and A. Klinkenburg, Rec. Trav. Chim., 76, 593 (1957).
11. J. J. Kipling, Proceedings of the Second International Congress of Surface Activity, Butterworths, London (1957), Vol. III, p. 462.
12. J. J. Kipling, Proceedings of the Third International Congress of Surface Activity (1960). Verlag der Universitats druckerei, Mainz, Vol. II, p. 77.
13. M. A. Gerovich and G. F. Rybalchenko, Zhur. Fiz. Khim., 32, 109 (1958).
14. A. N. Frumkin, A. Gorodetskaya and P. Chugunov, Acta phys. chim., U. R. S. S., 1, 12 (1934).
15. B. E. Conway, R. G. Barradas, P. G. Hamilton and J. M. Parry, J. Electroanal. Chem., 10, 485 (1965).

16. C. G. Gasser and J. J. Kipling, Proceedings of the Fourth Conference on Carbon, Pergamon Press, London and N. Y. (1960), p. 55.

17. A. Blackburn and J. J. Kipling, J. Chem. Soc., 3819 (1954).

18. A. I. Vogel, "A Textbook of Quantitative Inorganic Analysis," Longmans, Green and Co. (1951), p. 780.

19. E. A. Flood, in "The Solid-Gas Interface," Vol. I, pp. 11-75. (Ed. E. A. Flood), Marcel Dekker Inc., N. Y. (1967).

20. R. Parsons, Trans. Faraday Soc., 51, 1518 (1955).

21. B. B. Damaskin, J. Electroanal. Chem., 7, 152 (1964).

22. A. N. Frumkin, Z. Physik, 35, 792 (1926).

23. D. C. Grahame, J. Am. Chem. Soc., 80, 4201 (1958).

24. A. N. Frumkin, J. Electroanal. Chem., 7, 152 (1964).

25. E. Dutkiewicz, J. D. Garnish and R. Parsons, J. Electroanal. Chem., 16, 505 (1968).

26. R. Parsons, J. Electroanal. Chem., 7, 136 (1964).

27. D. M. Mohilner, Electroanalytical Chemistry, Vol. I, pp. 241-422, (Ed. A. J. Bard), Marcel Dekker Inc., N. Y. (1966).

28. H. L. F. von Helmholtz, Ann. Physik (2) 89, 211 (1853); (3) 7, 337 (1879).

29. G. Gouy, Compt. rend., 149, 654 (1910).

30. D. L. Chapman, Phil. Mag., (6) 25, 475 (1913).

31. O. Stern, Z. Elektrochem., 30, 508 (1924).

32. D. C. Grahame, Chem. Revs., 41, 441 (1947).

33. B. E. Conway, "Theory and Principles of Electrode Processes," Ronald Press, N. Y. (1965).

34. P. Delahay, "Double Layer Theory and Electrode Kinetics," Interscience Publishers, N. Y. (1965).

35. R. Parsons, J. Electroanal. Chem., 5, 397 (1963).

36. A. N. Frumkin, J. Electroanal. Chem., 7, 152 (1964).

37. J. A. V. Butler, Proc. Roy. Soc., London, A122, 399 (1929).

38. J. O'M. Bockris, E. Gileadi and K. Muller, Electrochim. Acta, 12, 1301 (1967).

39. B. E. Conway, Ph. D. Thesis, London (1949).

40. J. O'M. Bockris, M. A. V. Devanathan and K. Muller, Proc. Roy. Soc., London, A274, 55 (1963).

41. J. R. McDonald and C. A. Barlow, J. Chem. Phys., 36, 3062 (1962).

42. J. R. McDonald, J. Chem. Phys., 22, 1857 (1954).

43. R. J. Watts-Tobin, Phil. Mag., 6, 133 (1961).

44. N. F. Mott and R. J. Watts-Tobin, Electrochim. Acta, 4, 79 (1961).

45. M. J. Austin and R. Parsons, Proc. Chem. Soc., 239 (1961).

46. A. N. Frumkin and B. B. Damaskin, Modern Aspects of Electrochemistry, Vol. III, (Eds. J. O'M. Bockris and B. E. Conway), Butterworths, London, 1965, Chap. 3.

47. R. S. Hansen, D. J. Kelsh and D. H. Grantham, J. Phys. Chem., 60, 1185 (1956).

48. J. E. B. Randles and W. White, Z. Elektrochem., 59, 666 (1955).

49. R. Parsons, Reports of the Fourth Soviet Conference on Electrochemistry, Eng. Translation, Consultants Bureau, N. Y., (1958), pp.18-22.

50. N. K. Adam, Proc. Roy. Soc., London, A112, 362 (1926).

51. A. H. Hughes and E. K. Rideal, Proc. Roy. Soc., A140, 253 (1933).

52. J. T. Davies and E. K. Rideal, Proc. Roy. Soc., A194, 417 (1948).

53. K. J. Vetter, Z. Naturforsch., 7a, 328 (1952).

54. K. J. Vetter, Trans. Symp. Electrode Processes, Philadelphia (1959), (Ed. E. Yeager), Wiley, N. Y., p. 61.

55. B. E. Conway and M. Salomon, Electrochim. Acta, 9, 1599 (1964).

56. I. Langmuir, Colloid Symp. Monograph, Chemical Catalog Co. Inc., N. Y. (1925), p. 48.

57. W. B. Hardy, Proc. Roy. Soc., London, A88, 303 (1913).

58. G. J. Hills and R. Payne, Trans. Faraday Soc., [illegible] 326 (1965).

59. B. E. Conway and E. Gileadi, Trans. Faraday Soc., 58, 2493 (1962).

60. J. Lawrence, R. Parsons and R. Payne, J. Electroanal. Chem., 16, 193 (1968).

61. P. Delahay, J. Electrochem. Soc., 113, 967 (1966).

62. A. N. Frumkin, Z. Physik Chem., 116, 466 (1925).

63. R. Parsons, Can. J. Chem., 37, 308 (1959).

64. O. A. Esin and B. F. Markov, Acta Physicochim., U.R.S.S., 10, 353 (1939).

65. M. A. V. Devanathan and P. Peries, Trans. Faraday Soc., 50, 1236 (1954).

66. B. E. Conway and R. G. Barradas, Electrochim. Acta, 5, 319 (1961).

67. R. G. Barradas, P. G. Hamilton and B. E. Conway, J. Phys. Chem., 69, 3411 (1965).

68. R. G. Barradas and P. G. Hamilton, Can. J. Chem., 43, 2468 (1965).

69. J. D. Bernal and R. H. Fowler, J. Chem. Phys., 1, 515 (1933).

70. R. Parsons and M. A. V. Devanathan, Trans. Faraday Soc., 49, 673 (1953).

71. W. Anderson and R. Parsons, Second International Congress on Surface Activity, Vol. III, pp. 45-52, Butterworths, London (1957).

72. W. Paik, T. N. Anderson and H. Eyring, J. Phys. Chem., 71, 1891 (1967).

73. A. N. Frumkin, Z. Physik Chem., 164, 121 (1933).

74. B. E. Conway, E. J. Rudd and L. G. M. Gordon, Disc. Faraday Soc., 45, 87 (1968).

75. R. Parsons and K. M. Joshi, Electrochim. Acta, 4, 129 (1961).

76. D. C. Grahame, Chem. Rev., 41, 441 (1947).

77. R. Parsons, Rev. Pure and Appl. Chem., 18, 91 (1968).

78. E. Blomgren and J. O'M. Bockris, J. Phys. Chem., 63, 1475 (1959).

79. A. A. Zhukovitskii, Acta Physiochim., U.R.S.S., 19, 176 (1944).

80. P. J. Flory, J. Chem. Phys., 10, 51 (1942); M. L. Huggins, J. Phys. Chem., 46, 151 (1942).

81. C. Kemball and E. K. Rideal, Proc. Roy. Soc., London, A187, 53 (1946).

82. N. W. C. Cumper and A. I. Vogel, J. Chem. Soc., 4723 (1960).

83. S. Glasstone, "Theoretical Chemistry", D. van Nostrand Co. Inc., (1944).

84. B. E. Conway and R. G. Barradas, Electrochim. Acta, 5, 319, 349 (1961).

85. R. G. Barradas, P. G. Hamilton and B. E. Conway, Coll. Czech. Chem. Comm., 32, 1790 (1967).

86. B. E. Conway and L. Laliberte, "Hydrogen Bonded Solvent Systems" (Proc. Symp. on Equilibria and Kinetics in H-bonded Systems, Newcastle, 1968), p.139, Taylor and Francis, London (1968); see also J. Phys. Chem., 72, 4317 (1968).

87. R. M. Diamond, J. Phys. Chem., 69, 2513 (1963); W. Y. Wen and S. Saito, J. Phys. Chem., 69, 3589 (1965); H. S. Frank, Zeit. phys. Chem., Leipzig, 228, 364 (1965).

88. K. J. Laidler, Trans. Faraday Soc., 55, 1725 (1959); cf. P. Ruetschi, Zeit. phys. Chem., 14, 277 (1958).

89. D. D. Eley and M. G. Evans, Trans. Faraday Soc., 34, 1093 (1938).

90. B. Belleau and J. L. Lavoie, Can. J. Biochem., 46, 1397 (1968).

91. T. L. Hill, "Introduction to Statistical Thermodynamics", pp. 380-1, Addison Wesley Publ. Co., Reading, Mass., (1960).

92. G. Nemethy and H. A. Scheraga, J. Chem. Phys., 36, 3401 (1962); cf. A. Ben Naim, J. Phys. Chem., 69, 1922 (1965).

93. R. Parsons, Modern Aspects of Electrochemistry, Vol. I, Chap. 3, (Eds. J. O'M. Bockris and B. E. Conway), Butterworths (1954).

94. B. E. Conway, J. O'M. Bockris and I. A. Ammar, Trans. Faraday Soc., 47, 756 (1951).

95. R. N. Rampolla, R. C. Miller and C. P. Smyth, J. Chem. Phys., 30, 566 (1959); (cf. ref. 40).

96. E. A. Moelwyn-Hughs, "Physical Chemistry," Pergamon Press, London (1957); see also Fowler "Statistical Mechanics," Cambridge University Press (1936) and ref. 89.

97. R. J. L. Andon, J. D. Cox and E. F. G. Herrington, Trans. Faraday Soc., 53, 410 (1957); see also idem, J. Chem. Soc., London, 3188 (1954).

98. R. Parsons, Proc. Roy. Soc., London, A261, 79 (1961).

99. H. W. Nürnberg and G. Woolf, Coll. Czech. Chem. Comm., 30, 3997 (1965).

100. L. Gierst, Trans. Symp. on Electrode Processes, p. 294, (E. Yeager, Ed.) Wiley, N. Y. (1961).

101. V. Prelog and P. Wieland, Helv. Chim. Acta, 27, 1127 (1944).

102. A. McKenzie, J. Chem. Soc., 270 (1952).

103. A. Inesi, F. Rallo and L. Rampazzo, Trans. Faraday Soc., 64, 3340 (1968).

104. E. Gileadi and B. E. Conway, Modern Aspects of Electrochemistry, (Eds. J. O'M. Bockris and B. E. Conway) Butterworths, 1964, Vol. III, Chap. 5.

105. D. H. Everett and P. Norden, Proc. Roy. Soc., London, A259, 341 (1960).

106. M. Johnson, H. Wroblowa and J. O'M. Bockris, Electrochim. Acta, 9, 639 (1964).

107. D. Gilroy and B. E. Conway, J. Phys. Chem., 69, 1259 (1965).

108. G. H. Nancollas, D. S. Reid and C. A. Vincent, J. Phys. Chem., 70, 3300 (1966).

109. L. Pauling, "Nature of the Chemical Bond," Cornell University Press, 1940.

110. E. A. Guggenheim, J. Chem. Phys., 4, 689 (1936).

111. R. Parsons, Proc. Roy. Soc., (London), A261, 79 (1961).

112. F. W. Schapink, M. Oudeman, K. W. Leu and J. W. Helle, Trans. Faraday Soc., 56, 415 (1960).

113. L. G. M. Gordon, J. Halpern and B. E. Conway, J. Electroanal. Chem., 21, p. 3 (1969).

114. T. L. Hill, J. Chem. Phys., 16, 181 (1948).

115. J. L. deBoer, "The Dynamical Character of Adsorption," Oxford University Press (1968).

116. H. K. Livingstone, J. Colloid Sci., 4, 447 (1949).

117. N. K. Adam, "The Physics and Chemistry of Surfaces," Oxford University Press, 1952.

118. M. H. Armbruster and J. B. Austin, J. Am. Chem. Soc., 66, 159 (1944).

119. G. Jura, E. H. Loeser, P. R. Basford and W. D. Harkins, J. Chem. Phys., 14, 117 (1946); see also ibid., 13, 535 (1945) and 14, 344 (1946).

120. D. A. Haydon and F. H. Taylor, Phil. Trans., A252, 225 (1960).

121. B. E. Conway and L. G. M. Gordon, J. Electroanal. Chem., 15, 7 (1967).

122. B. E. Conway and L. G. M. Gordon, J. Phys. Chem. In Press.

123. T. L. Hill "Introduction to Statistical Thermodynamics", Addison-Wesley Pub. Co., Mass., U.S.A. (1962).